



Brunel
University
London

Experimental and Analytical Study of Water Production of Solar Still

A thesis submitted in partial fulfilment of the requirements for
the degree of Master of Philosophy

by

Thamer Alheefi

College of Engineering, Design and Physical Sciences

Brunel University London

May 2019

Abstract

Rapid population growth and industrialization have increased the demand on potable water dramatically, and there are many rural areas and communities around the world which suffer from the shortage of potable water. However, many of these communities inhabit desert areas where the weather is hot and solar energy is plentiful. Therefore, the present study suggests basin-type solar stills for desalination, which uses solar energy to evaporate the saline water. The use of solar stills in large scale commercial systems is limited by the low production rate of desalinated water. Therefore, the present study focuses on the effects of different parameters on the thermal performance and productivity of a single basin double slope solar still. It is well known that the performance of a solar still can vary from one country to another due to the effect of meteorological conditions. The experiments of the present study were conducted in Kuwait. A double slope solar still was designed and fabricated, and the data were collected over a long period of time to achieve high accuracy. The effects of several parameters on the performance of the examined solar still were investigated. These parameters include the following: (1) type of energy storing materials, (2) basin water depth, (3) the cooling of the solar still cover plate. The experimental data were verified using a theoretical model. The investigated energy storage materials included steel metal pieces in different shapes, gravel in two different sizes and encapsulated paraffin wax as a phase change material.

This study has concluded that the basin water depth has a significant effect on the daily water production and the water production rate. This rate increases as the water depth in the basin decreases. A correlation was developed to express the relation between the daily water production and the basin water depth. The study has also found that the performance of the solar still with the energy storing materials depends on the material density and specific heat capacity. A new dimensionless factor called “energy storing material factor (β)” was introduced. It was found that the performance of the energy storing materials is proportional to the values of β . For $\beta < 1$, the energy storing materials can improve the water productivity. Among the studied energy storing materials, the phase change material has achieved the highest total water production per square meter (about 53% improvements). This present study contributes to improving the design of passive basin-type solar stills which can be used for water production in many rural and desert areas which do not have access to electricity. The study also discusses some ideas to enhance the water productivity of passive solar stills, which is still a big limitation to the widespread use of solar stills.

Acknowledgments

Firstly, I would like to express my sincere gratitude to my supervisor Prof. Ibrahim Esat for his continuous support of my postgraduate study and research, his patience, motivation and immense knowledge. His guidance has helped me throughout my research and the writing of this thesis. I could not have imagined better support for my study.

Also, I would like to express my profound gratitude to my parents and to my family, especially my wife for providing me with unfailing support and continuous encouragement throughout my years of study and the process of research and writing this thesis at Brunel University London. This accomplishment would not have been possible without them.

Thamer Alheefi

Table of Contents

Abstract.....	i
Acknowledgments	ii
Abbreviations.....	v
Nomenclature.....	vi
Greek Letters	vii
List of Figures.....	vii
List of Tables	xi
1. Chapter One: Introduction.....	1
1.1 Background.....	1
1.2 Desalination Technologies	2
1.2.1 Solar Still Distillation (SD).....	3
1.2.2 Humidification-Dehumidification (HDH)	5
1.2.3 Membrane Distillation (MD)	6
1.2.4 Multi Effect Distillation (MED).....	7
1.2.5 Multistage Flash Distillation (MSF)	7
1.2.6 Vapour Compression (VC)	8
1.2.7 Crystallization Process	8
1.2.8 Reverse Osmosis	8
1.2.9 Distillation:.....	10
1.3 Research Objectives	11
1.4 Organization of the Thesis.....	12
2. Chapter Two: Literature Review.....	13
2.1 Introduction	13
2.2 Effect of Energy Storing Materials.....	15
2.2.1 Sensible Heat Energy Storing Materials	15
2.2.2 Phase Change Energy Storing Materials.....	20
2.3 Effect of Basin Water Depth	22
2.4 Effect of Solar Still Cover	23
2.5 Effect of Solar Still Cover Tilt Angle.....	25
2.6 Summary.....	27
3. Chapter Three: Experimental Set-Up	31

3.1	Introduction	31
3.2	Experimental System.....	31
3.3	Experimental Plan and Methodology	34
4.	Chapter Four: Experimental Results and Discussions	37
4.1	Introduction	37
4.2	The Effect of the Shape of Metallic Energy Storing Materials	39
4.3	Solar Still with Hollow and Solid Steel Pieces	44
4.4	The Effect of External Cooling	46
4.5	The Effect of a Combination of External Cooling and Solid Steel Rods.....	48
4.6	The Effect of Water Depth	50
4.7	The Effect of the Type of Energy Storing Material	51
4.8	Summary.....	53
5.	Chapter Five: Empirical and Theoretical Study of Solar Still Productivity	55
5.1	Introduction	55
5.2	Empirical Study of Total Production (Y)	55
5.3	The Effect of Ambient Temperature	56
5.4	Energy Storing Materials.....	58
5.5	Heat Capacity of Energy Storing Materials.....	59
5.5.1	Energy Storing Factor (β).....	61
5.5.2	The Effect of The Shape of Energy Storing Materials.....	64
5.6	Theoretical Analysis	66
5.7	Summary.....	71
6.	Chapter Six: Conclusions and Future Work	72
6.1	Conclusions	72
6.2	Future Work.....	74
	REFERENCES.....	75
	Appendix 1: On Balance Mtt-500 Mini Table Top Scale.....	88
	Appendix 2: Derivation of Equation (5.8)	89
	Appendix 3: Figures – Experimental Setup	90

Abbreviations

UN	The United Nations
MSF	Multi Stage Flash
PVC	Polyvinyl Chloride
PUF	Poly Urethane foam
STDEV.P	Product standard deviation
Ec	Electrical conductivity
TDS	Total dissolved solids
Sa	Salinity
IMechE	Institution of Mechanical Engineers

Nomenclature

A	Area	m^2
M	mass	kg
M	hourly distilled water production	kg/h
G	solar radiation intensity	W/m^2
D	depth	m
Y	total water production	l/m^2
K	thermal conductivity	$W/m\ K$
A	cover tilt angle	degree
T	Temperature	$^{\circ}C$
E	Experiment number	-
X	Maximum production rate	ml/ m^2h
X	Production rate	ml/ m^2h
t_o	Start of production	min
t_e	End of production	min
r_{xy}	Correlation Coefficient	-
R_t	Critical correlation Coefficient	-
Q	Energy	J
C	Specific heat capacity	$J/kg.K$
QL	Heat loss	J
V	Volume	m^3
H	heat transfer coefficient	W/m^2K

Greek Letters

α	absolute relative temperature percentage	
β	Energy storing factor	
ΔT	Duration of production	min
η	Efficiency	-
ρ	Density	kg/m ³
Υ	specific vapour latent heat	kJ/kg

List of Figures

FIGURE 1.1 AN IMMEDIATE ACTION NEEDS TO BE TAKEN TO FIND A SOLUTION FOR WATER SHORTAGE GLOBALLY (WWW.UNWATER.ORG).....	2
FIGURE 1.2 THE MAIN DESALINATION TECHNOLOGIES, (BELESSIOTIS, (2016)).....	3
FIGURE 1.3 SKETCH OF THE EVAPORATION/CONDENSATION INSIDE A SINGLE EFFECT SOLAR STILL (BELESSIOTIS, 2016).....	4
FIGURE 1.4 SCHEMATIC DRAWING FOR THE HUMIDIFICATION-DEHUMIDIFICATION DISTILLATION SYSTEM (KUCERA, 2014).....	6
FIGURE 1.5 SCHEMATIC DRAWING FOR THE MEMBRANE DISTILLATION	7
FIGURE 1.6 SCHEMATIC DRAWING SHOWING THE MULTI-EFFECT DISTILLATION PROCESS (EL-DESSOUKY AND ETTOUNEY, 2002)	7
FIGURE 1.7 ADELAIDE DESALINATION PLANT (WWW.EN.WIKIPEDIA.ORG, 2014)	9
FIGURE 2.1 NUMBER OF RESEARCH PAPERS ON SOLAR STILLS PUBLISHED BY SCIENCEDIRECT.COM DURING THE PERIOD FROM 2004 TO 2016	13
FIGURE 2.2 (A) SINGLE SLOPE ACTIVE SOLAR STILL THAT CONVERTS SOLAR ENERGY TO THERMAL ENERGY AND HEATS UP WATER IN THE BASIN. (B) SINGLE SLOPE ACTIVE SOLAR STILL THAT USES SOLAR PANEL TO CONVERT SOLAR ENERGY TO ELECTRIC ENERGY (TIWARI ET AL., 2003A).....	14

FIGURE 2.3 SCHEMATIC DIAGRAM OF THE SINGLE SLOPE SOLAR STILL WITH SUSPENDED BAFFLE PLATE (EL-SEBAIL ET AL., 2000).....	16
FIGURE 2.4 EXPERIMENTAL SET-UP SHOWING JUTE CLOTH AS AN ENERGY STORING MATERIAL (SAKTHIVEL ET AL., 2010).....	17
FIGURE 2.5 SCHEMATIC OF THE EXPERIMENTAL SETUP BY SAMUEL ET AL. (2016).....	18
FIGURE 2.6 EXPERIMENTAL SET-UP SHOWING SENSIBLE HEAT ENERGY STORING MATERIAL (DESHMUKH AND THOMBRE, 2017)	18
FIGURE 2.7 SCHEMATIC OF A FINNED LINER BASIN STILL (EL-SEBAIL AND EL-NAGAR, 2017)	19
FIGURE 2.8 BLUE METAL STONE IN VARIOUS SIZE (6, 12, 20 MM) (NITHYANANDAM ET AL., 2017)	20
FIGURE 2.9 SOLAR STILL DESIGN WITH V-CORRUGATED ABSORBER INTEGRATED WITH PHASE CHANGE MATERIAL (SHALABY ET AL., 2016).....	21
FIGURE 2.10 VARIATION OF DAILY PRODUCTION Y AGAINST THE WATER DEPTH.....	23
FIGURE 2.11 SOLAR STILL DAILY YIELD (L) BY USING THREE DIFFERENT MATERIALS (GLASS, PVC AND COPPER) FOR COVER (TIWARI ET AL., 2009).....	24
FIGURE 2.12 VARIATION OF DAILY YIELD AGAINST THICKNESS OF GLASS COVER FOR ACTIVE STILL AND PASSIVE STILL, (TIWARI ET AL., 2009)	25
FIGURE 2.13 THE SCHEMATIC DIAGRAM OF EXPERIMENTAL SET-UP (KHALIFA AND IBRAHIM, 2010).....	26
FIGURE 2.14 VARIATION OF SOLAR STILL COVER TILT ANGLE IN EACH MONTH DURING A YEAR (AL OTAIBI AND AL JANDAL, 2011)	27
FIGURE 2.15 SUN HOURS IN EVERY MONTH OF A YEAR.....	28
FIGURE 2.16 VARIATION OF AVERAGE MAXIMUM AND MINIMUM TEMPERATURE (oC) IN A YEAR.....	28
FIGURE 2.17 VARIATION OF SEA WATER AVERAGE TEMPERATURE IN A YEAR	29
FIGURE 2.18 VARIATION OF AVERAGE PRECIPITATION (MM) IN A YEAR	29
FIGURE 2.19 NUMBER OF RAINY DAYS IN EVERY MONTH OF A YEAR.....	29
FIGURE 2.20 VARIATION OF AVERAGE HUMIDITY IN A MONTH (%) OF A YEAR.....	30
FIGURE 2.21 VARIATION OF AVERAGE MONTHLY WIND SPEED (M/S) DURING A YEAR.....	30
FIGURE 3.1 SCHEMATIC DRAWING FOR THE EXPERIMENTAL SET-UP WITH THE LOCATIONS OF TEMPERATURE MEASUREMENTS	32
FIGURE 3.2 PHOTOGRAPH SHOWING THE TESTED DOUBLE SLOPE PASSIVE SOLAR STILL	32

FIGURE 3.3 (A) PHOTOGRAPH FOR THE 2.5 CM INSULATION THICKNESS AND (B) COMPOSITE WALL CROSS SECTIONAL VIEW	33
FIGURE 3.4 THE SOLID AND HOLLOW STEEL RODS, A) TOP VIEW, B) SIDE VIEW AND C) THE IMAGE OF SOLID AND HOLLOW STEEL RODS	35
FIGURE 3.5 THE LAYOUT OF THE WATER COOLER.....	36
FIGURE 4.1 VARIATION OF THE AMBIENT TEMPERATURE DURING THREE CONSECUTIVE DAYS AT DIFFERENT TIME OF THE DAY AT THE TEST SITE IN KUWAIT	37
FIGURE 4.2 THE HOURLY MEASURED INTENSITY OF SOLAR RADIATION	38
FIGURE 4.3 THE CONFIGURATIONS AND SHAPE OF THE TESTED STEEL ENERGY STORING MATERIAL	40
FIGURE 4.4 TEMPERATURE DISTRIBUTIONS INSIDE THE CONVENTIONAL SOLAR STILL (WITHOUT MODIFICATIONS)	41
FIGURE 4.5 TEMPERATURE DISTRIBUTIONS INSIDE THE SOLAR STILL WITH SOLID ROUND RODS	41
FIGURE 4.6 TEMPERATURE DISTRIBUTIONS INSIDE THE SOLAR STILL WITH HOLLOW ROUND RODS	42
FIGURE 4.7 TEMPERATURE DISTRIBUTIONS INSIDE THE SOLAR STILL WITH SOLID SQUARE RODS	42
FIGURE 4.8 THE CUMULATIVE WATER PRODUCTION CURVE FOR THE SOLAR STILL MODIFIED WITH ROUND SOLID RODS, HOLLOW ROUND RODS AND SOLID SQUARE RODS COMPARED WITH THE CONVENTIONAL SOLAR STILL.	43
FIGURE 4.9 THE RATE OF WATER PRODUCTION FOR THE SOLAR STILL MODIFIED WITH ROUND SOLID RODS, HOLLOW ROUND RODS AND SOLID SQUARE RODS COMPARED WITH THE CONVENTIONAL SOLAR STILL.	44
FIGURE 4.10 THE TEMPERATURE DISTRIBUTION INSIDE A SOLAR STILL MODIFIED WITH A COMBINATION OF SOLID AND HOLLOW ROUND STEEL RODS	45
FIGURE 4.11 THE RATE OF WATER PRODUCTION FOR A SOLAR STILL MODIFIED WITH A COMBINATION OF SOLID AND HOLLOW ROUND STEEL RODS COMPARED WITH THE CONVENTIONAL SOLAR STILL	45
FIGURE 4.12 THE CUMULATIVE WATER PRODUCTION CURVE FOR A SOLAR STILL MODIFIED WITH A COMBINATION OF SOLID AND HOLLOW ROUND STEEL RODS COMPARED WITH THE CONVENTIONAL SOLAR STILL	46
FIGURE 4.13 THE TEMPERATURE DISTRIBUTION INSIDE A SOLAR STILL MODIFIED WITH AN EXTERNAL COOLING ON THE OUTER SURFACE OF GLASS COVER PLATE	47
FIGURE 4.14 THE RATE OF WATER PRODUCTION FOR A SOLAR STILL MODIFIED WITH AN EXTERNAL COOLING ON THE OUTER SURFACE OF GLASS COVER PLATE	47

FIGURE 4.15 THE CUMULATIVE WATER PRODUCTION CURVE FOR A SOLAR STILL MODIFIED WITH AN EXTERNAL COOLING ON THE OUTER SURFACE OF GLASS COVER PLATE.....	48
FIGURE 4.16 THE TEMPERATURE DISTRIBUTION INSIDE A SOLAR STILL MODIFIED WITH A COMBINATION OF EXTERNAL COOLING AND SOLID RODS.....	49
FIGURE 4.17 THE RATE OF WATER PRODUCTION FOR A SOLAR STILL MODIFIED WITH A COMBINATION OF EXTERNAL COOLING AND SOLID STEEL RODS	49
FIGURE 4.18 THE CUMULATIVE WATER PRODUCTION CURVE FOR A SOLAR STILL MODIFIED WITH A COMBINATION OF EXTERNAL COOLING AND SOLID STEEL RODS	50
FIGURE 4.19 VARIATION OF TOTAL DAILY PRODUCTION (L/M ²) IN TERMS OF WATER DEPTH (CM).....	51
FIGURE 4.20 EFFECT OF THE TYPE OF ENERGY STORING MATERIAL ON THE RATE OF WATER PRODUCTION COMPARED TO THE CONVENTIONAL SOLAR STILL WITH NO MODIFICATIONS	52
FIGURE 4.21 EFFECT OF THE TYPE OF ENERGY STORING MATERIAL ON THE CUMULATIVE WATER PRODUCTION CURVE COMPARED TO THE CONVENTIONAL SOLAR STILL WITH NO MODIFICATIONS.	53
FIGURE 5.1 THE DAILY WATER PRODUCTION AS A FUNCTION OF WATER DEPTH INSIDE THE BASIN.....	56
FIGURE 5.2 VARIATION OF BASIN TEMPERATURE (T ₁), BASIN WATER TEMPERATURE (T ₂), VAPOUR TEMPERATURE (T ₃), AMBIENT TEMPERATURE (T ₄) AND COVER TEMPERATURE (T ₅) IN AUGUST IN KUWAIT.....	57
FIGURE 5.3 THE VARIATION OF DAILY WATER PRODUCTION AGAINST THE AMBIENT AVERAGE TEMPERATURE	58
FIGURE 5.4 A TYPICAL DOUBLE SOLAR STILL WITH NO ENERGY STORING MATERIALS USED IN THE BASIN	59
FIGURE 5.5 DOUBLE SOLAR STILL WITH ENERGY STORING MATERIALS USED IN THE BASIN..	60
FIGURE 5.6 WATER TEMPERATURE RISE FOR A MODIFIED SOLAR STILL USING ENERGY STORING MATERIALS VERSUS WATER TEMPERATURE RISE FOR A SOLAR STILL WITHOUT MODIFICATIONS	62
FIGURE 5.7 VARIATION OF ENERGY STORING FACTOR, B FOR STEEL, COPPER, ALUMINIUM, STONE AND GLASS.....	63
FIGURE 5.8 THE ENERGY FLOW INSIDE A DOUBLE SLOPE SOLAR STILL	66
FIGURE 5.9 THE MEASURED BASIN WATER TEMPERATURE VERSUS TIME COMPARED WITH THE PREDICTION USING THE THEORETICAL MODEL.....	70
FIGURE 5.10 THE MEASURED GLASS TEMPERATURE VERSUS TIME COMPARED WITH THE PREDICTION USING THE THEORETICAL MODEL.....	71

FIGURE 5.11 THE MEASURED CUMULATIVE WATER PRODUCTION VERSUS TIME COMPARED WITH THE PREDICTION USING THE THEORETICAL.....	71
--	----

List of Tables

TABLE 1.1 THE GENERAL TECHNICAL INFORMATION OF ADELAIDE DESALINATION PLANT, (WWW.EN.WIKIPEDIA.ORG, 2014)	9
TABLE 1.2 MAJOR OIL RESERVES IN THE MIDDLE EAST, (WWW.IMECHE.ORG, 2015)	10
TABLE 5.1 MEASURED TOTAL PRODUCTION IN TERMS OF WATER DEPTH.....	55
TABLE 5.2 DAILY AMBIENT TEMPERATURE AGAINST DAILY WATER PRODUCTION	57
TABLE 5.3 MAXIMUM WATER PRODUCTION RATE VERSUS THE DAILY AMBIENT AVERAGE TEMPERATURE	58
TABLE 5.4 DENSITY AND SPECIFIC HEAT CAPACITY VALUES	63

1. Chapter One: Introduction

1.1 Background

Water is one of the most important factors for the lives of humans, animals and plants. In the past, there was an impression that water resources are unlimited and the balance between demand and supply always exists through the hydrological cycle in nature. In the last few decades, it has been revealed that there is a significant imbalance between the supply and demand for fresh water. Such findings have led to the conclusion that water resources are extremely limited. It is well known that more than three quarters of the earth's surface is covered with water. However, the majority of this water is not drinkable. Oceans, which consist of salt water, constitute about 97% of the earth's water. The remaining 3%, which represents fresh water, is reserved in icecaps and glaciers (68.7%), ground water (30.1%) and surface water such as lakes and rivers (0.3%), (Manju and Sagar, 2017). This means that less than 1% of the earth's water is available for human use in the form of potable water.

Thus, it is expected that there will be an acute water shortage in the near future. This shortage arises from the increased demand induced by population growth, urbanization and industrialization. Some researchers (Rijsberman, 2006) reported that a water shortage occurs when the water supply falls below 1000 m³ per person per year. Additionally, it was reported by the United Nations that about 40% of the world population will face water shortage by 2030 (WAAP, 2015). Also, the World Health Organization (2010) reported that the demand will exceed the supply by 56% by 2025. It is commonly known that water shortage is a multi-dimensional problem that can lead to poverty, hunger, ecosystem degradation, desertification, climate change and even the threat to world peace directly and indirectly.

Owing to the seriousness of the global water crisis, the United Nations has declared that the 22nd of March of every year is the World Water Day since 1993. This is to highlight the importance of water, to encourage the sustainable management of water resources and to increase the public awareness of this issue worldwide. Since this date, the interest in the global water crisis has increased dramatically, and noticeable improvements were detected in some regions in the last twenty years. However, the United Nations has issued a shocking report in 2014, showing that 4000 children die every day (about 1.5 million/year) due to diseases such as diarrhoea, dysentery and cholera caused by dirty water and unhygienic living conditions. Moreover, the report indicates that the lack of access to water, sanitation and potable water is

extremely serious and needs immediate action so that a solution is reached globally. **Error! Reference source not found.** illustrates that an appropriate action can prevent 20% of child death.

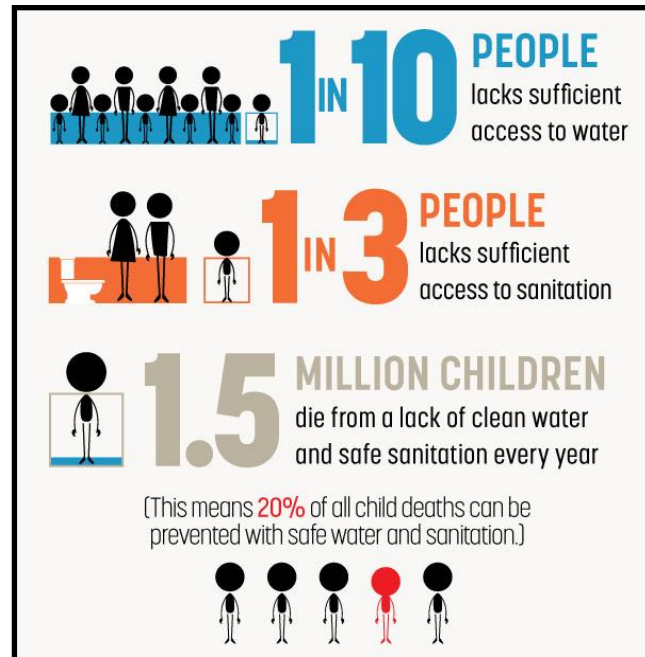


Figure 1.1 An immediate action needs to be taken to find a solution for water shortage globally (www.unwater.org).

1.2 Desalination Technologies

Desalination can be defined as the process of removing dissolved salts and minerals from saline water to produce potable water with the permissible salinity limit 500 – 1000 ppm, (Rao and Mamatha, 2004). The objective of this section is present a summary of the existing desalination techniques. Figure 1.2 summarizes the classifications of desalination techniques based on the adopted desalination process, (Kucera, 2014) and Belessiotis, 2016). The figure classifies the desalination methods into thermal and non-thermal processes. The conventional thermal methods (commercially available) are usually driven by steam supplied from external sources and include Multistage Flash evaporation (MSF), Multi-Effect Distillation (MED) and Thermal Vapour Compression (TVC). The non-conventional thermal methods (not commercially available) include Solar Distillation (SD), Membrane Distillation (MD) and Humidification-Dehumidification (HDH) which are suitable for small capacities. The non-conventional thermal methods are still under investigation by researchers. The conventional (commercialized) non-thermal methods are driven by direct electric energy and include

Reverse Osmosis (RO), Electro-Dialysis Reversal (EDR) and Mechanical Vapour Compression (MVC). The non-conventional non-thermal methods include crystallization (freezing and hydrates) and ion exchange, which did not find a wide range of applications. A brief description to each process is given below.

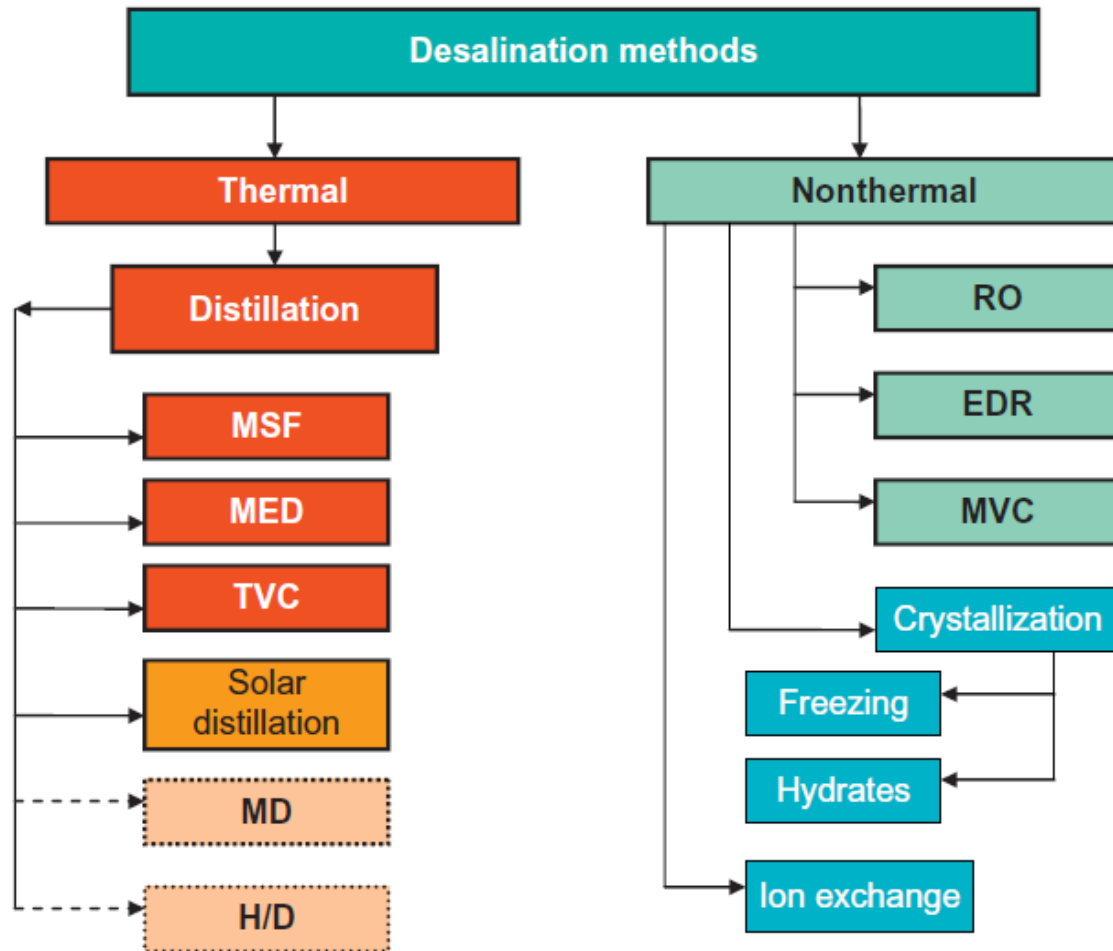


Figure 1.2 The main desalination technologies, (Belessiotis, (2016).

1.2.1 Solar Still Distillation (SD)

In its simplest form, solar stills are basins which are partially filled with saline water and covered from the top side with a transparent cover; see Figure 1.3. The basins are thermally insulated from each side except from the top transparent side. Basically, the operation of solar stills is based on a distillation process. The incident solar radiation is absorbed by water in the basin of the still; thus, the solar energy is used to evaporate the saline water. The created vapor moves towards the top transparent cover by natural convection and condenses on the cold interior surface of the transparent cover. The pure water vapour condenses on top and drips down to the sides where it is collected and removed by gutters.

Because the created vapour is already mixed with the air inside the still, this process includes humidification-dehumidification process occurring simultaneously in the same device. The advantages of solar stills include simplicity, low cost, ease of maintenance and low environmental impact, while the most significant disadvantage is the low efficiency and productivity. Ahsan et al. (2014) designed and fabricated a solar still using local, available, cheap and durable materials and provided the fabrication cost. The designed still occupied a land area of 0.8 m² and produced about 1.5 L/day. The total cost of fabricating this solar still was estimated, based on their local currency, as RM 112 or (\$35, USD). Recent reviews on this technique were also given by Kaviti et al. (2016), Omara et al. (2017) and Shukla et al. (2017).

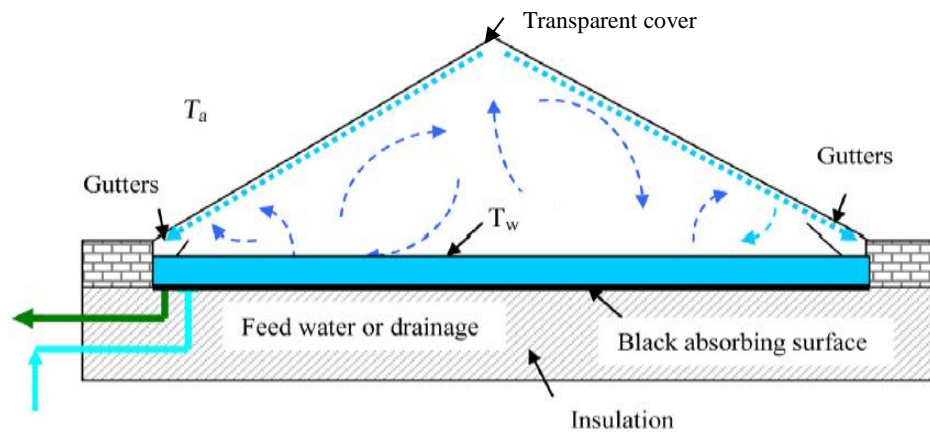


Figure 1.3 Sketch of the evaporation/condensation inside a single effect solar still (Belessiotis, 2016)

Solar stills have been studied by researchers extensively in terms of their advantages and disadvantages compared to other techniques. The main points extracted from the published literature can be summarized as follows:

Advantages:

- A Free energy source: Sunlight, as an available energy source, exists almost in all countries, and it is a renewable energy. For example, the average daily solar radiation in India is 4–7 kWh/m² compared to the global average of 2.5 kWh/m². Therefore, despite its relatively high capital cost, solar energy driven desalination is known to be more feasible than other methods (Arjunan et al., 2009).
- Low maintenance cost: Solar stills are very simple and consist of no moving parts. Hence, there is no need to have regular maintenance which can be very costly in remote areas.

- A reliable system: Solar stills use sunlight to produce the potable water and there is no risk of losing the energy source. Therefore, solar stills are known as a reliable water producer.
- Availability: Solar stills use a renewable energy source, which is available in most countries. It represents a good option especially in remote areas where there is a shortage of electricity and good quality water (Eltawil and Omara, 2014).
- Better water taste: the water produced by solar stills has better taste compared to the other systems which boil the water to produce the drinking water. In solar stills the water is not boiled.
- Neutral PH: Water production in solar stills is a chemical free process, which can produce neutral PH water.

Disadvantages:

Solar stills, like any other devices, have some disadvantages that render this technology very controversial in the field of fresh water production. Some of the disadvantages that were claimed by researchers can be listed as follows:

- Bacteria and harmful chemicals: Solar stills do not boil the water and therefore, the bacteria and harmful chemicals could contaminate the produced water.
- Bugs and insects: The area for the tilted glass cover could be an attractive area for insects and bugs, which could reduce the efficiency of produced water in terms of quality and quantity.
- Low water production: One of the main problems associated with the use of solar stills, as identified in many studies, is the productivity issue. A single solar still can be installed in one square metre and it weighs about 30 kg. The produced water when it is in direct sun shine can be about 6 litres per day in summer time and it could drop to half in winter time.

1.2.2 Humidification-Dehumidification (HDH)

In the solar still system, evaporation (humidification) and condensation (dehumidification) occurs in the same compartment. On the other hand, in the humidification-dehumidification (HDH) systems, evaporation and condensation occurs in separate compartments and the carrier gas moves also either by natural convection (closed cycle) or by a blower (open cycle). Figure 1.4 depicts the simplest HDH process. The cold feed seawater is used to condense the water vapour in the dehumidifier unit and thus the feed water temperature increases. The feed water is further pre-heated in a separate heating unit then it is sprayed over a packed bed in the humidifier (evaporator). This is an updated version of solar stills. Because

some of the energy can be recovered in the dehumidifier and is used for preheating the feed water, the performance is improved compared to solar stills. Thus, the HDH process is a low to medium capacity method.

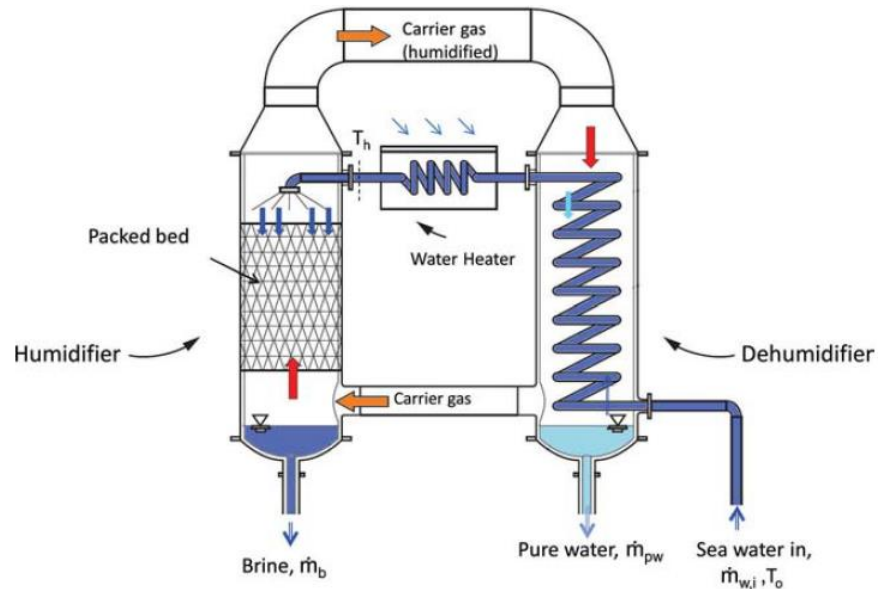


Figure 1.4 Schematic drawing for the humidification-dehumidification distillation system (Kucera, 2014)

1.2.3 Membrane Distillation (MD)

Membrane distillation (MD) is a desalination process that is driven by temperature gradient across a microporous hydrophobic membrane between a hot feed solution and a cold permeate. The temperature gradient across the membrane creates a vapour pressure gradient, and thus the vapour flows from the high pressure side (hot side) to the low pressure side (cold side). It involves evaporation of the water molecules at the hot interface, the transport of water vapor across the porous membrane and condensation of water vapor at the cold interface. A schematic drawing for this process is shown in Figure 1.5. It has the following advantages:

- (1) low sensitivity to salt concentration,
- (2) almost 100% salt rejection can be achieved,
- (3) it can utilize low-grade heat and renewable energy (e.g., industrial waste heat, solar power or geothermal energy),
- (4) there is a low chance of membrane fouling,
- (5) it is characterized by low equipment cost and good performance under mild operating conditions as compared to conventional, multi-stage distillation or pressurized process like RO.

More details about this technique can be found in Abu-Zeid et al. (2015) and González et al. (2017) who have conducted an extensive review on this method.

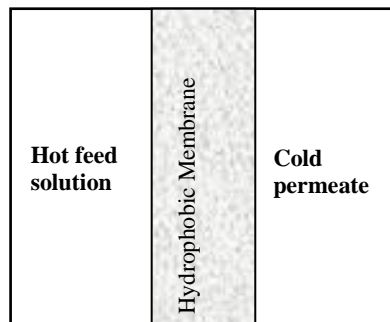


Figure 1.5 Schematic drawing for the membrane distillation

1.2.4 Multi Effect Distillation (MED)

The feed seawater is evaporated in several stages called effects (see Figure 1.6). In the first effect, the feed water is heated and partially evaporated by steam supplied from an external source. Afterwards, the feed water passes through a series of consecutive chambers where it is partially evaporated. The vapour created in the previous chamber is condensed in the next chamber giving the latent heat of condensation to the incoming feed seawater.

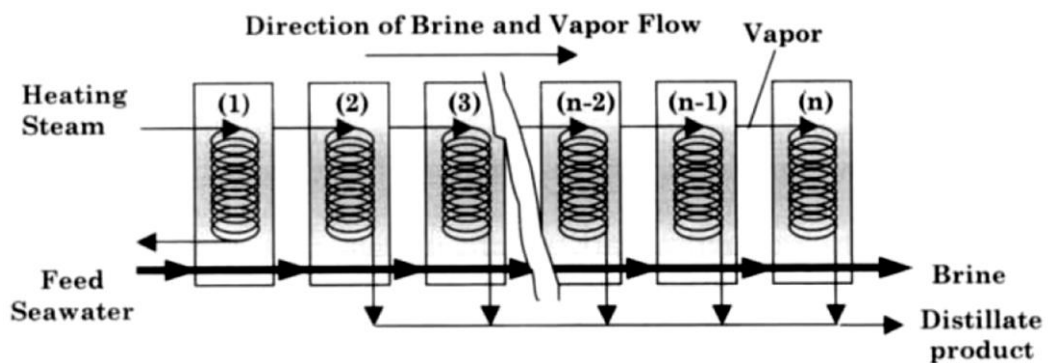


Figure 1.6 Schematic drawing showing the multi-effect distillation process (El-Dessouky and Ettouney, 2002)

1.2.5 Multistage Flash Distillation (MSF)

The Multi Stage Flash (MSF) process consists of several elements, called stages. The hot feed water heated by steam in the first stage enters a series of compartments, each at lower pressure than the previous stage. The hot water expands (flashes) into each chamber releasing vapor, which condenses to fresh water and exchange simultaneously the latent heat of condensation with the incoming feed seawater.

1.2.6 Vapour Compression (VC)

In this process, the heat required to vaporise the saline water is obtained from compressed steam supplied from an external source, i.e. the steam temperature increases as the pressure increases. The compression process could be done mechanically or thermally using steam ejector.

1.2.7 Crystallization Process

This process comprises of the freezing of seawater and hydrate formation. Both processes, despite their simplicity, have found no wide industrial applications. During the freezing process, seawater crystallizes nearly to pure ice. Small crystals are not easily separated from the ice brine slurry and almost half of the fresh water produced is used to wash out the salts from the ice surface, considerably reducing the efficiency of the method and increasing product cost. Hydrate formation is an alternative to produce pure crystals. Water combines with other substances to form hydrate crystals. For desalination purposes, hydrocarbons like propane or butane have been studied. During crystal formation, all impurities like the dissolved salts in seawater are excluded and the crystals formed are pure hydrates. After hydrate formation, the gas is released giving pure water. The process found no large-scale commercial applications due to many problems arising during operation.

1.2.8 Reverse Osmosis

In this process, saline water is pushed at pressures higher than the osmotic pressure (mechanical energy) through special semi-permeable membranes allowing water molecules to pass selectively while blocking the dissolved salts.

Reverse osmosis and distillation processes constitute the most widely used techniques due to their efficiency and economic viability. A brief illustration of these two technologies is presented below.

The reverse osmosis: These systems are generally preferred to distillation systems where the fresh water production is considered in a large scale (Ghaffour et al., 2013 and Greenlee et al., 2009). A water desalination plant that uses reverse osmosis process can provide fresh water for a city in scale of Adelaide in Australia by using sea water. After a pre-treatment process, seawater is pumped into a multi layers membrane at a high pressure (about 7 MPa). In order to improve the taste and disinfection properties, calcium carbonate (CaCO₃) and chlorine (Cl₂)

are added to the water. In a typical water desalination plant that uses reverse osmosis technology, similar to the Adelaide Desalination Plant in Australia in **Error! Reference source not found.**, about 40% of the saline water can be converted to potable water (en.wikipedia.org, 2014). This plant has been providing 3×10^8 litres per day since 2012, which represents almost 50% of the city's drinking water needs. Depending on the availability of energy and the ability of affording the costs, a reverse osmosis plant can be a suitable solution to produce fresh water. **Error! Reference source not found.** presents the general technical information of Adelaide Desalination plant, which uses reverse osmosis technology.



Figure 1.7 Adelaide Desalination plant (www.en.wikipedia.org, 2014)

Location	Lonsdale, South Australia
Daily capacity	300 megalitres per day
Annual capacity	100 gigalitres per annum
Cost	A\$1.83 billion
Energy generation offset	Renewable (TBA)
Technology	Reverse Osmosis
Percent of water supply	50% of Adelaide
Completion date	Dec-12
Website	www.sawater.com.au

Table 1.1 The general technical information of Adelaide Desalination plant, (www.en.wikipedia.org, 2014)

It was reported that the price of desalinated seawater has been reduced to under US\$0.50/m³ at reverse osmosis plants. This price could be increased in some locations depending on the location conditions and facilities. The price also depends on local government policy and some subsidies may be contributed in calculating final price (Ghaffour et al., 2013).

1.2.9 Distillation:

After heating a liquid up to the evaporation phase, the process of capturing and cooling the resultant hot vapour until it condenses is called distillation. Distillation has been used to produce potable water for many years. It is a fundamental process in many water producing systems. The source of the heat energy required for the distillation process could be electrical energy or energy due to combustion of fossil fuels (oil or natural gas). Due to the cost of energy and the availability of energy sources in the form of electricity or fuel, producing low cost fresh water is not possible by using distillation in many remote areas (Ghaffour et al., 2015). According to the literature, it is estimated that 8.78 million tons of oil per year is required to produce one million m³/day of fresh water by desalination, which indicates that there is an important need to find an alternative energy source for the desalination systems (Kalogirou, 2005). According to the report by the Institution of Mechanical Engineers (*IMechE*), there are an estimated 1.3 trillion barrels of proven oil reserve left in the world's major fields (www.imeche.org, 2015). Considering such a huge rate of oil consumption, the present oil reserves will be sufficient to last for 40 years only. Table 1.2 illustrates the major oil reserves in the Middle East. It is estimated that two-thirds of the world's remaining reserves are in the Middle East.

Country	Billions of barrels
Saudi Arabia	261.8
Iraq	112.5
United Arab Emirates	97.8
Kuwait	96.5
Iran	89.7

Table 1.2 Major oil reserves in the Middle East, (www.imeche.org, 2015)

By 2040, the production levels may decrease down to 15 million barrels per day – around 20% of what is currently consumed. It is likely that by then that the world's population will be

twice as large as it is now. Therefore, the demand for potable water will be increased significantly in the future. It can be concluded that there is a real need to find an alternative source of energy for the increasing demand of potable water. Theoretically, any kind of energy can be considered as a heating source in potable water production. However, not many energy sources are available to replace the existing energy sources.

In the last decades, researchers have focused on solar energy as a suitable alternative energy source that has many benefits in terms of availability and cleanliness (Kannan et al., 2014 and Omara et al., 2013). The process of producing potable water by using solar energy is called solar desalination. The history and installation of solar desalination technology dates back to 2000 years ago (Velmurugan and Sritha, 2011 and Samee et al., 2007). Solar desalination was used to produce potable water from brackish water as well as salt. A number of advantages and disadvantages were reported in the literature for solar desalination. The main benefits of using solar energy are as follows (www.technologystudent.com, 2015):

1. Solar energy is free,
2. Solar energy does not cause pollution,
3. Solar energy can be used in remote areas,
4. Solar energy is not as limited as oil reserves.

There are also several disadvantages for solar energy, namely:

1. Solar energy is available on sunny days only,
2. Solar energy is available at day time,
3. Solar energy is not practically available in some countries,
4. Solar energy requires a large area of land to capture sunlight.

Having considered both advantages and disadvantages of solar energy, many researchers have concluded that solar stills are suitable devices to produce potable water especially in remote areas (Zerrouki et al., 2014; Malaeb et al., 2014; Sathyamurthy et al., 2014).

1.3 Research Objectives

As mentioned above, the future limitations in water resources have urged researchers to enhance the performance of the existing treatment units. However, the existing desalination technologies are energy intensive processes where the production of 1000 m³ of potable water per day requires about 27.4 ton of fossil fuel per day (Methnani, 2007). These technologies

require the availability of energy sources (external steam or electricity). In fact, in rural and remote areas, conventional energy sources (external steam or electricity) are not available. Thus, there is the need for an alternative energy source for deriving small-scale desalination systems suggested for these rural and remote areas. Due to the abundant availability of solar energy, solar desalination systems are one of the options suggested for these areas. Accordingly, the objective of the present study is to investigate the effect of different parameters on the thermal performance of a double-slope solar still for water production in rural or remote areas. The objectives of the present study are summarized as follows:

1. to study the effect of the type of energy storing material on the thermal performance of solar stills. Three materials will be tested namely steel, gravel and phase change material (PCM).
2. to study the effect of the geometrical shape of steel pieces, which are used as a sensible heat energy storing material.
3. to study the effect of gravel size on the thermal performance of the solar still.
4. to compare the experimental results with a theoretical model.

1.4 Organization of the Thesis

The thesis is organised as follows. Chapter 2 reviews the previous studies on solar stills. Chapter 3 describes the experimental system. Chapter 4 presents the results and discussions. Chapter 5 presents the modelling and comparison with the experimental data. Chapter 6 gives the conclusions and suggestions for future work.

2. Chapter Two: Literature Review

2.1 Introduction

As mentioned in chapter 1, conventional desalination systems consume large amounts of fossil fuel. Thus, there is a need for either reducing the energy consumption in these conventional systems or using an alternative renewable energy sources. Solar stills are one option that uses solar energy for water desalination. According to the published literature, the number of published journal papers on solar stills during the last ten years has increased significantly; see Figure 2.1. Thus, research on solar stills is growing considerably. Based on the source of energy used to evaporate the saline water, solar stills can be classified into passive and active solar stills. In passive solar stills, water evaporation occurs naturally using direct solar radiation and no external energy source is supplied to the basin. The basin is fed with water every morning and there is no feed water circulation.

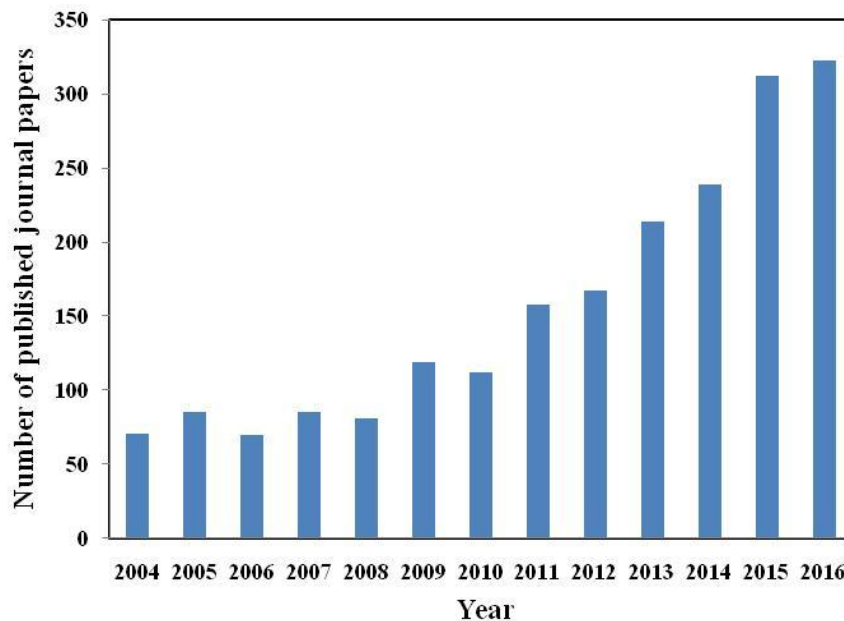


Figure 2.1 Number of research papers on solar stills published by sciencedirect.com during the period from 2004 to 2016

In active solar stills, water evaporation is assisted by an external energy source such as solar collectors or solar panel or any waste heat, which is used to increase the water temperature and thus increase the evaporation rate. The feed water is circulated at very low flow rates using a circulation pump. Figure 2.2 illustrates an example on active solar stills assisted with a solar

collector (Figure 2.2a) or a solar panel that converts solar energy into electrical energy, which is used to heat the water using an electric heater (Figure 2.2b).

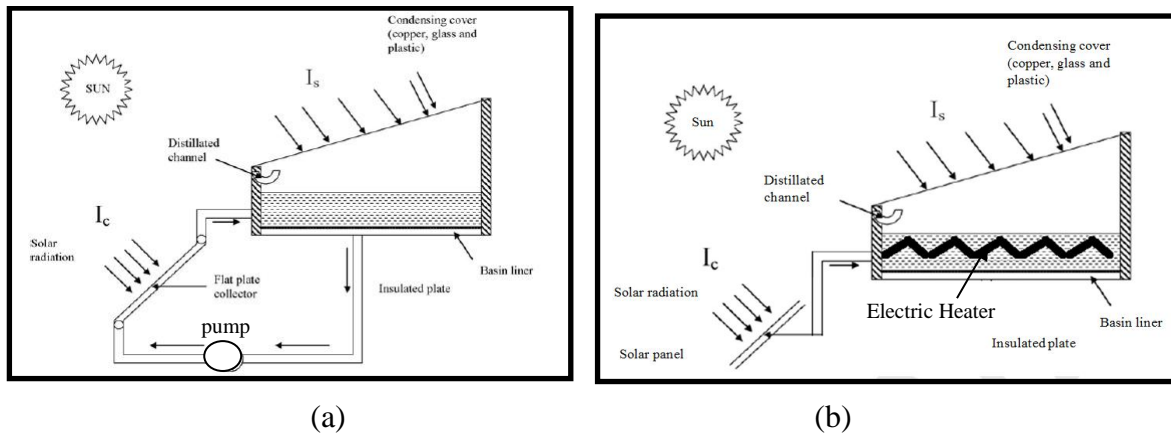


Figure 2.2 (a) Single slope active solar still that converts solar energy to thermal energy and heats up water in the basin. (b) Single slope active solar still that uses solar panel to convert solar energy to electric energy (Tiwari et al., 2003a).

The performance of solar stills is usually evaluated using thermal efficiency defined by Eq. (2.1) below (Xiao et. al, 2013):

$$\eta = \frac{\sum m \cdot \gamma}{3.6 \times \sum A_a \cdot G} \quad (2)$$

where m is the hourly distilled water production rate (kg/h), γ is the specific latent heat of vaporization (kJ/kg), A_a is the total area of an absorber (m^2) and G is the solar radiation intensity over the area of A_a (W/m^2). Note that, the value of m varies along the day depending on the time, i.e. morning, afternoon, etc.

This chapter presents a review of the factors affecting the thermal performance of solar stills. In section, 2.2, the effect of using energy storage materials is presented. Section 2.3 presents the effect of initial water depth on the daily productivity of solar stills. Section 2.4 presents the effect of transparent cover material while section 2.5 presents the effect of the tilt angle. Finally, section 2.6 gives a summary to the chapter.

2.2 Effect of Energy Storing Materials

Solar still is not so much attractive in the market due to its low productivity, so researchers have tried to improve the distillate output of solar stills. The productivity of solar still can be enhanced by increasing the brine temperature in the basin (Xiao et al., 2013) and Voropoulos et al., 2003). It was also found that the temperature of the brine depends on water free surface temperature (Sivakumar and Sundaram, 2013). The use of energy storing materials can affect the brine temperature and thus can make enhancements in the productivity of solar stills (El-Sebaili et al., 2009). Energy storing materials store the excess energy during the sunshine hours and release it during sunless hours in order to increase distillate production. These materials can be divided into sensible heat materials (energy stored without phase change) and latent heat materials (energy stored with phase change). Some of the most effective energy storing materials is reviewed in this section.

2.2.1 Sensible Heat Energy Storing Materials

Akash et al. (1998) studied the effect of using different absorbing materials on enhancing the productivity of a double slope solar still. They tested three types of absorbing materials, namely; black absorbing rubber mat, black ink in water solution and black dye in water solution. The results demonstrated that the productivity has increased by 60% with black dye, 45% with black ink and 38% with black rubber mat. El-Sebaili et al. (2000) investigated the effect of using baffle suspended absorber plates on the performance of a single basin single slope solar still; see Figure 2.3. The still basin was made of a galvanized iron sheet with an area of 1 m^2 . A movable suspended absorber plate made of aluminium was provided inside the basin water. Two plates were tested: a solid plate and a perforated plate, i.e. a plate with some vents. The suspended absorber plate can be moved up and down and thus the mass ratio of the water above and below the plate can be varied, i.e. the water height above and below the plate can vary. The results demonstrated that the modified still with baffle plates operates at higher water temperature compared to the conventional solar still. Thus, the daily productivity has increased from 4.736 kg/m^2 to 5.737 kg/m^2 (increased by 21.1%). Additionally, they reported that when the plate is perforated, the optimum position of the baffle plate should be in the middle of the basin while the mass of water above the plate should be as low as possible in case of solid plate. The reason for the improvement in productivity is mainly because of the increase in water free surface temperature induced by the absorber plate. In fact, this plate divides the water in the basin to upper and lower portions. The level of water column in upper portion plays a main

role in productivity enhancement. It was found out that the highest productivity can be achieved for the lowest water column in upper portion.

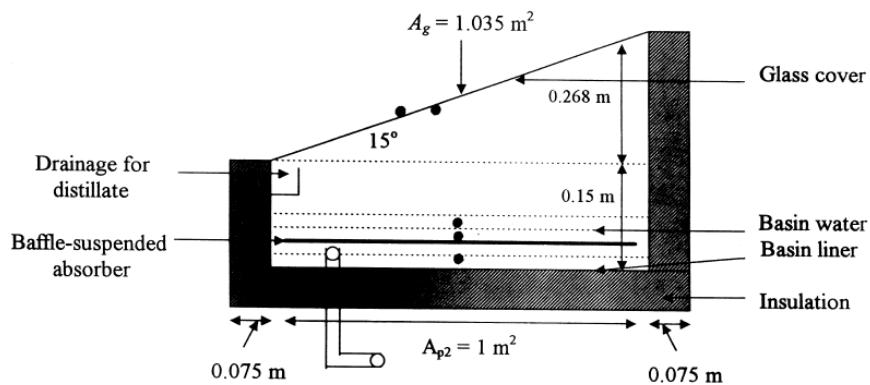


Figure 2.3 Schematic diagram of the single slope solar still with suspended baffle plate (El-Sebaai et al., 2000)

Nafey et al. (2001) used black rubber and black gravel materials as energy storage materials in order to enhance the productivity of a single slope solar still. They tested the effect of rubber thickness (2 mm, 6 mm, 10 mm) and gravel size (7 - 12 mm, 12 - 20 mm, 20 - 30 mm). They concluded that the maximum enhancements occurred using black rubber with 10 mm thickness (20% enhancement) and using gravel which measure 20 – 30 mm (19% enhancement). Naim et al. (2002) studied the improvement of productivity of solar still using charcoal particles to work as an energy absorbing material. They designed and fabricated a solar still made of Perspex with basin area 0.5 m^2 . A layer of charcoal particles of 20 mm thickness was placed uniformly underneath the basin. The effect of charcoal particle size was investigated (1.5, 5, 7 mm). The results showed that the coarse charcoal particles yielded the best results in terms of productivity. The experimental results showed a 15% improvement in solar still efficiency in comparison with conventional solar stills.

Sakthivel et al. (2010) studied experimentally the effect of using jute cloth as an energy storing material on the performance of conventional solar still. The jute cloth was kept in the middle of the still as well as at the surface of the side wall (see Figure 2.4). Most of the incident solar energy is absorbed by the blackened surface of the basin through the saline water, portion of energy is absorbed by the jute cloth. The jute cloth provides more evaporation surface and as the heat capacity of the jute cloth is low, it can attain high temperatures. This leads to rapid evaporation of water. The still has an effective basin area of 0.5 m^2 . The experimental results

showed that the productivity of the solar still was improved by 12% using Jute cloth and the efficiency increased by 8% compared to the conventional solar still. This improvement is due to the fact that the latent heat released from the glass cover (condensation) is used to evaporate the water absorbed by the capillary action in the Jute cloth. Consequently, the water yield in solar still increased and the temperature of the bottom of the glass cover decreased.

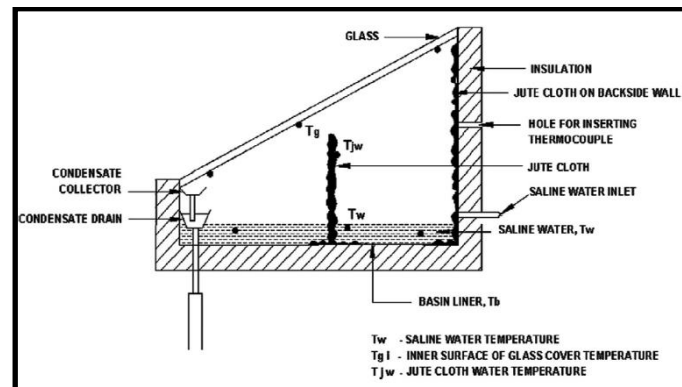


Figure 2.4 Experimental set-up showing Jute cloth as an energy storing material (Sakhivel et al., 2010).

Samuel et al. (2016) conducted an experimental study on improving the performance of a single slope solar still using the following: (1) spherical balls filled with rock salt as sensible heat storage material and (2) different sponge materials for better capillary action that enhances the evaporation process. Their experimental setup is shown in Figure 2.5. The results demonstrated that the daily yield was 3.7 kg/m^2 with spherical ball salt energy storage whereas for the single slope solar still with and without sponges, the value was 2.4 and 2.6 kg/m^2 , respectively. It was found also that sponges need to be replaced every 14 days as rust and salt from saline water gets accumulated on the pores, thus reducing the capillary effect. Additionally, the cost of the produced water using the ball energy storage material was lower compared to that with the sponge material.

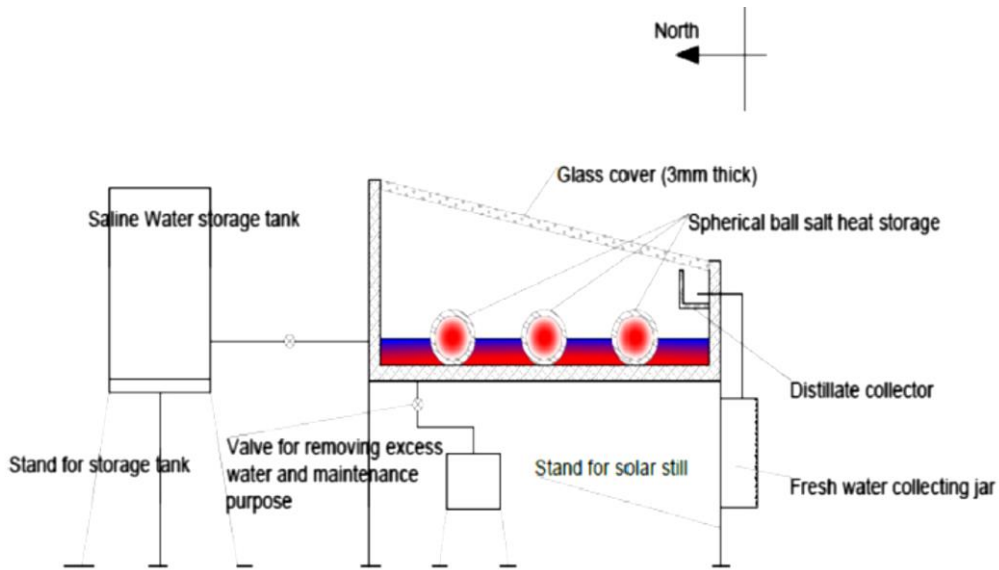


Figure 2.5 Schematic of the experimental setup by Samuel et al. (2016).

Deshmukh and Thombre (2017) studied experimentally the effect of using sensible heat storage materials on the performance of a single slope solar still (0.5 m^2 basin area) as shown in Figure 2.6. Sand and Servotherm medium oil (SM) were used as energy storing materials. Three depths of the energy storage material were tested namely; 0.5 cm (4.1 kg), 1 cm (8.2 kg) and 1.5 cm (12.3 kg). The water depth was kept fixed at 0.6 cm (3 kg) for all cases. The results demonstrated that the overnight productivity for solar stills with energy storage materials increased with increasing the mass of water and energy storing material compared to the base case (without storage material). The daylight productivity decreased with increasing the mass of water and energy storage material. Thus, they concluded that there is an optimum value for the mass of the energy storing material. This optimum value was such that the heat capacity equals 8.

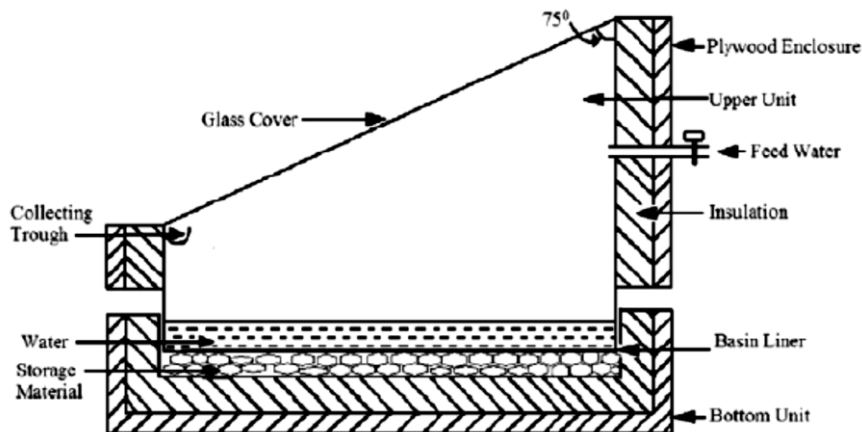


Figure 2.6 Experimental set-up showing sensible heat energy storing material (Deshmukh and Thombre, 2017)

Panchal et al. (2017) investigate the effect of energy storage material on the productivity of a single slope solar still. Marble pieces and sand stones were used as energy storage materials, and the water depth in the basin was kept constant at 4 cm. The results indicated that the productivity of the still with sand stone increased by 16% and the productivity of the still with marble pieces increased by 8%, compared to the still without energy storage materials. El-Sebaili and El-Nagar (2017) investigated the performance of a finned solar still. Black-painted seven fins made of copper were attached to the flat plate basin liner as shown in Figure 2.7. It was found that the daily productivity of the conventional and finned stills were 4.235 kg and 5.065 kg respectively (16.4% improvements). Additionally, the annual productivity of the conventional and finned solar stills were found to be 1467.4 kg and 1898.8 kg. The cost of 1 (L) of distillate water has been calculated as 0.28, 0.21 and 0.20 (LE/L) when copper, glass and mica were used in manufacturing the finned basin liner, respectively. The corresponding cost of 1 (L) of fresh water obtained from the conventional still is found to be 0.31 (LE/L).

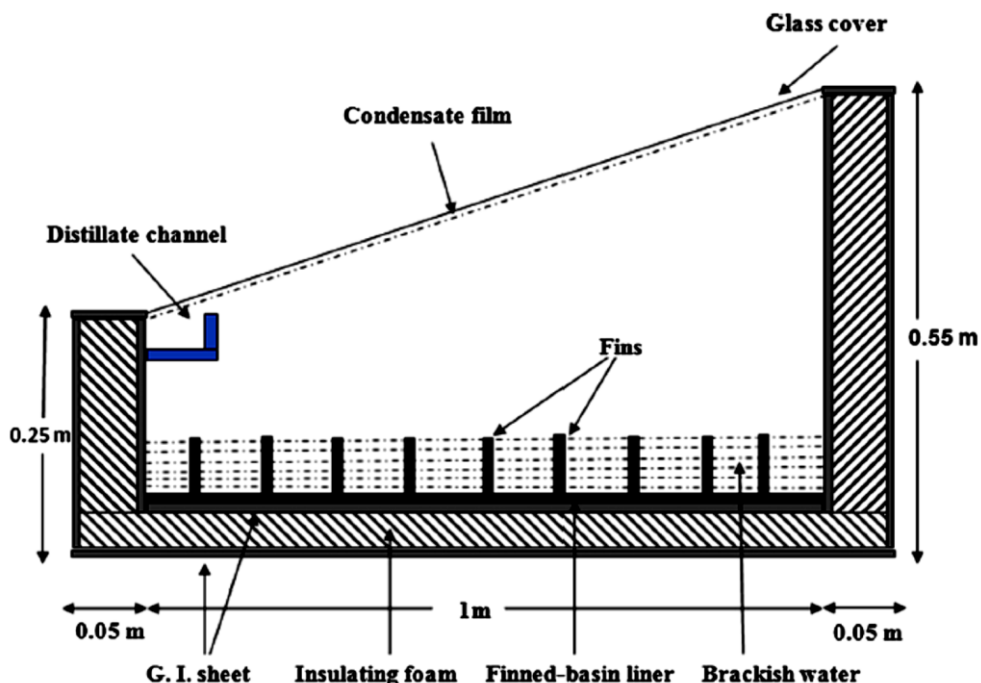


Figure 2.7 Schematic of a finned liner basin still (El-Sebaili and El-Nagar, 2017)

Nithyanandam et al. (2017) investigated the effect of various energy storage materials and the sizes of blue metal stone on the performance of the single-slope solar distillation system. The picture of the metal stone used as energy storing material is shown in Figure 2.8. The results demonstrated that blue metal stone with size 12 mm gave the highest thermal efficiency:

34.9% compared to 29.84% for the solar still without blue metal stones, i.e. about 17% improvement in the thermal efficiency.



Figure 2.8 blue metal stone in various size (6, 12, 20 mm) (Nithyanandam et al., 2017)

2.2.2 Phase Change Energy Storing Materials

Naim et al. (2002b) studied the improvement in the productivity of a solar still using phase change energy storage material (PCM). The material used was a mixture of paraffin wax, paraffin oil and water. It was found that the use of PCM material promoted the heat transfer process and increased the still productivity noticeably by allowing distillation to take place at night time. Shalaby et al. (2016) proposed a new design for a v-corrugated absorber solar still with built-in phase change material (PCM) (see Figure 2.9). This design allowed for the expansion of melting wax through a net of tubes extended inside the storage tank. The system was tested with and without the PCM using different water masses. Adding a wick over the corrugated plate using PCM is also investigated. Paraffin wax is chosen as a PCM due to its medium storage, safety, reliability, uniform melting and moderate cost.

The experimental investigation showed that the solar still with the PCM beneath the corrugated plate with less basin water mass achieves the best thermal performance among other studied configurations. Using the PCM causes a little decrease in the daylight productivity with a considerable increase in the still's overnight productivity. The daily productivity of the still with the PCM was 12% and 11.7% better than those for the v-corrugated still without the PCM and with the PCM using wick, respectively. Cost analysis is also performed where the cost per litre (CPL) for the still without PCM, with PCM and with PCM using a wick are estimated as 0.07182, 0.08369 and 0.09558 \$/L, respectively

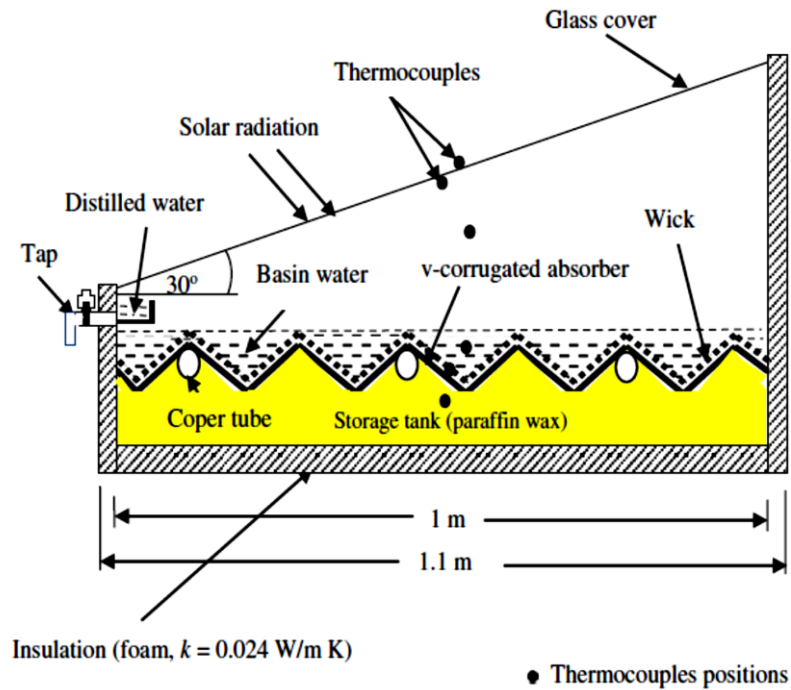


Figure 2.9 Solar still design with v-corrugated absorber integrated with phase change material (Shalaby et al., 2016)

Kabeel and Abdelgaied (2016) investigated the improvement of the performance of a solar still using a phase change material (PCM), which was paraffin wax. Two solar stills were designed, constructed and tested; a solar still with PCM and a conventional solar still. The experimental results indicated that the daily freshwater productivity for solar still with PCM is higher than that of conventional solar still. The daily freshwater productivity approximately reached 7.54 L/m^2 a day for solar still with PCM, while its value is recorded 4.51 L/m^2 day for the conventional solar still. The results show that the daily freshwater productivity for solar still with PCM is 67.18% higher than that of the conventional solar still. Also, the solar still with PCM is superior in daily freshwater productivity (67%–68.8% improvement) compared to a conventional solar still in the period from June to July 2015 under the ambient conditions of Tanta city in Egypt. In this case study, the estimated cost of 1 L of distillate water reached approximately 0.24 LE/L (0.03\$/L) and 0.252 LE/L (0.032\$/L) for solar still with PCM and conventional solar still, respectively

Elfasakhany (2016) studied the effect of paraffin wax mixed with copper nano-particles as energy storage material on the performance of a single slope solar still. They have tested three cases. In case 1 a simple solar still without modification (base case) was tested. Case 2 had a solar still with paraffin wax as an energy storage material. In case 3, paraffin wax was

combined with copper nano-particles as energy storage materials. It was found that the paraffin wax with copper nano-particles showed better energy storage performance compared to the paraffin wax only. The total daily productivity has increased by 125% and 106% compared to case 1 and case 2, respectively.

Sharsher et al. (2017) investigated experimentally the effect of graphite nanoparticles, phase change material and film cooling on the performance of a single slope solar still. They tested the following four modifications: modification A: flake graphite nano-particle (FGN) mixed with water, modification B: flake graphite nano-particle (FGN) mixed with water and encapsulated phase change material (paraffin wax), modification C: flake graphite nano-particle (FGN) mixed with water and using film cooling on the glass cover (using water flowing at low flow rate), modification D: flake graphite nano-particle (FGN) mixed with water and encapsulated phase change material (paraffin wax) combined with film cooling on the glass cover. Compared to the non-modified solar still, the results indicated that the productivity has improved by 50.3% for modification (A), 65% for modification (B), 56.2% for modification (C) and 73.8% for modification (D).

2.3 Effect of Basin Water Depth

The effect of brine depth on the productivity of a solar still has been studied widely in the published literature by Srivastava and Agrawal (2013), Sathyamurthy et al. (2014), Rajaseenivasan and Murugavel (2013a), Manokar et al. (2014) and Mamouri et al. (2014). They agreed that as the water depth in the basin decreases, the productivity of the solar still increases. In contrast, Taghvaeia et al. (2014) reported that the productivity of solar still improves by increasing the water depth in the basin. They studied experimentally the effect of water depth on the productivity of solar still. Khalifa and Hamood (2009) collected data from literature on the effect of water depth on the productivity of solar still and used the least square method to fit the data in the form given by Eq. (2.2) below.

$$y = 3.884e^{-0.0458d} \quad (2.2)$$

where y is the still daily productivity in l/m^2 and d is the basin water depth in cm . According to this Equation, the solar still production is increased by reducing basin water depth. Also Equation (2.2) indicates that the effect of water depth is insignificant for depths $d > 40$ cm . Kandasamy et al. (2013) proposed correlations for the daily production y as a function of the

water depth d and are expressed by Eq. (2.3) for single slope and Eq. (2.4) for double slope solar stills, respectively.

$$y = 2.833d^{-0.2}, R^2 0.829 \quad (2.3)$$

$$y = 5.885d^{-0.292}, R^2 0.869 \quad (2.4)$$

Ahsan et al. (2014) have investigated experimentally the effect of water depth on the daily water productivity and proposed the following correlation defined by Eq. (2.5). **Error! Reference source not found.** 2.10 compares the daily water production predicted using Eqs. (2.2) to (2.5). The figure indicates that there is agreement on the effect of water depth, where the daily water productivity increases as the water depth decreases. Also, the figure shows that some correlations predict small effect (Kandasamy et al. and Ahsan et al.), while some other correlations (Sivakumar et al.) predict a strong effect.

$$y = 3.84 - 0.47d \quad (2.5)$$

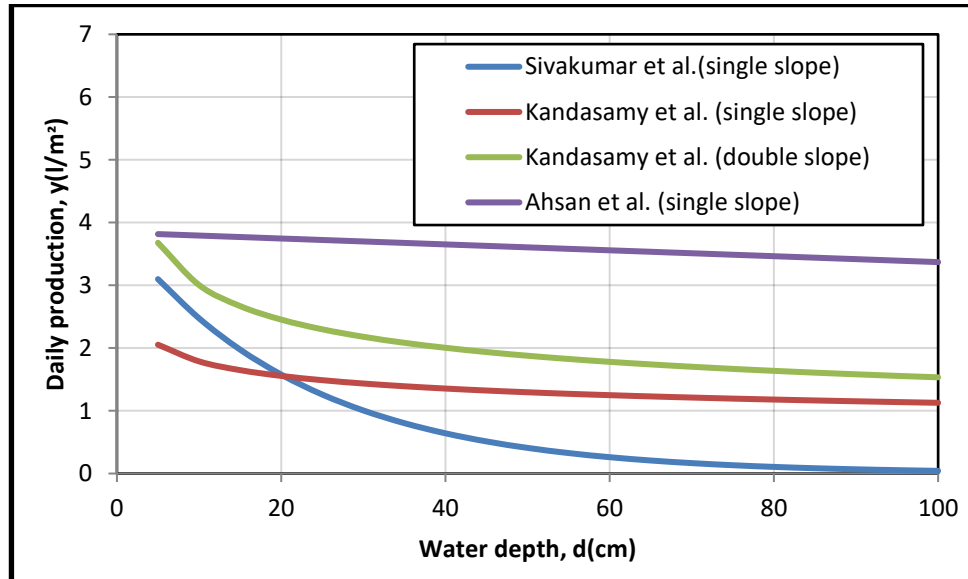


Figure 2.10 Variation of daily production y against the water depth

2.4 Effect of Solar Still Cover

Different materials could be used for the solar still cover. Plastic transparent nylon sheets are widely used in solar stills. Nylon sheets are cheaper in comparison to metal and glass sheets.

In Tiwari et al. (2009), the performance of solar still was studied by using glass, copper and PVC sheets as still cover material. Figure 2.11 shows the daily yield for a solar still using the three different cover materials (Glass, PVC and Copper).

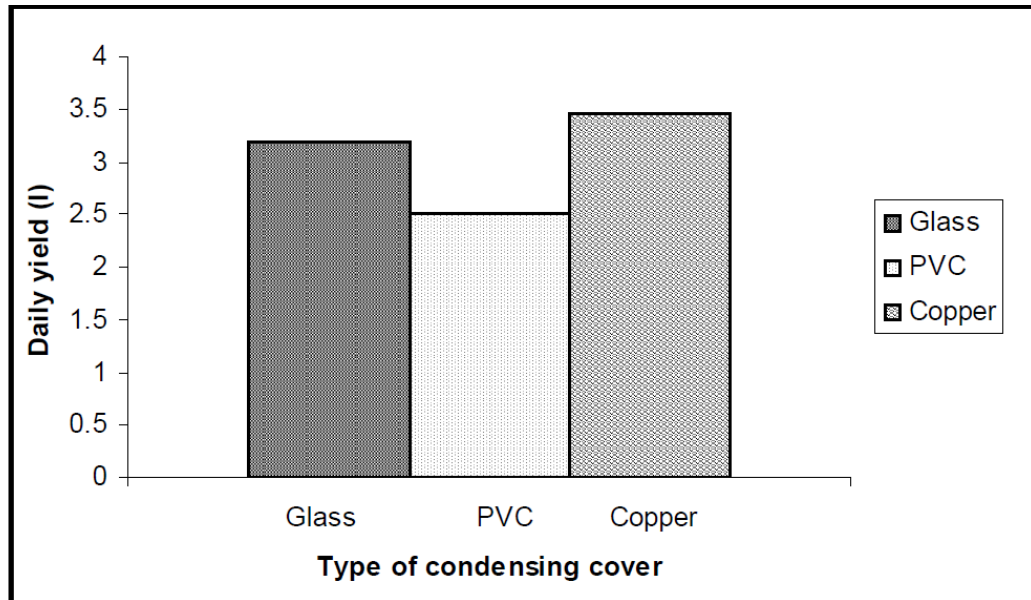


Figure 2.11 Solar still daily yield (l) by using three different materials (Glass, PVC and Copper) for cover (Tiwari et al., 2009)

They have found that the performance of the solar still with a cover plate made of copper was better than that made of glass and PVC, with PVC giving the lowest performance. The high performance of copper was attributed to the high thermal conductivity of copper, which results in higher overall top loss heat transfer coefficient.

Martin and Goswami (2005) studied the performance of a solar still with cover plate made of copper, aluminium and steel. They found that the performance of the still with copper and aluminium cover plates is much better than that of steel and it was attributed to the thermal conductivity. Copper and aluminium have higher thermal conductivity in comparison with steel ($k=200\text{Wm}^{-1}\text{K}^{-1}$ for aluminium, $k=390\text{Wm}^{-1}\text{K}^{-1}$ for copper and $k=48\text{Wm}^{-1}\text{K}^{-1}$ for steel). In terms of cost of materials, copper and aluminium are more expensive than steel; more than two times the cost of galvanized steel (Manokar et al. 2014).

Apart from the cover material, the cover thickness is another parameter that can affect the solar still productivity. Tiwari et al. (2009) studied the effect of glass cover thickness on solar still daily yield for active and passive stills. They found that the daily yield is linearly related to the thickness of the glass cover. Figure 2.12 shows the variation of daily yield against the

glass cover thickness in the range of 2mm to 6 mm. They concluded that the highest daily yield was achieved for 2 mm glass cover thickness.

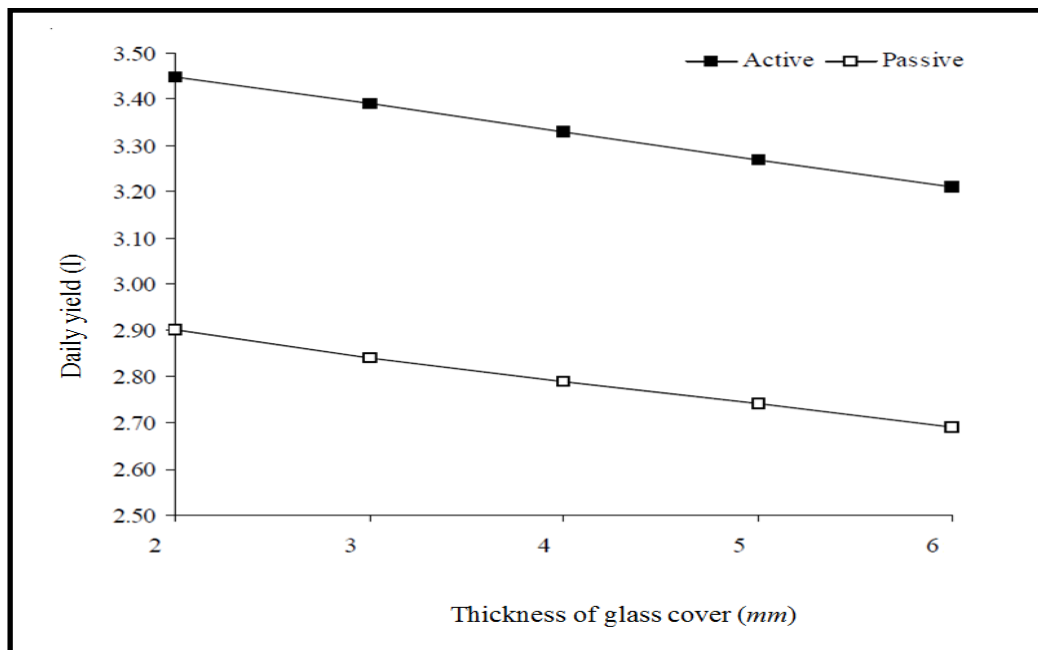


Figure 2.12 Variation of daily yield against thickness of glass cover for active still and passive still, (Tiwari et al., 2009)

2.5 Effect of Solar Still Cover Tilt Angle

The solar still cover tilt angle is another important factor which can affect the still productivity as reported by Kamal (1988) and Aybar and Assefi (2009). It was revealed that there is an optimum value for the tilt angle to achieve the best performance of solar stills. This optimum value mainly depends on various parameters such as season, latitudes as and design parameters. A wide range of optimum values was reported for tilt angles in experimental and theoretical studies. The most reported tilt angle was 10° (Tiwari et al., 2003 and Velmurugan and Srithar, 2007), and the second most reported tilt angle was 30° (Tiwari et al., 2003 and Mathioulakis and Belessiotis, 2003). A low angle of 4° was reported in Porta et al. (1997) and E1-Bahi and Inan (1999), and high angle value of 85° in Aybar and Assefi (2009). Other tilt angles include 20° by Fatani et al (1994), Ghoneyem and Lleri (1997) and between 11° to 13.5° by Kamal (1988), Farid and Hamad (1993) and Namprakai and Hirunlabh (2007). In some studies, the tilt angle was equal to the test site latitude angle.

Khalifa and Ibrahim (2010) studied the effect of solar still tilt angle and reflector on the still productivity experimentally and presented a list of tilt angles in a table. The investigation was carried out in winter and location latitude angle of 33.3° N. The experimental set-up for their tests is shown in **Error! Reference source not found.2.13**.

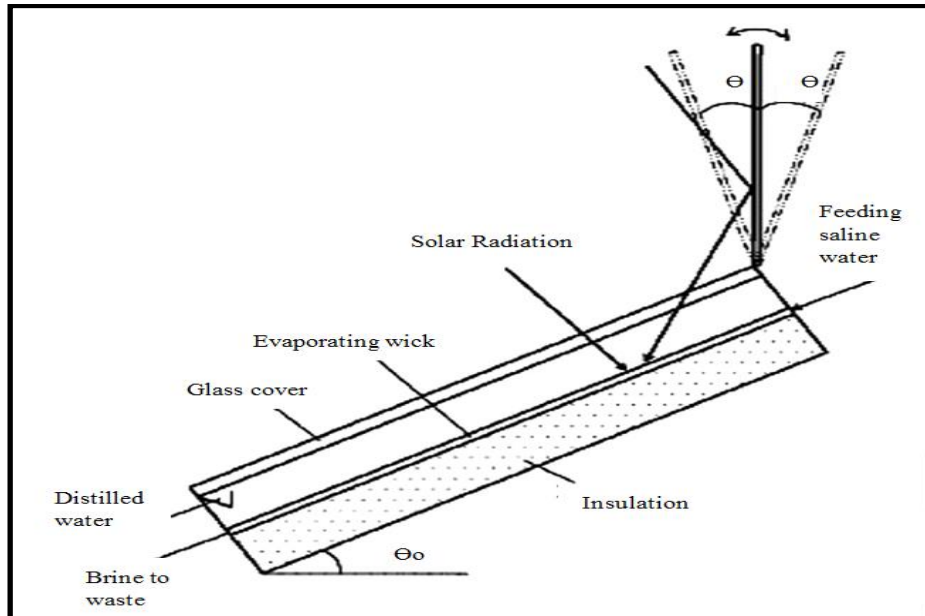


Figure 2.13 The schematic diagram of experimental set-up (Khalifa and Ibrahim, 2010)

They have found that the daily yield remained almost the same for all tilt angles (0°, 10°, 20° and 30°). Consequently, no significant effect of tilt angle on the daily yield was observed. In terms of productivity, the best performance of the solar still in winter weather condition was achieved at 20° cover tilt angle for solar still with reflectors. The daily yield for solar still with reflector was recorded 2.45 times that of solar still with no reflectors. It was also concluded that cover tilt angle rises by increasing the test site latitude angle. The effect of tilt angle on productivity was studied in Sivakumar and Sundaram (2013), and the relation between productivity and tilt angle was presented by Eq. (2.6).

$$y = -0.0025a^2 + 0.1562a + 0.843 \quad (2.6)$$

where y is the relative daily productivity (l/m^2) and a is the cover tilt angle (*degree*). According to this Equation there is only one optimum value for cover tilt angle and this value can be calculated by differentiating Eq. (2.6) with respect to a .

$$\frac{dy}{da} = -0.005a^2 + 0.1562 \quad (2.7)$$

By equating Eq. (2.7) to zero, the value of cover tilt angle which corresponds to maximum value of productivity was calculated $a \approx 31^\circ$.

Otaibi and Al Jandal (2011) discussed the relation between solar still cover tilt angles and the time of the year. They found that the optimum value of tilt angle depends on the time of the year in Kuwait. Figure 2.14 shows the variation of the best tilt angle that corresponds to absorbing the highest solar radiation and daily water productivity in each month.

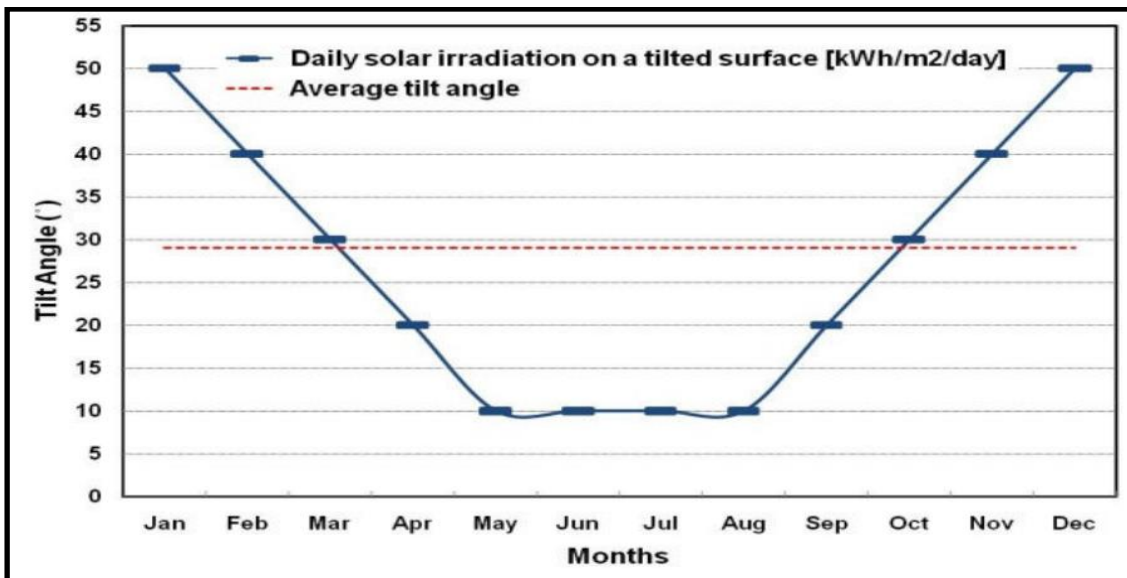


Figure 2.14 Variation of solar still cover tilt angle in each month during a year (Al Otaibi and Al Jandal, 2011)

According to Figure 2.14, the optimum tilt angle during winter is much greater than that in summer time. It is mainly because of variation of sun light angle in summer and winter.

2.6 Summary

The different parameters affecting the performance of solar stills are reviewed and discussed in this chapter. These parameters included energy storing materials, water depth in the basin, still cover plate material and tilt angle. The review indicated that a great deal of research is still needed to increase the productivity of solar stills and thus transfer the process from the laboratory scale into commercial applications. The focus of the present study is on

weather conditions in Kuwait, which have not been considered extensively by researchers. Figures 2.15 to 2.22 indicate the variation of sun hours, average maximum and minimum temperature in every month, water temperature, precipitation, number of rainy days, relative humidity and wind speed during a year, respectively (weather and climate.com, 2015).

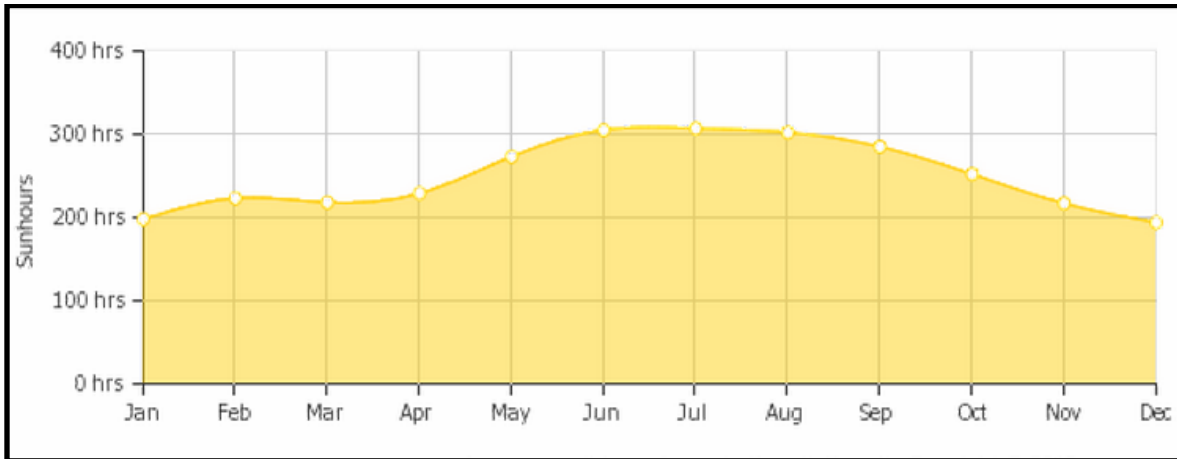


Figure 2.15 Sun hours in every month of a year

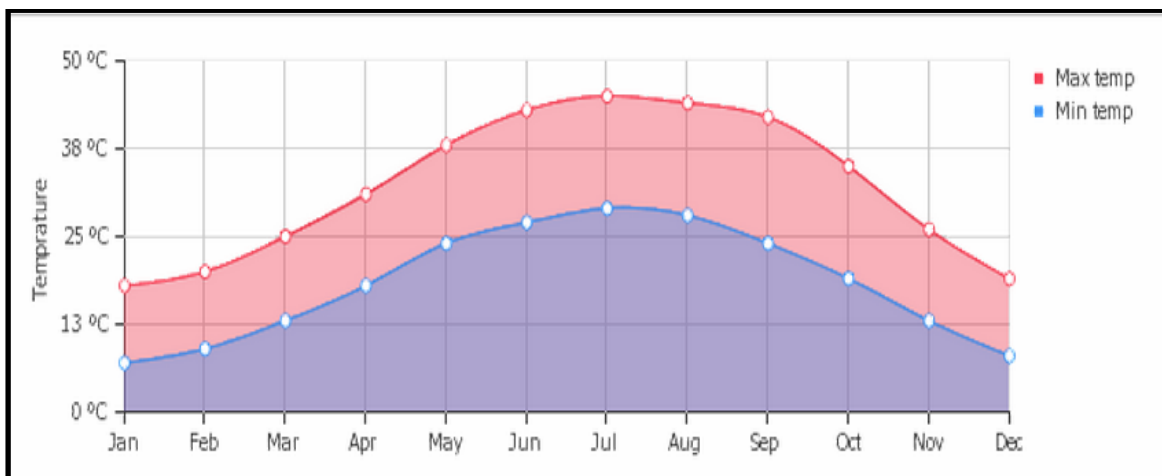


Figure 2.16 Variation of average maximum and minimum temperature (oC) in a year

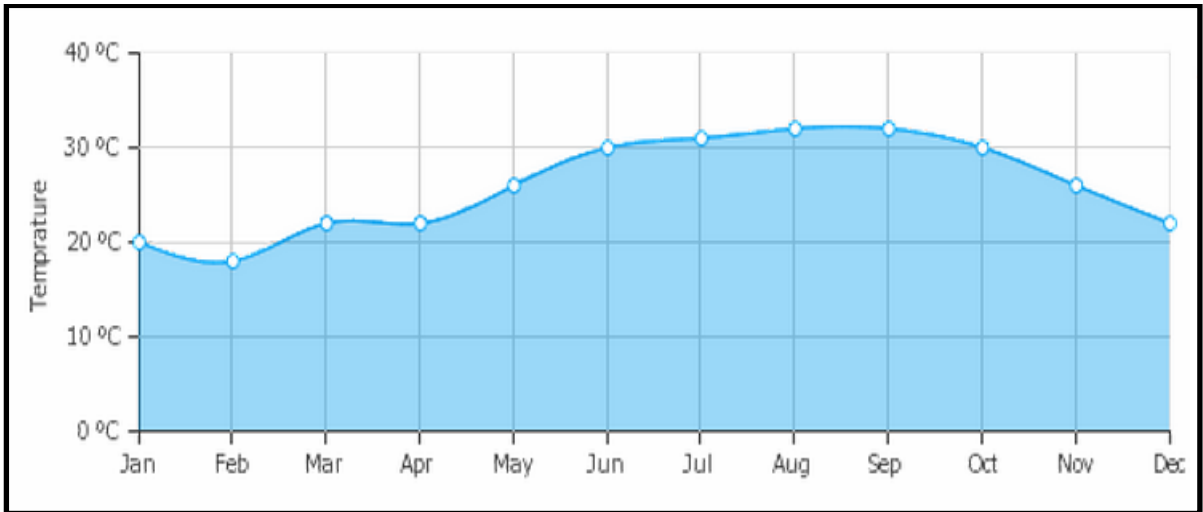


Figure 2.17 Variation of sea water average temperature in a year

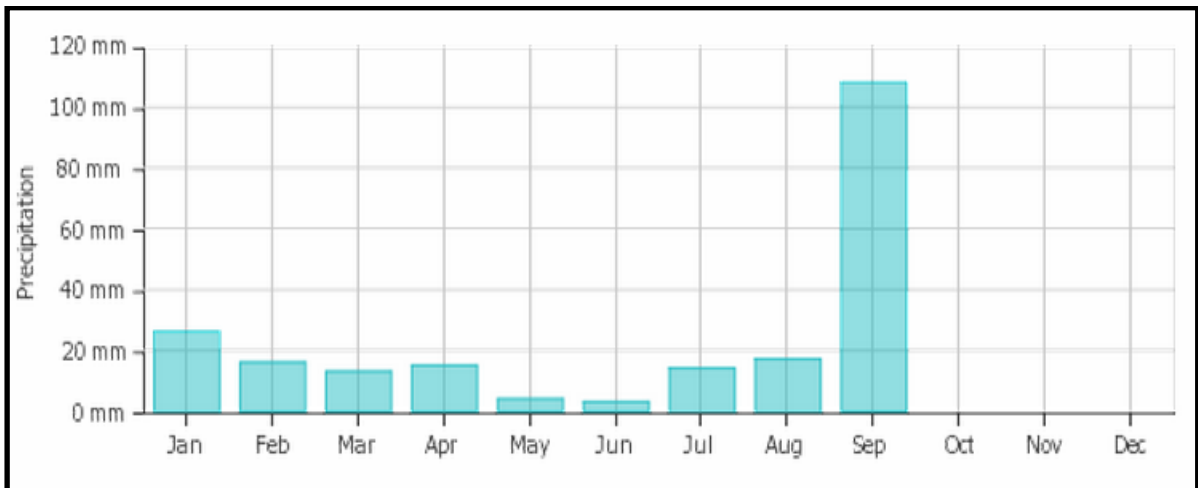


Figure 2.18 Variation of average precipitation (mm) in a year

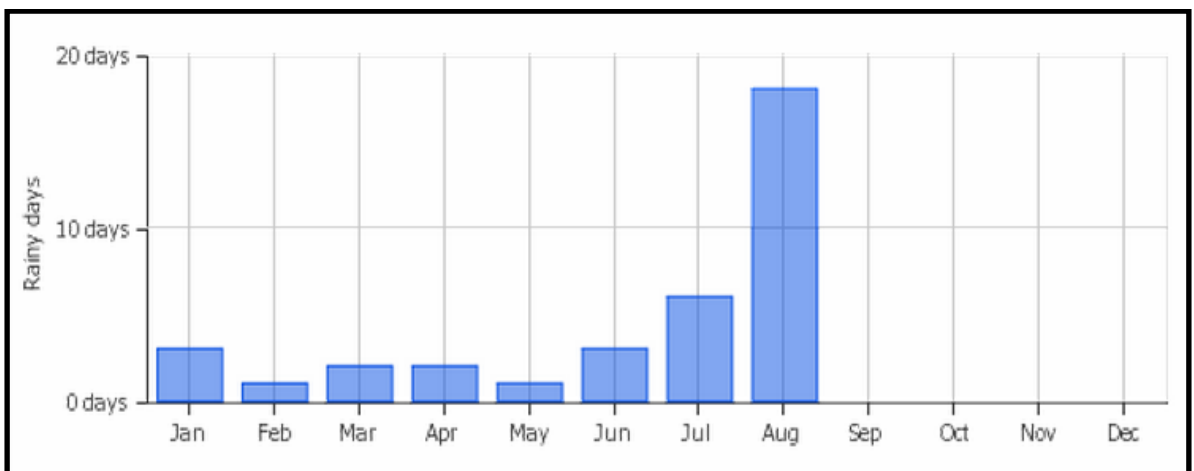


Figure 2.19 Number of rainy days in every month of a year

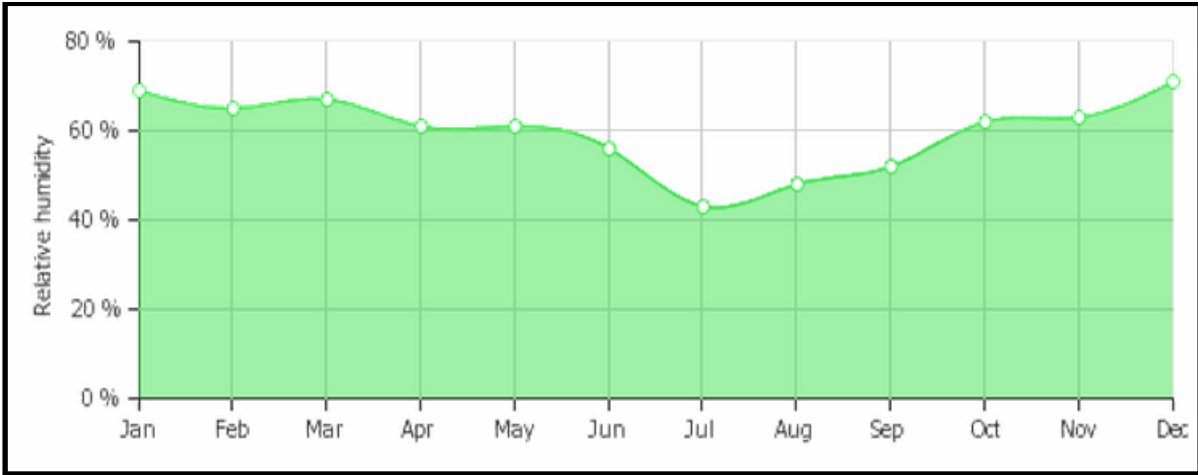


Figure 2.20 Variation of average humidity in a month (%) of a year

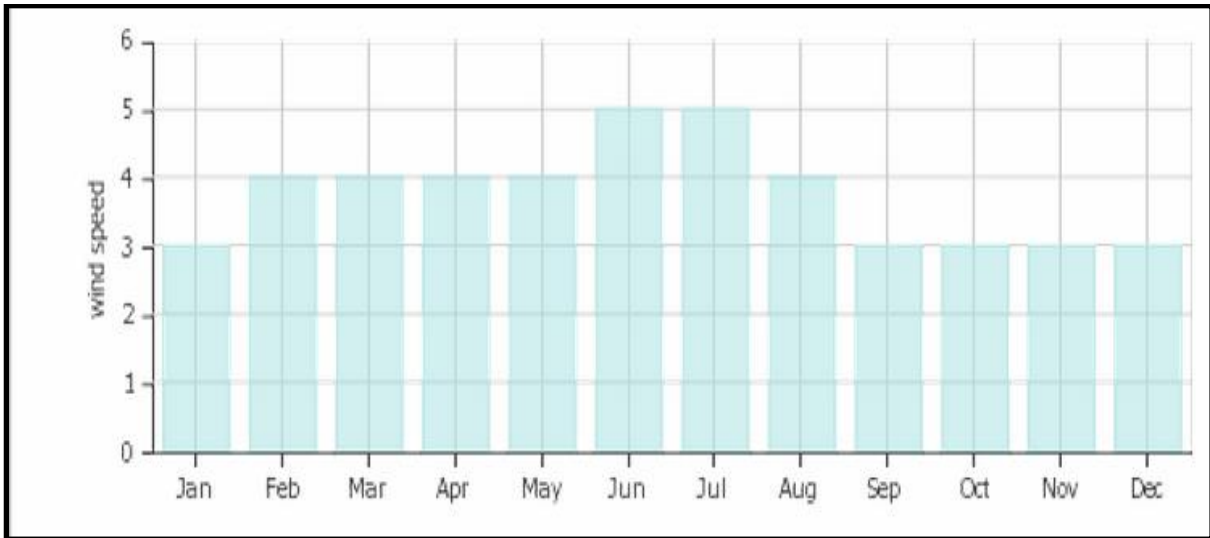


Figure 2.21 variation of average monthly wind speed (m/s) during a year

The abundant sunny days in Kuwait constitute one of the main reasons why Kuwait has recently built a 5 MW solar power plant. The main parameters that affect solar still productivity are studied experimentally and analytically in the present study. The data were collected in Kuwait for some time and a wide range of time slots were considered to capture any variation in the measurement.

3. Chapter Three: Experimental Set-Up

3.1 Introduction

Based on the literature reviewed in chapter 2, there is a need to improve the thermal performance of passive solar stills. Thus, the present study focuses on investigating experimentally the effect of different parameters on the performance of a double slope passive solar still. This chapter presents the description of the experimental and measurements system used in the present study. Additionally, the experimental plan and methodology are also presented.

3.2 Experimental System

The experimental set-up is installed at a personal workshop in Al Ahmadi, Kuwait (latitude of 29.3667° N and longitude of 47.9667° E). Al Ahmadi is a city which has more than 250 sunny days in a year, and the daily solar insolation can reach more than 7 kWh/m^2 (Al Otaibi and Al Jandal, 2011). Hence, this city is one of the best locations that could be chosen for solar energy experiments.

The experimental set-up consists of two parts; a) the double slop solar still cover and b) the basin. Figure 3.1 shows the schematic drawing of the single basin double slope solar still and Figure 3.2 shows a photograph for the investigated solar still. According to section 2.4, different materials could be used for the solar still cover. Plastic nylon sheet, glass, copper, aluminium and steel have been used in literature. Plastic transparent nylon sheets are widely used in solar stills because of their low cost and availability even though their performance is not as good as that of glass. In terms of the cost and performance of materials, it was decided to use glass for cover instead of metals (copper, aluminium and steel) and transparent nylon sheet. The basin was fabricated by using a galvanized steel sheet of 2 mm thickness. The thickness of the steel sheet was selected so that the still can be durable and light. The basin was 1m long, 0.5 m wide and 0.5 m deep.

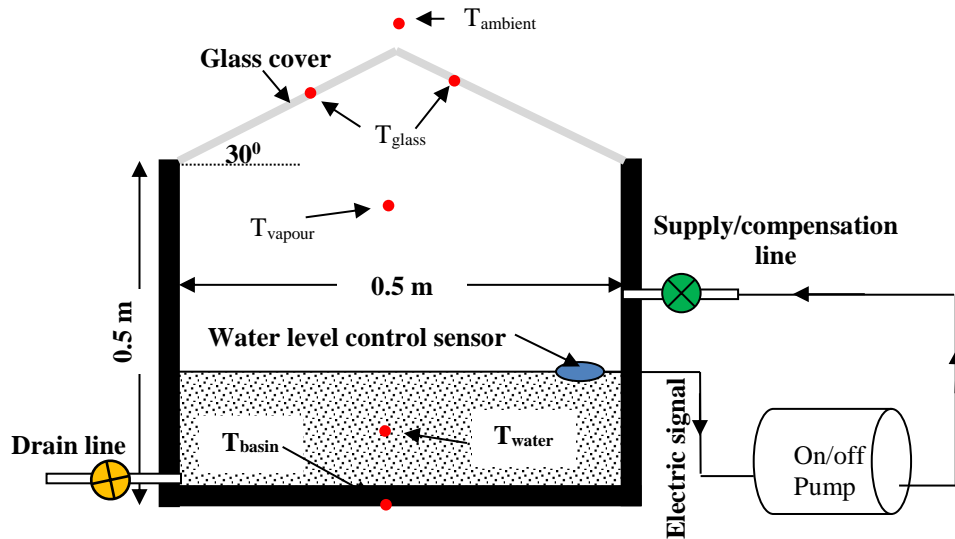


Figure 3.1 Schematic drawing for the experimental set-up with the locations of temperature measurements



Figure 3.2 Photograph showing the tested double slope passive solar still

The basin was painted black to improve the absorbability of solar energy. The supply pipe was connected to the basin from the side wall, while a drain line was considered at the other side wall of the basin. To control the water level inside the basin, a level sensor was inserted. When the water level in the basin decreases below the required value, the level sensor sends an

electric signal to the water supply pump to make it run and compensate the evaporated amount of water in the basin. K-type thermocouples were used to measure the basin temperature, the water temperature, the vapour temperature, the glass cover temperature and the ambient temperature (see Figure 3.1).

The basin was enclosed by a wooden box of 2 cm wall thickness so that there was a clearance of 2.5 cm between the walls of the basin and the wooden box (see Figure 3.3a and Figure 3.3b). This clearance was filled with *PUF* (poly Urethane foam) insulating material in order to reduce the heat losses to the ambient. The thermal conductivity of the foam material is $0.025 \text{ W/m}^2\text{K}$. The wood sheets were attached to the insulation by an adhesive: flexible anti-mould and waterproof silicone sealant. This kind of attachment results in uniform mechanical and heat transfer properties on all basin area. A temperature selector switch was attached on the side of outer basin to monitor the temperature at different parts of the still. The detailed photographs of the different components of the still are summarized in appendix 3.

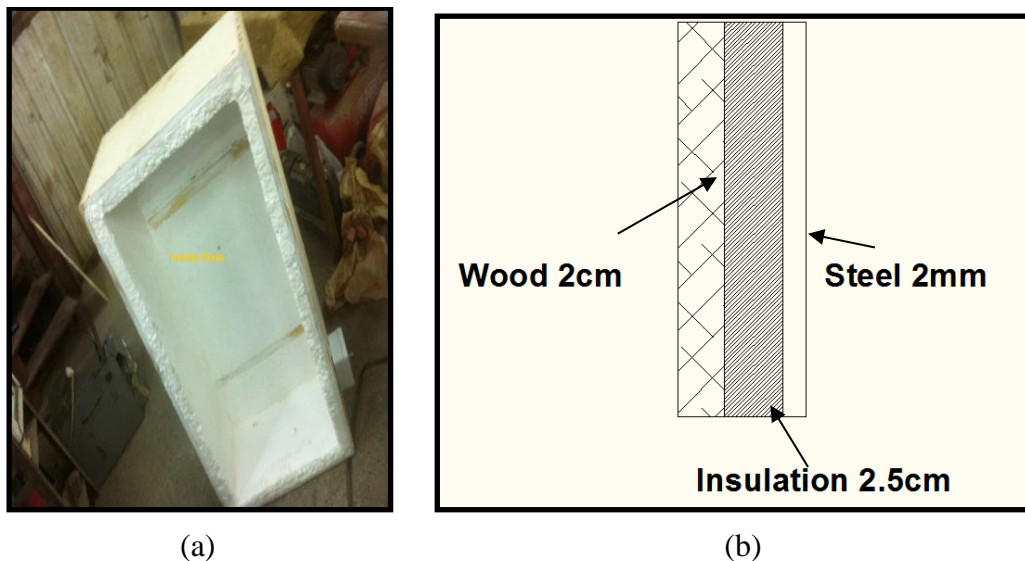


Figure 3.3 (a) Photograph for the 2.5 cm insulation thickness and (b) composite wall cross sectional view

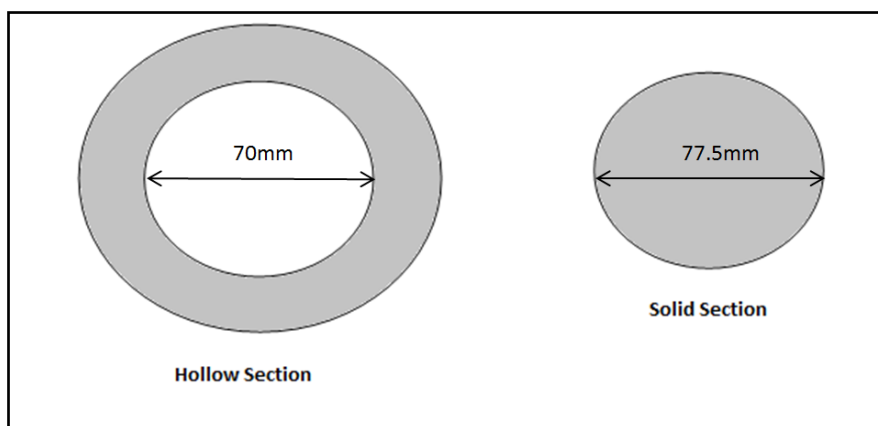
It was discussed in Tiwari et al. (2009) that the daily yield is proportional to the thickness of the glass cover. It was reported that the daily water productivity decreases linearly as the thickness of the glass cover increases. It was also found that the best performance of solar still was achieved with a 2 mm thick glass. Since the 2 mm thick glass is not strong enough, a clear glass sheet with 3 mm thickness was used to construct the double slope solar still cover used

in the present study. The angle of glass sheets with horizontal plane were considered 30° and remained constant for all experiments. The selection of the tilt angle was based on the Kuwait latitude, which is about 30° . The solar still cover was connected to the basin using flexible anti-mould waterproof silicone sealant. This type of sealant is strong and can keep the parts together. The experiments were carried out by placing the solar still in an open area, where the solar radiation could hit the glass cover directly during the experiments.

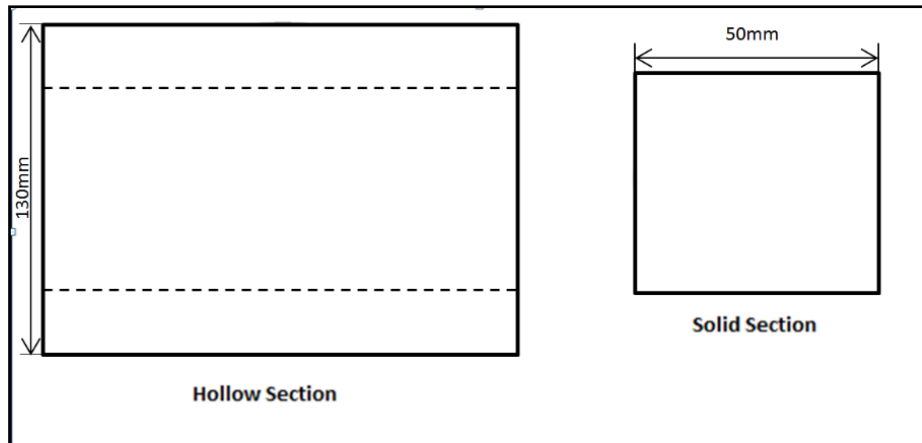
3.3 Experimental Plan and Methodology

In the present study, two approaches were used to enhance the performance of solar stills; namely, the use of energy storing materials and cooling the glass cover plate. The effect of energy storing materials and glass cover temperature on the productivity of passive double slope solar still were studied experimentally. The experiments were conducted first in a solar still without any modifications, which was considered as a base case for comparison. The following modifications were investigated:

1. Steel metal was used as the energy storing material. Three different shapes were tested. The first shape was solid cylindrical rods cut in small pieces with each piece having diameter 77.5 mm and length 50 mm. The second shape was hollow cylindrical rods cut in small pieces with each piece having an inner diameter of 70 mm, 130 mm outer diameter and 25 mm in length. The third shape has square cross-sectional area of 150 mm \times 150 mm and 12 mm length. These dimensions were selected so that the mass is kept fixed at about 2 kg. Figure 3.4 shows the dimensions of the solid and hollow steel rods.



(a)



(b)



(c)

Figure 3.4 The solid and hollow steel rods, a) top view, b) side view and c) the image of solid and hollow steel rods

2. The second modification includes the use of gravel of different sizes as energy storing materials. Two sizes of gravel were used: 6.3 mm and 12.7 mm.
3. The third modification includes the use of copper tubes of 25.4 mm diameter and 120 mm length filled with paraffin wax as energy storing material. The copper tubes were closed at both ends.
4. The fourth modification includes cooling the glass cover using water flow to enhance the condensation and thus the productivity of the solar still. Figure 3.5 shows the layout of the water cooler on the solar still schematically.

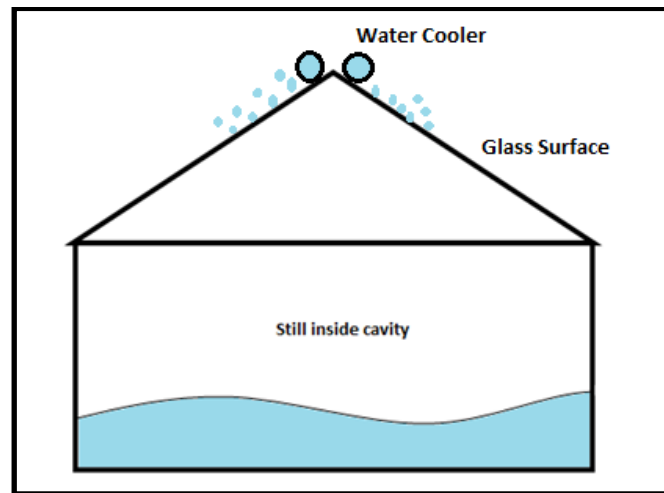


Figure 3.5 The layout of the water cooler

In terms of accuracy of measurements, the experiments were carried out in three consecutive days in order to minimize the effects of variation in weather conditions. The measurements were carried out three times, and the average values were used in the calculations. During the three consecutive days, the solar still's location in the test site remained constant and it was covered during the night to protect the glass surfaces from dust. The solar still was cleaned at start of each day to make sure that the condition of the solar still was identical during the measurement period. Therefore, it can be assumed that the design parameters were kept constant during the measurement.

4. Chapter Four: Experimental Results and Discussions

4.1 Introduction

In this chapter the experimental results of the effect of energy storing materials on the productivity of solar still were studied experimentally. According to chapter 2, the performance of solar still can be affected by weather conditions (temperature, wind speed, relative humidity and solar radiation intensity) and design parameters. In the present study, the ambient temperature was measured on an hourly basis. The variation of the ambient temperature was studied in three consecutive days. It was found that the variation of the ambient temperature during these three consecutive days was less than 5% (see Figure 4.1). According to this Figure, the high ambient temperature was recorded between hours 12 to 16 for the three consecutive days.

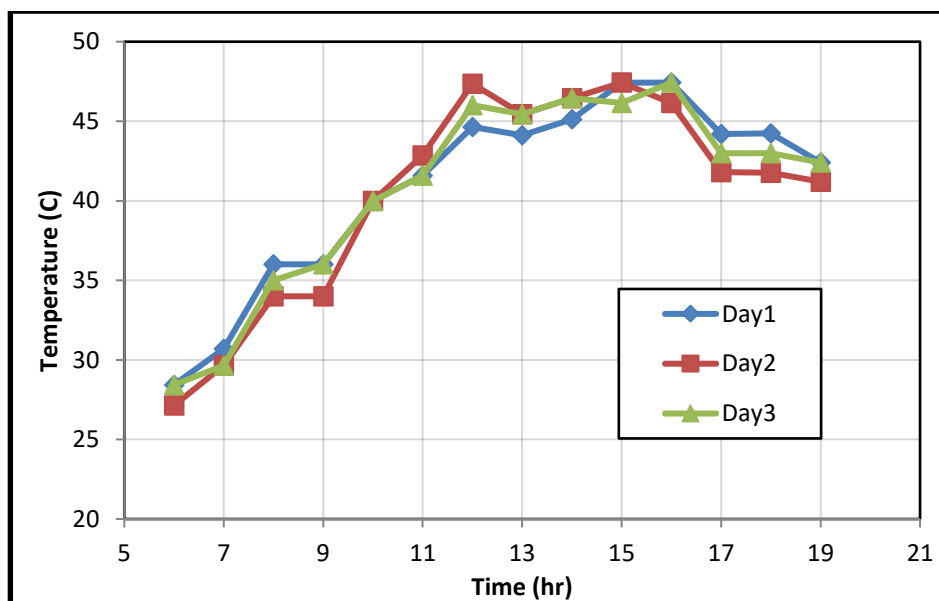


Figure 4.1 Variation of the ambient temperature during three consecutive days at different time of the day at the test site in Kuwait

The results in Figure 4.1 indicate that the variation of the ambient temperature during the three consecutive days is not significant and hence the effect of the temperature variation could be considered negligible. Similar measurements were carried out for the temperature of the basin, water, vapour and glass inner side and a similar conclusion was obtained, i.e. the variation of the temperatures over the three consecutive days was not significant.

As presented in chapter 2 in Figs. 2.20 and 2.21, the variations of wind speed and relative humidity in the test site during the measurements period (9:00 to 19:00) were considered negligible at this time of the year. Solar radiation is another main factor which can affect the solar still productivity significantly. The solar radiation was measured in the present study on hourly basis using digital instrument SOLAR SURVEY 100 and the results are presented in Figure 4.2. The instrument gives the incident solar radiation in W/m^2 . The maximum value was recorded at hour 13. The measurements of the solar radiation in several days indicated that the maximum deviation from the mean value was less than 9.5%. In other words, the variation in solar radiation during the time of conducting the experiments could be negligible. This agrees with the conclusion given by Taghvaei et al. (2014) who also measured the solar radiation and reported variations of about 11%. It can be concluded that the variation of weather condition during the test measurements are negligible in the present study.

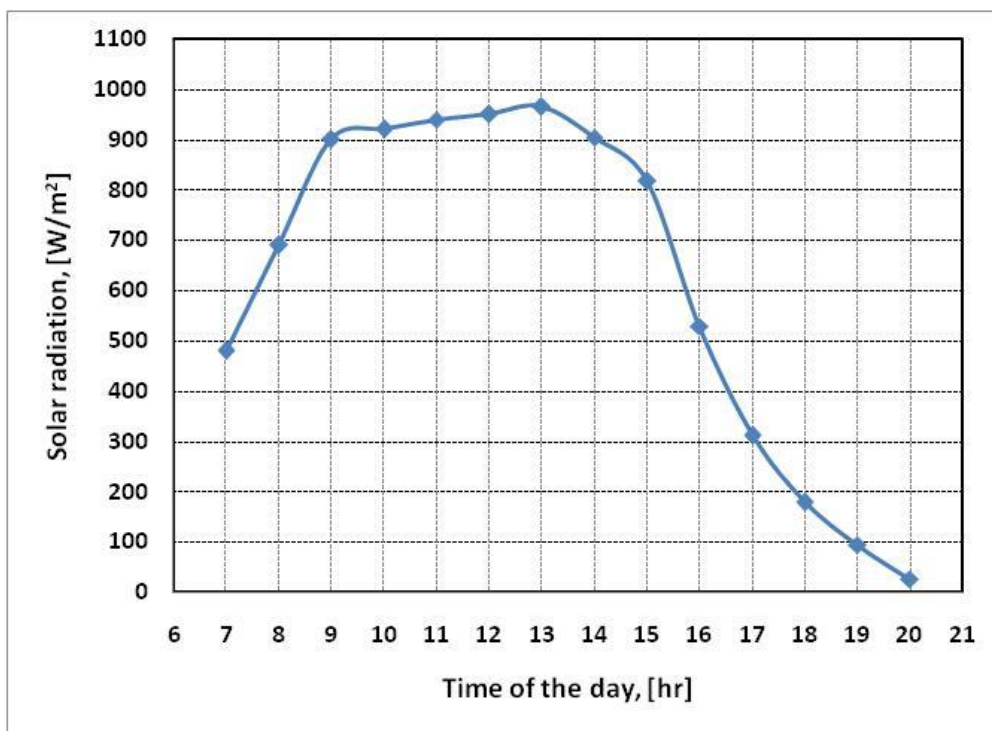


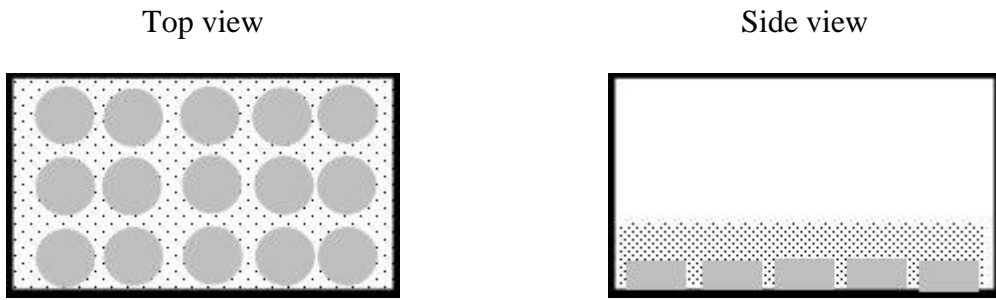
Figure 4.2 The hourly measured intensity of solar radiation

This chapter presents the experimental results and discussion for the examined experimental parameters. In what follows, the solar still with no modification is termed conventional solar still, which was used as a bench mark for comparison with the solar still with modification. In this study, “no modification” means no energy storing material or no external cooling for the glass cover plate.

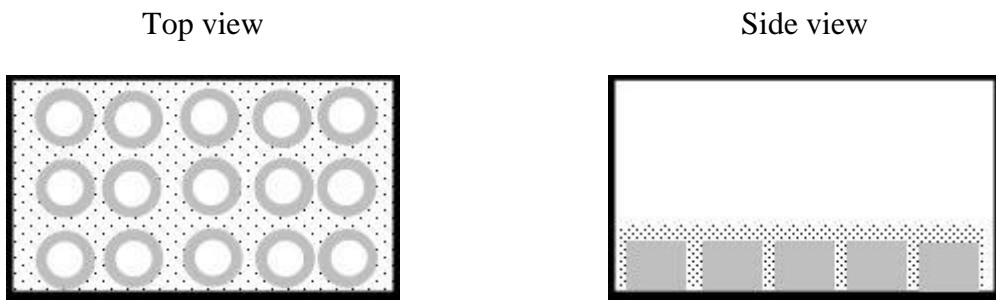
The chapter is organised as follows. In section 4.2, the effect of the shape of metallic energy storing material is presented. Section 4.3 presents the effect of water depth. Section 4.4 presents the effect of water cooling on the glass cover. Section 4.5 presents the effect of gravel as an energy storing material and its size. Section 4.6 presents the effect of using phase change material as an energy storing material. Finally, section 4.7 gives concluding remarks.

4.2 The Effect of the Shape of Metallic Energy Storing Materials

Three geometrical shapes of steel pieces were used as energy storing material. The three shapes are depicted schematically in Figure 4.3 and they are as follows: solid round rod, hollow round rod and solid square rod. Although the shapes were different, the total mass of the energy storing materials was kept fixed. The solar still was tested with no modifications as a base case for comparison, i.e. a conventional solar still. The design parameters in terms of cleanliness, location of the still and experimental set-up were kept unchanged during the measurements and it is assumed that the variation of weather conditions is not significant during experiments. At this stage the basin water depth was kept fixed at 10 cm and the water level was controlled by the height sensor. Figure 4.4 shows the distribution of temperature in the conventional solar still. According to this figure, the maximum temperatures for basin, water in the basin, vapour, ambient and glass inner side do not appear at the same time, but they occur about hour 12:00 – 16:00. Moreover, the highest temperature was recorded for vapour inside the still as high as 60 °C. The temperature of water in the basin was slightly higher than the basin temperature; up to 12:00 and the difference became more pronounced after 12:00. Figures 4.5 - 4.6 demonstrate the measured temperature versus time of the day for the solar still with solid round rods, hollow round rods and solid square rods. These figures demonstrate that the measured temperature distribution in the modified solar stills exhibited similar behaviour to that found in the conventional solar still. The vapour temperature showed some variation between hours 8:00 and 16:00. The variation in the vapour temperature can be attributed to the variation in basin temperature which affects the natural air circulation currents inside the solar still. As result, a temperature gradient was formed inside the solar still. Also, it is observed that the vapour temperature is the highest.



a. Solar still with solid round rods sitting on the bottom side of the basin



b. Solar still with hollow round rods sitting on the bottom side of the basin



c. Solar still with solid square rods sitting on the bottom side of the basin

Figure 4.3 The configurations and shape of the tested steel energy storing material

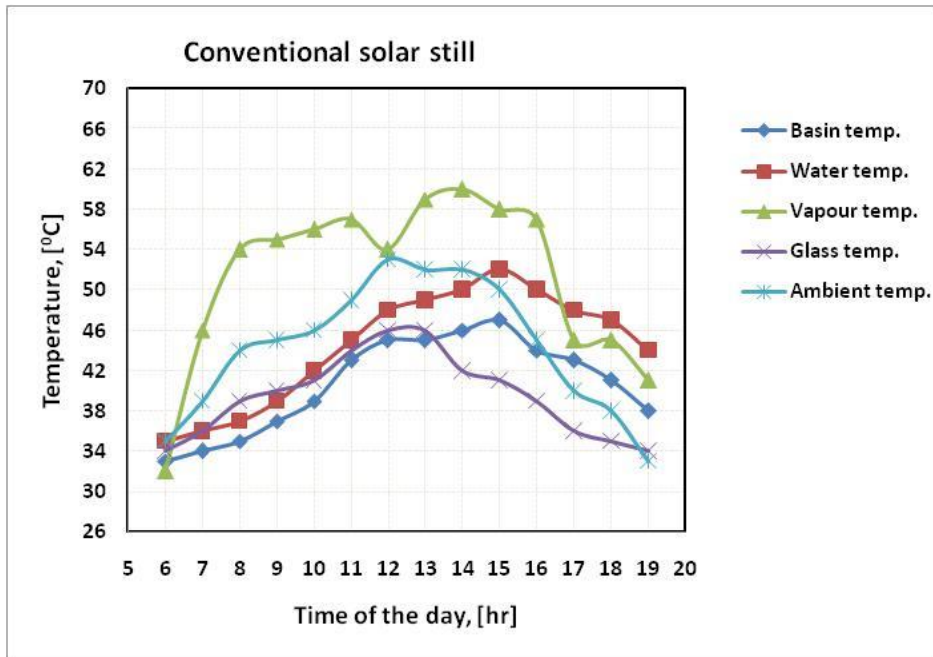


Figure 4.4 Temperature distributions inside the conventional solar still (without modifications)

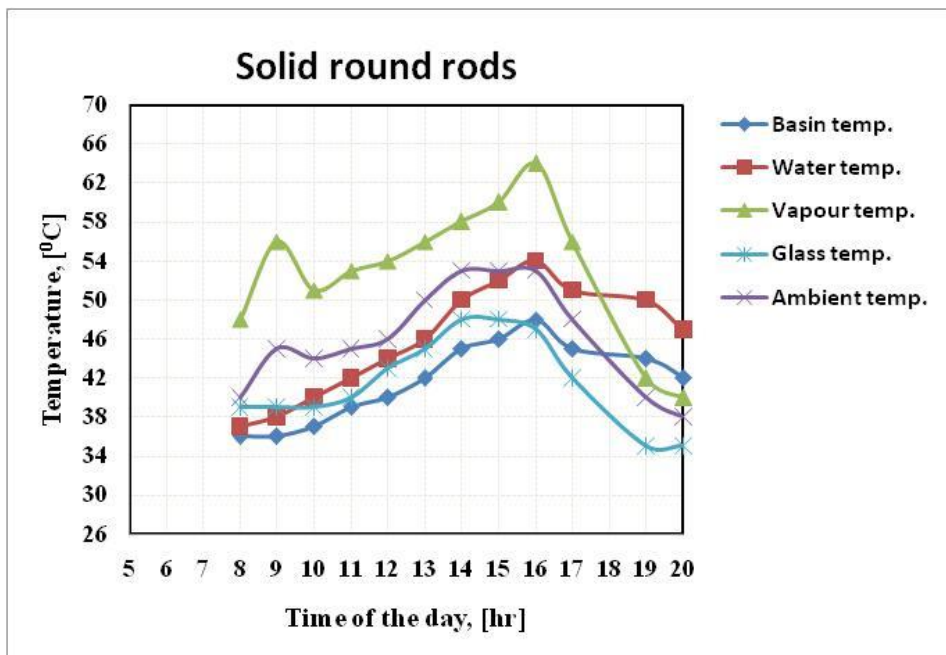


Figure 4.5 Temperature distributions inside the solar still with solid round rods

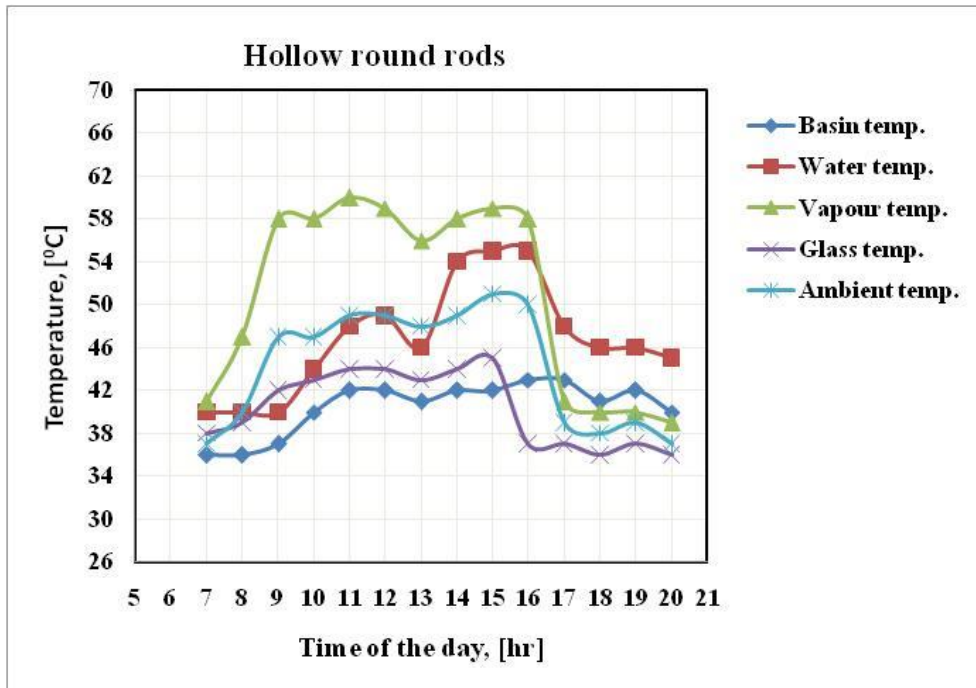


Figure 4.6 Temperature distributions inside the solar still with hollow round rods

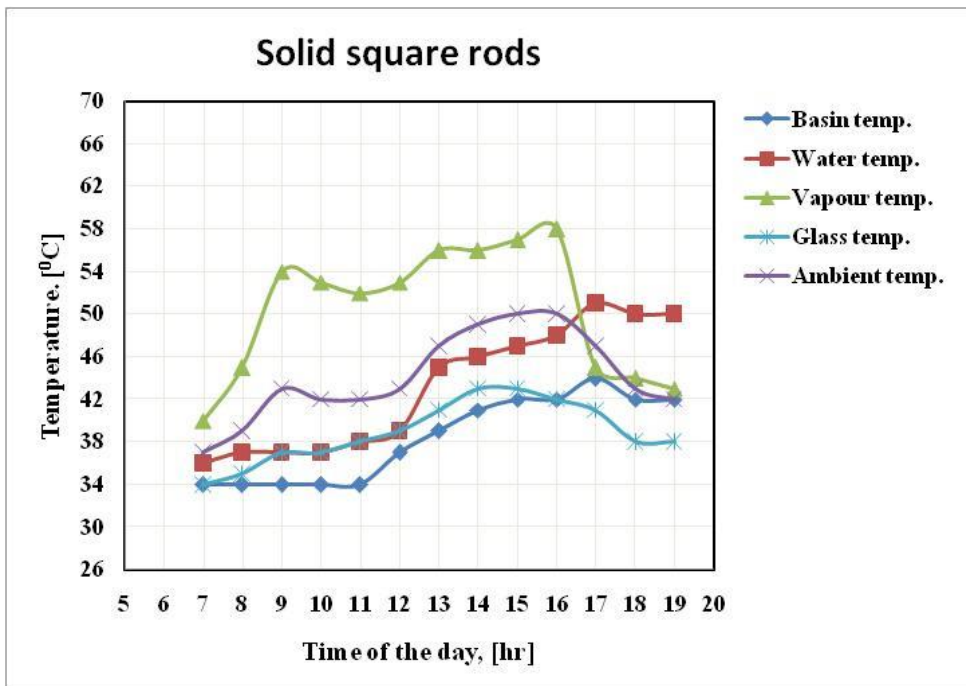


Figure 4.7 Temperature distributions inside the solar still with solid square rods

Figure 4.8 depicts the cumulative water production curves for the above three steel shapes compared with the cumulative water production curve for the conventional solar still. Time 0 means the starting time (6:00 am) and time increases as we move forward on the time axis. It is obvious that there is a clear improvement in the cumulative water production for solar stills

with steel pieces compared to the base case especially after about 6 hours from operation (nearly 12:00 am). The round hollow rods gave the best performance where the total daily water production has increased by 28.3%, followed by the round solid rods, which improved the total daily production by 21.3%. On the other hand, the steel pieces of square solid shapes exhibited insignificant improvements. This could be due to the fact that a considerable part of this shape was not fully immersed in water as was the case with the other two shapes (see Figure 4.3). The enhancements with the solid and hollow round shapes could be due to the reduction in the water depth above the immersed steel pieces. Figure 4.9 depicts the water production rate versus time for the three shapes compared with the conventional solar still. It is obvious that the production rate was nearly the same for all cases in the first five hours and there is a small peak after 5 hour (at nearly 11:00 am) for the conventional still and after about 6 hours (nearly at 12:00 am) for the other cases. After this peak, there is another big peak, which occurred at different times for the three modifications. For the round solid rods, the peak occurred at time = 11 hr (17:00 pm). For the round hollow rods, it occurred at time = 13 hr (19:00 pm). For the square solid rods, it occurred at time = 12 hr (18:00 pm). These peaks are nearly in agreement with the temperature peaks reported in Figs. 4.4 – 4.7. The difference in the total production for the three pieces is related to the shape of energy storing material.

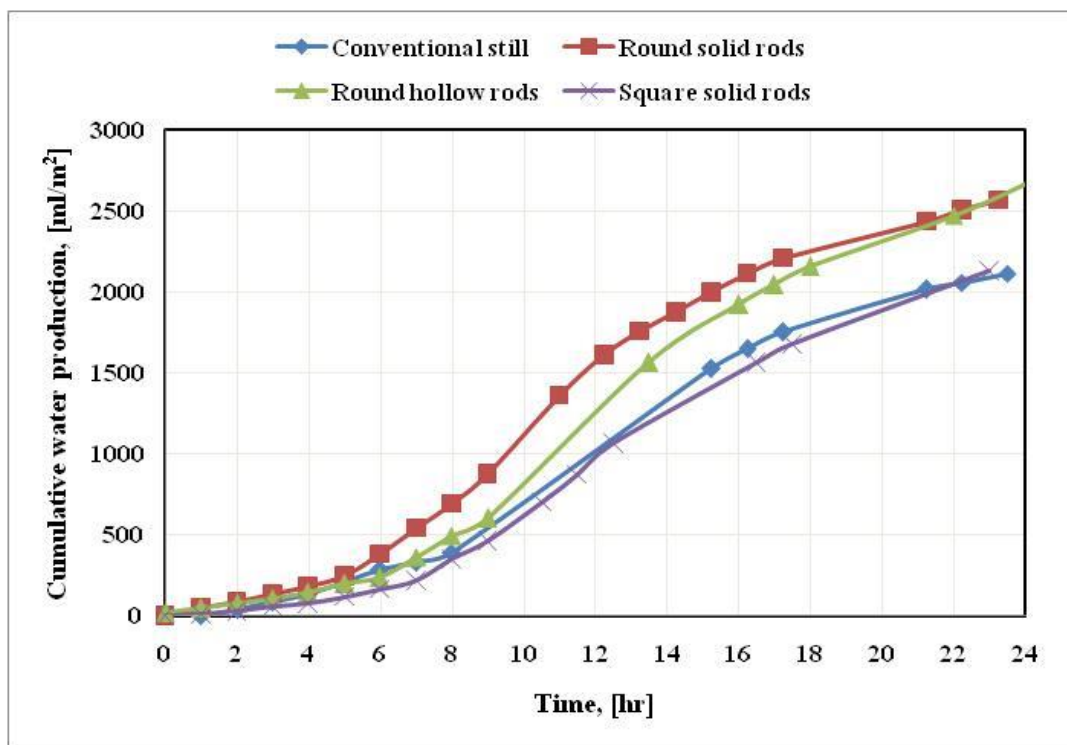


Figure 4.8 The cumulative water production curve for the solar still modified with round solid rods, hollow round rods and solid square rods compared with the conventional solar still.

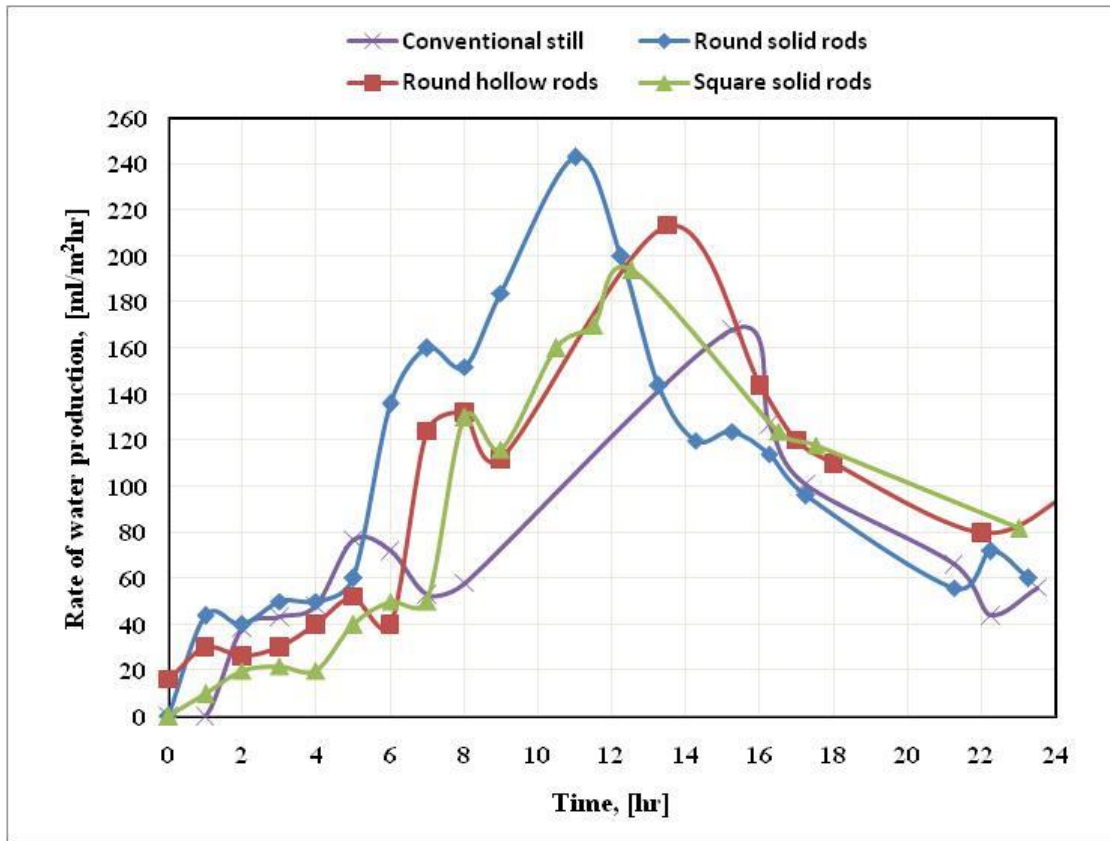


Figure 4.9 The rate of water production for the solar still modified with round solid rods, hollow round rods and solid square rods compared with the conventional solar still.

4.3 Solar Still with Hollow and Solid Steel Pieces

In this section, the solar still was tested using a combination of hollow and solid section steel rods together at the same time. Figure 4.10 presents the temperature distribution in the still. The figure indicates that the highest and lowest temperatures were recorded for water in the basin and the ambient respectively. The peak temperature occurs at the maximum ambient temperature with some delay. Figures 4.11 and 4.12 present the variation of the rate of water production and the cumulative production with time respectively. In comparison with the conventional solar still with no modifications, no significant changes were observed in the total water production. However, the peak value of production rate for the modified solar still was 10% lower, which occurs when the basin reaches its maximum temperature. The peak value of the basin, water, glass and vapour temperature occurs when the ambient temperature reaches close to its maximum value. Also, it was observed that the delay in water production at the beginning was longer.

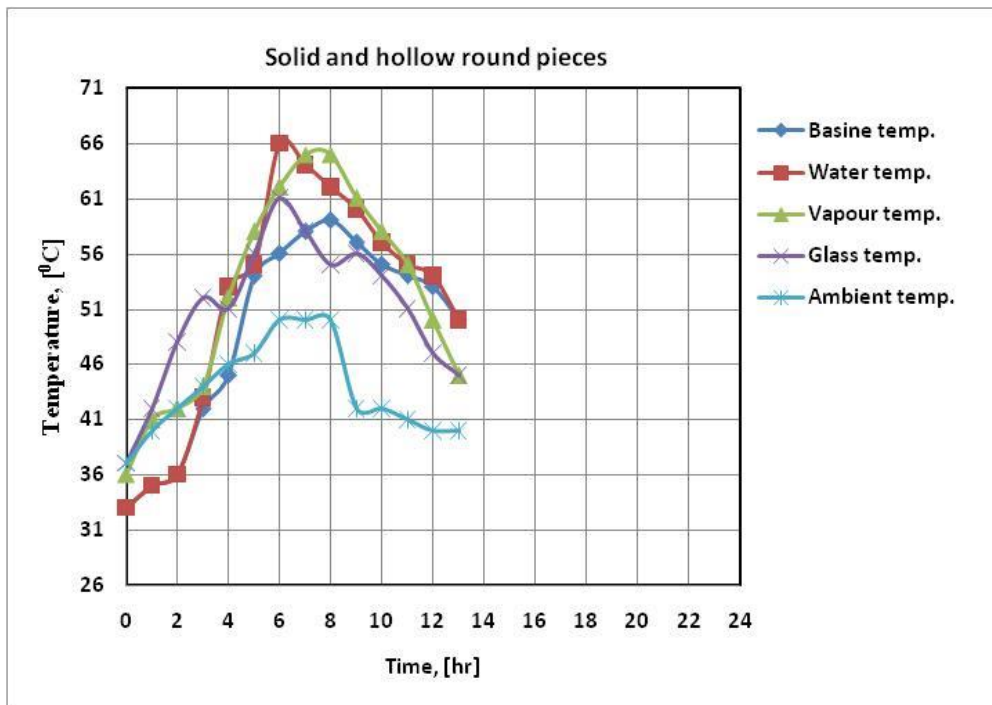


Figure 4.10 The temperature distribution inside a solar still modified with a combination of solid and hollow round steel rods

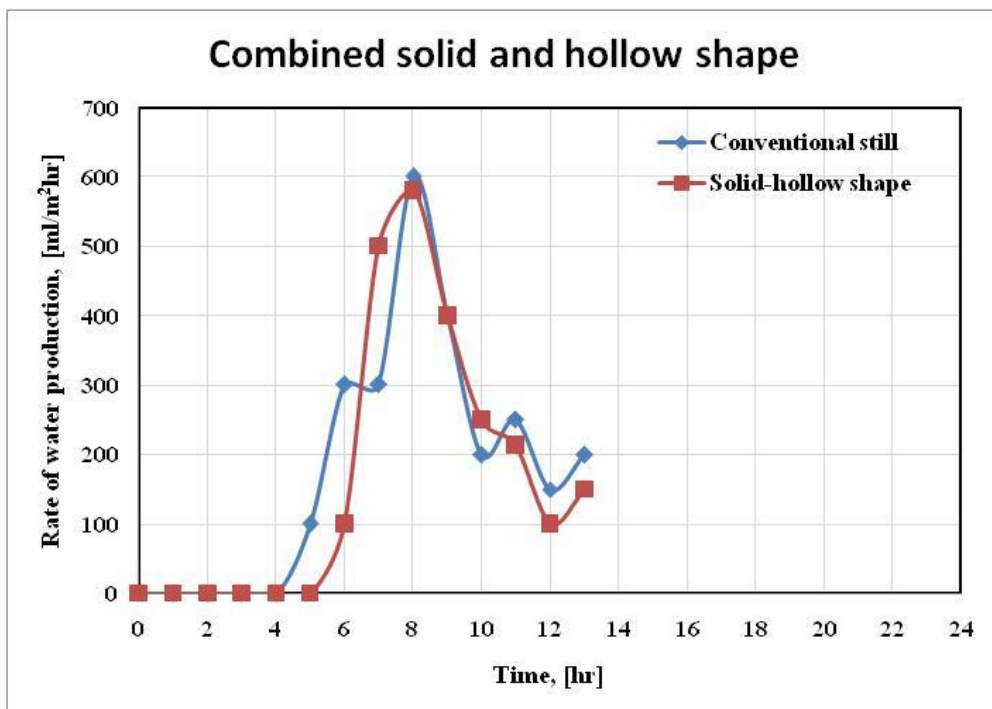


Figure 4.11 The rate of water production for a solar still modified with a combination of solid and hollow round steel rods compared with the conventional solar still

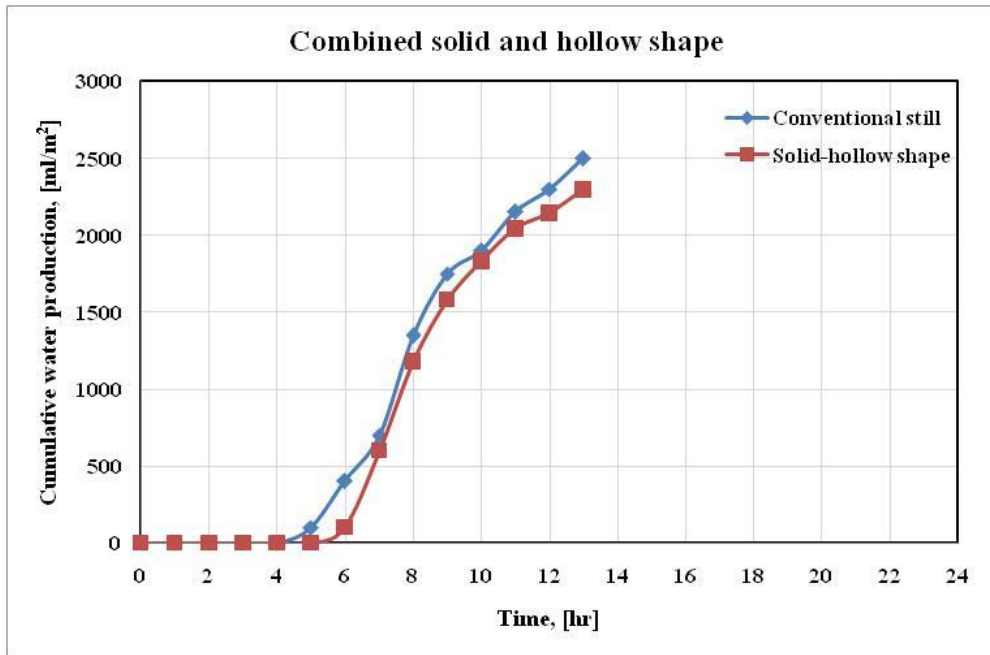


Figure 4.12 The cumulative water production curve for a solar still modified with a combination of solid and hollow round steel rods compared with the conventional solar still

4.4 The Effect of External Cooling

In this section, the conventional solar still was tested with water flow on the outer surface of the glass cover as external cooler. Figure 4.13 indicates the temperature distribution inside the solar still. No significant temperature reduction in the glass cover was observed by using the water flow on the outer surface of the glass cover and it was due to the high temperature of the water flowing on the cover. The water volumetric flow rate was considered *0.5 lit/min* in this test. Due to the large surface of the hoses exposed to the environment, the water inside the hoses warmed up before reaching the cover, rendering the cooling function less efficient. It was found that increasing the volumetric water flow rate of water from 0.5 to 1 lit/min was not making a significant difference. Figures 4.14 and 4.15 present the rate of water production and the cumulative production curves as a function of time respectively. In comparison with the conventional solar still with no modification, almost no significant changes were observed in the total production and the peak value of the production rate. It took a long time for the production rate to reach its peak value and *2-hour* time difference was recorded between the maximum temperatures for the basin and the glass cover. Moreover, it was observed that the delay in water production at the beginning was one hour longer.

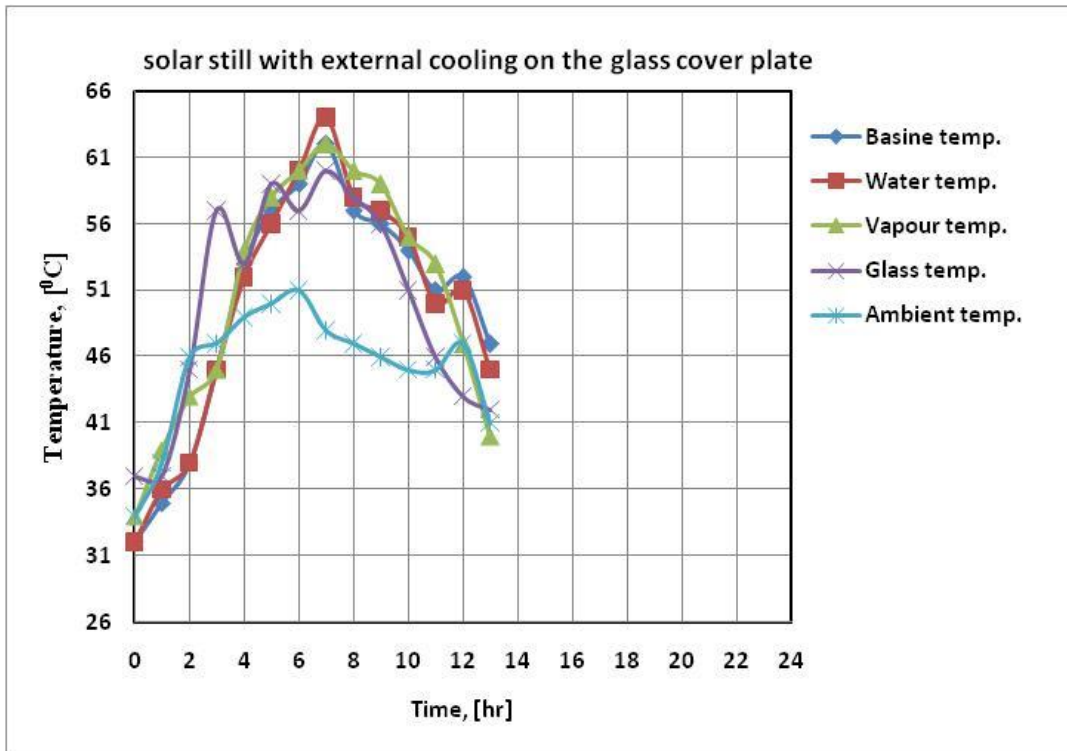


Figure 4.13 The temperature distribution inside a solar still modified with an external cooling on the outer surface of glass cover plate

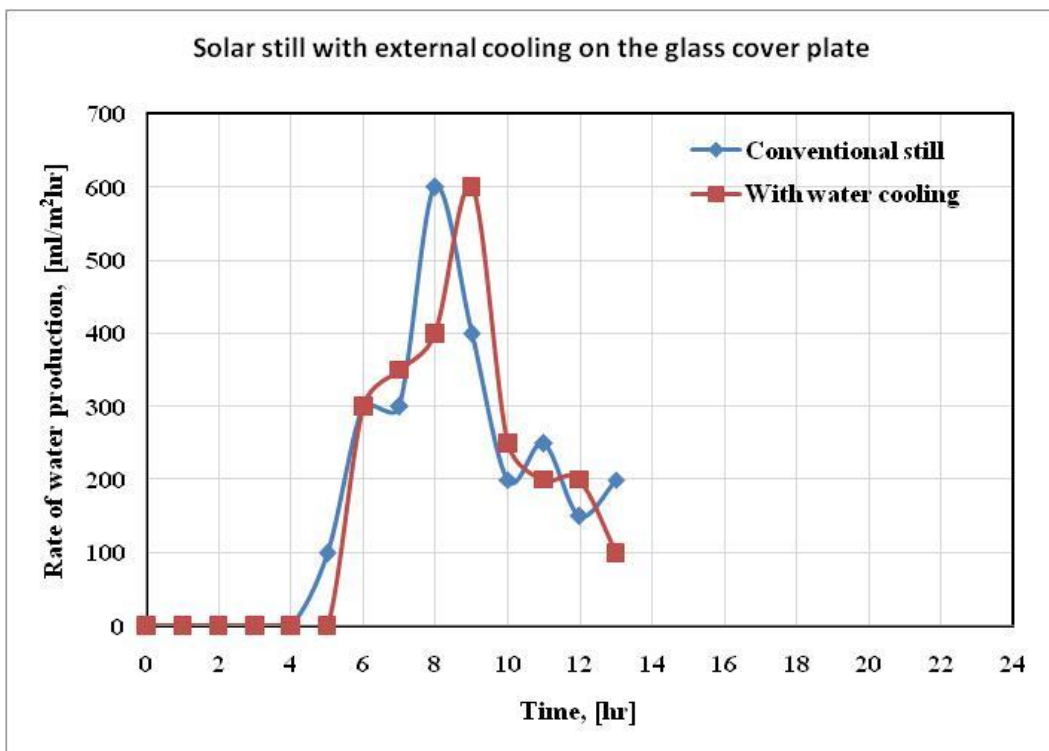


Figure 4.14 The rate of water production for a solar still modified with an external cooling on the outer surface of glass cover plate

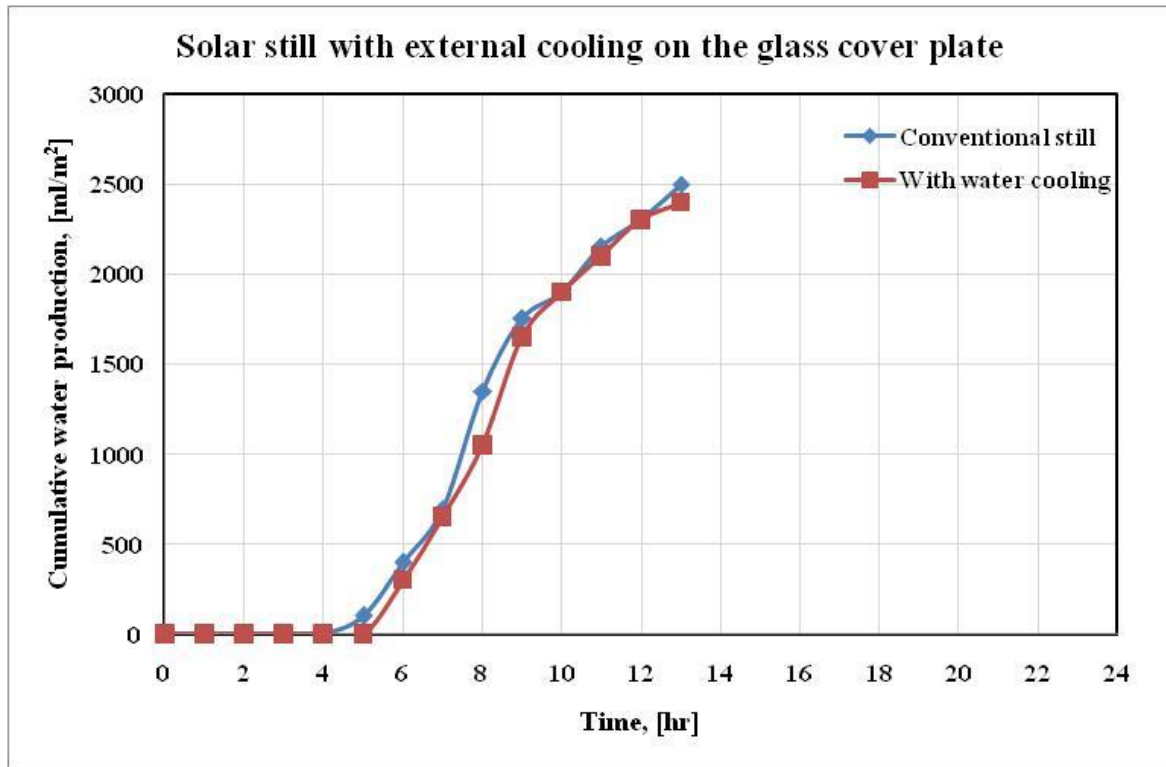


Figure 4.15 The cumulative water production curve for a solar still modified with an external cooling on the outer surface of glass cover plate

4.5 The Effect of a Combination of External Cooling and Solid Steel Rods

In this section, the solar still was modified by a combination of external water cooling and solid steel rods. The temperature distribution in the solar still was recorded and the results are depicted Figure 4.16. According to this figure, the peak values of the basin temperature, the water temperature, the vapour temperature and the glass temperature occur at the maximum ambient temperature with some delay. The highest and lowest temperatures were recorded for the water and ambient temperature, respectively. Figure 4.17 and 4.18 present the rate of water production and the cumulative water production versus time respectively. The figures demonstrate that there was a reduction in the total water production and the production rate. In comparison with the conventional solar still with no modifications, the total water production showed 17% reduction. The maximum production rate was also reduced by 17%.

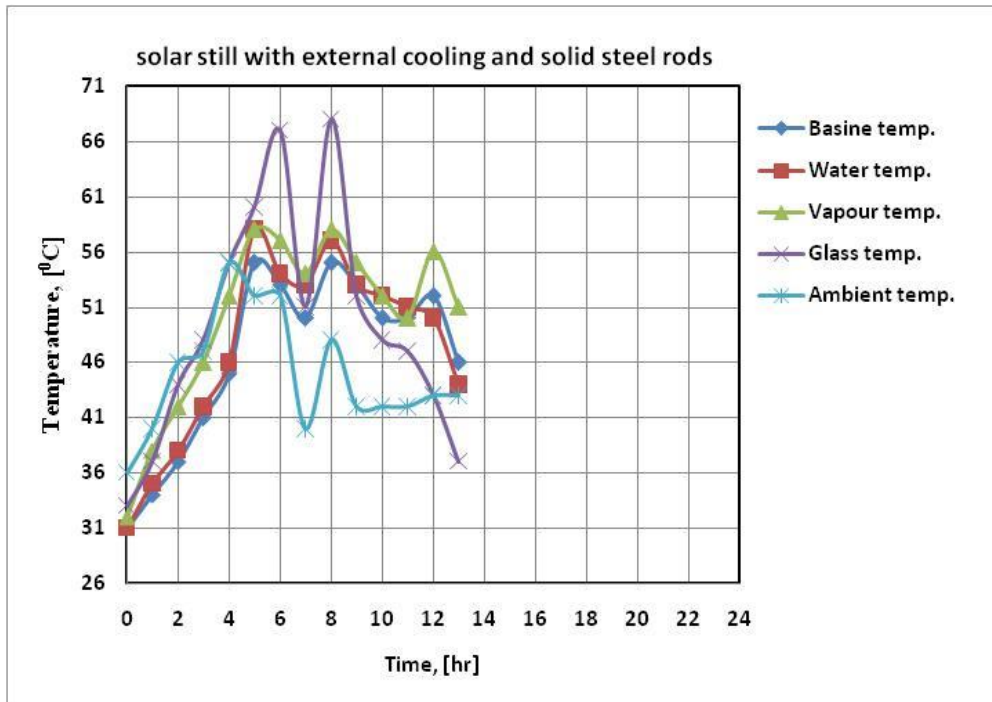


Figure 4.16 The temperature distribution inside a solar still modified with a combination of external cooling and solid rods

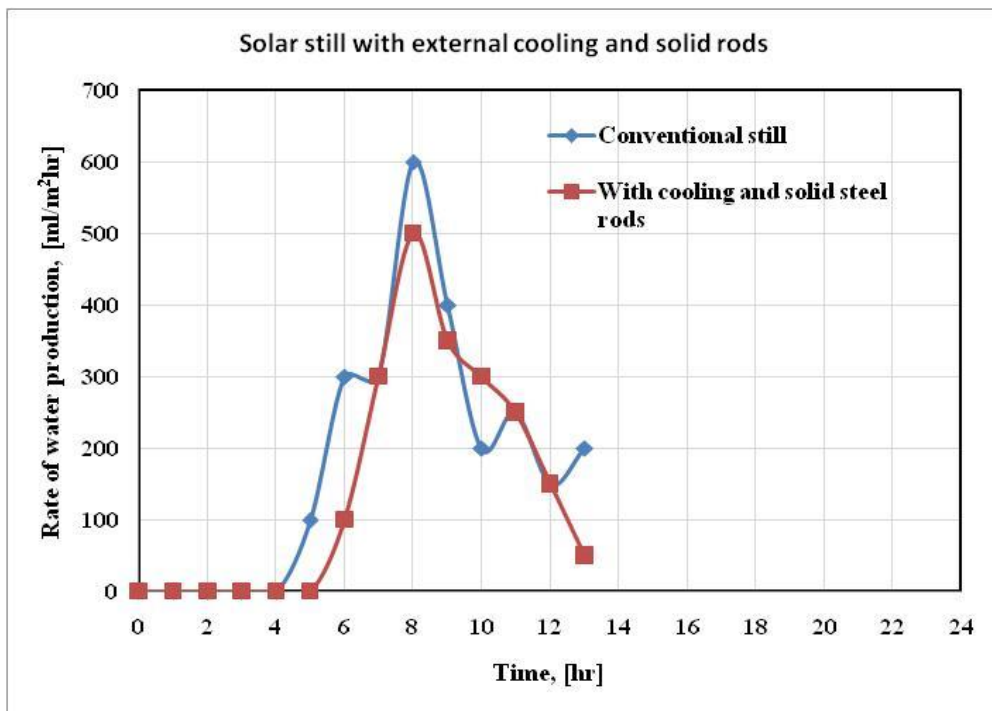


Figure 4.17 The rate of water production for a solar still modified with a combination of external cooling and solid steel rods

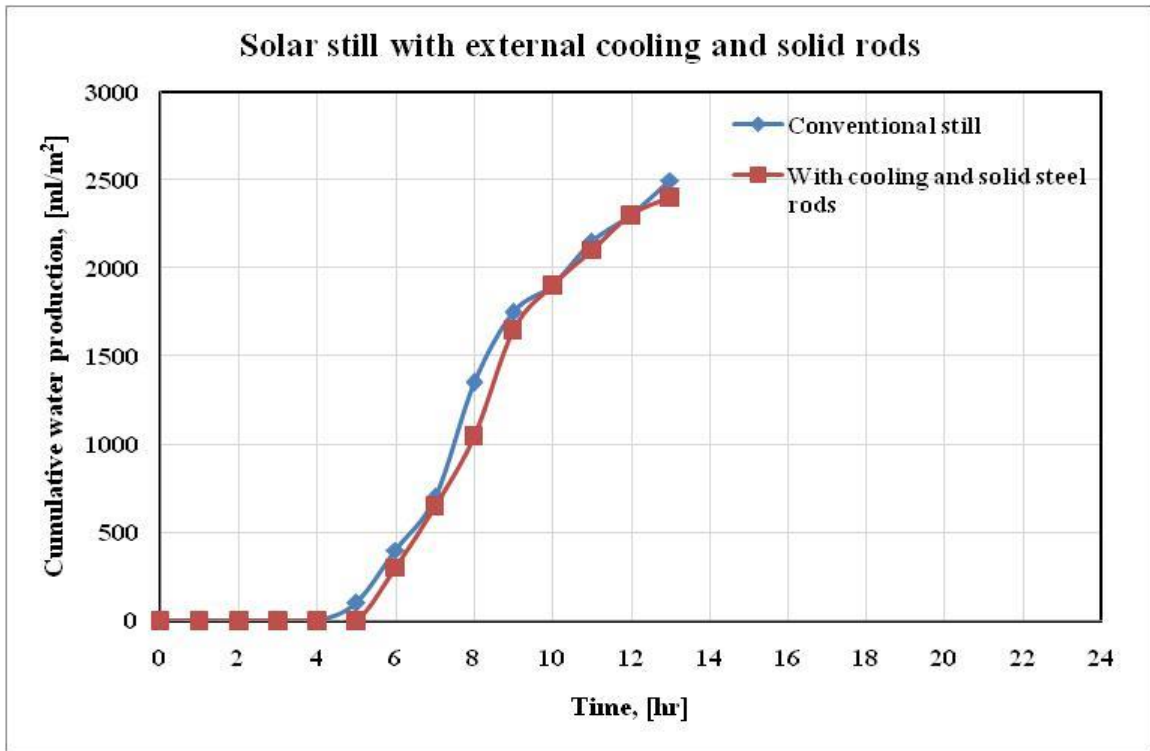


Figure 4.18 The cumulative water production curve for a solar still modified with a combination of external cooling and solid steel rods

4.6 The Effect of Water Depth

The effect of the basin water depth on the total water production has been investigated extensively in the literature. Some researchers proposed correlations for the prediction of the total water production in terms of the basin water depth. However, these correlations may not be general; they depend on the region in which the experiments were conducted, and they need to be checked. In the present study, the water depth in a conventional solar still was varied from 5 cm to 25cm in 5 cm intervals. Figure 4.19 presents the variation of the total production in terms of basin water depth. The figure demonstrates that the maximum daily production depends on the water depth and it increases as the water depth decreases. The effect of water depth can be explained as follows: as the water depth decreases the volumetric heat capacity of the water in the basin decreases and thus the water temperature increases rapidly. The increase in water temperature can increase the rate of water evaporation in the basin. Thus, the production rate is expected to increase as the water depth decreases.

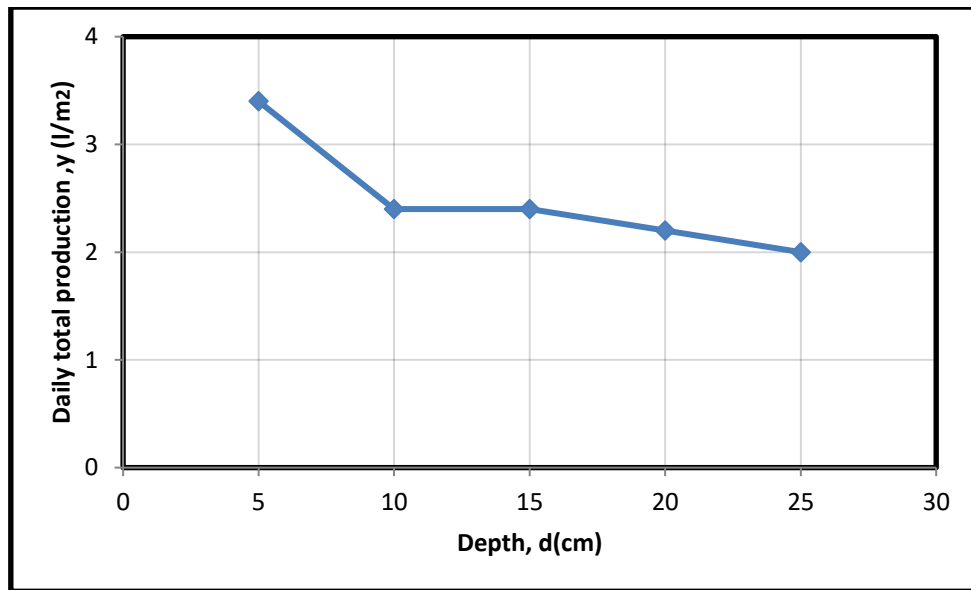


Figure 4.19 Variation of total daily production (l/m²) in terms of water depth (cm)

4.7 The Effect of the Type of Energy Storing Material

This section presents and discusses the performance of the solar still with different energy storing materials. Two types of the energy storing media were tested, namely; sensible heat media and phase change media. The sensible heat media include steel pieces (round solid, round hollow and square solid) and gravel stones (small size, 0.25 inch, and big size, 0.5 inch). The phase change material tested in this study was paraffin wax filled in short pieces of copper tubes having 1-inch diameter and 12 cm length. After filling the tube with the paraffin wax, the two ends of the tube were closed and sealed. All materials were painted black in order to enhance the absorption of solar radiation. Figure 4.20 compares the rate of water production using different energy storing media with the conventional solar still with no modifications.

The figure demonstrates nearly similar behaviour but with some differences in the peak value. The solar still with small and big gravel sizes exhibits nearly similar production rate to the conventional solar still without any modifications. There is a delay in the peak where it occurred at time = 15 hr. The round hollow rods and the square rods gave nearly similar trend and the peak value occurred at time = 12-14 hr with the hollow rods exhibiting better production rate. Finally, the round solid rods and the phase change material showed similar trend and the peak value occurred at time = 11 hr with the phase change material giving significantly higher peak value.

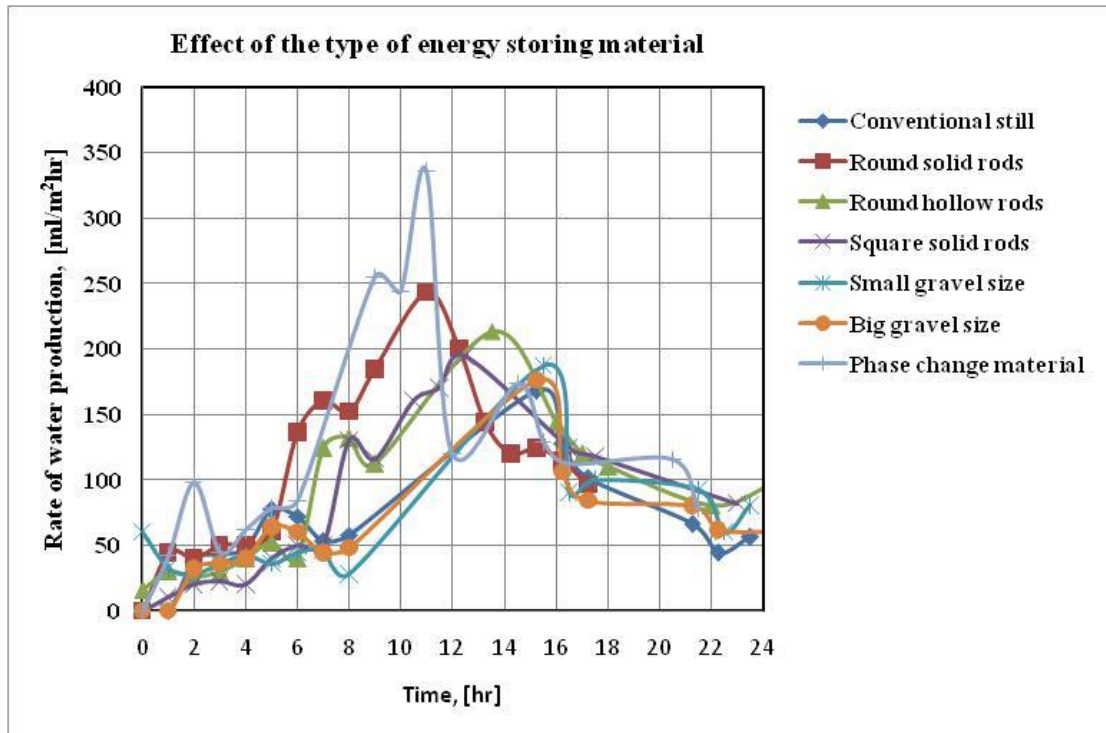


Figure 4.20 Effect of the type of energy storing material on the rate of water production compared to the conventional solar still with no modifications

Figure 4.21 shows the cumulative water production curve for the different types of energy storing materials. The figure demonstrates that after 21 hours of operation the total water production was 3.1L/m², 2.44 L/m², 2.47 L/m², 2.3 L/m², 2.1 L/m², 2 L/m², 2.05 L/m² respectively for the phase change material, the round solid rods, the round hollow rods, the small size gravel, the big size gravel, the square solid rods and the conventional solar still. This means that the percent improvements in the total water production ranged from 5 – 53% with the highest value achieved with the phase change material. Additionally, the use of gravel with small size has achieved slightly higher production compared to the gravel with the big size. This could be due to the increase in the exposed surface area (area in contact with water) as the gravel size decreases. The enhancements in the total water production and production rate that were achieved with the phase change material could be attributed to the high thermal conductivity of copper compared to the other examined materials. This improves the response time of the material (fast release of heat/fast storing of energy). Additionally, with phase change the material can release a significant amount of energy over the night when the wax solidifies due to the decrease in the ambient temperature and the absence of solar radiation.

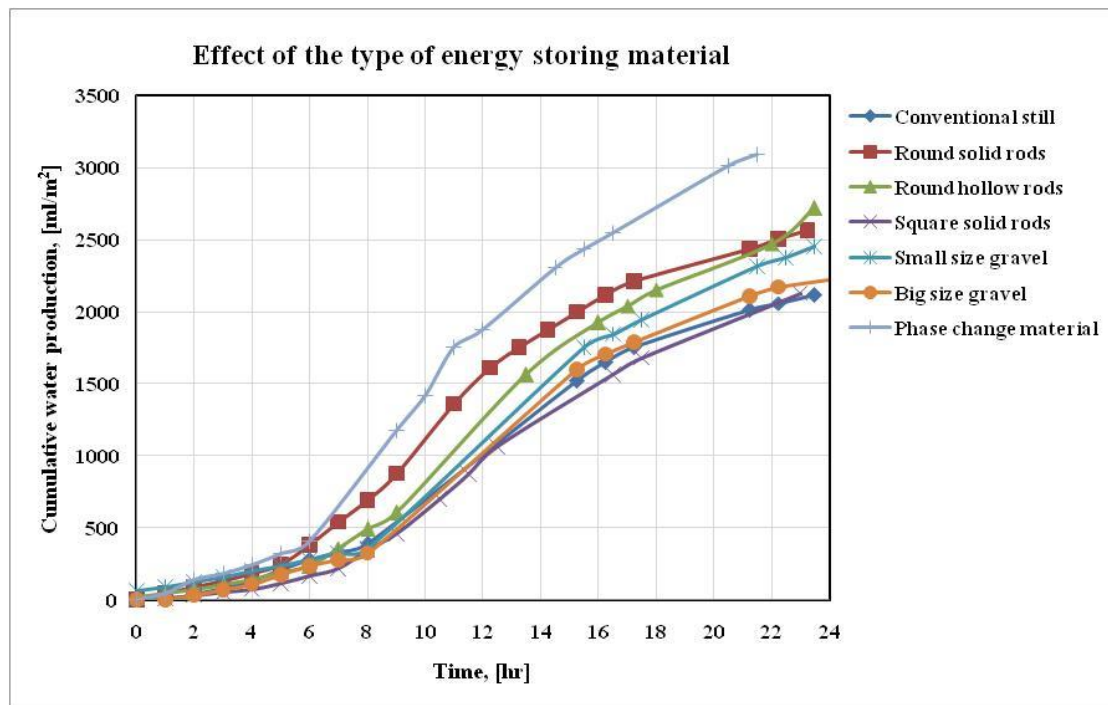


Figure 4.21 Effect of the type of energy storing material on the cumulative water production curve compared to the conventional solar still with no modifications.

4.8 Summary

This chapter presents the effects of several parameters on the thermal performance and total water production of a double slope basin-type solar still. The investigated parameters include the following: (1) the geometrical shape of steel pieces that were used as energy storing material, (2) the external cooling on the outer glass surface, (3) the combination of external cooling and steel pieces, (4) the water depth and (5) the type of the energy storing material. It was found that all the investigated parameters can affect the performance of solar stills. The results have indicated the following conclusions:

- (1) the round hollow steel pieces were the best among the investigated shapes.
- (2) The external cooling of the glass cover plate is not very effective.
- (3) The total water production increases significantly as the water depth decreases.
- (4) Using gravel as energy storing material can improve the productivity of a solar still, which is slightly lower than the productivity of solar stills with metallic energy storing materials. If the cost is considered, gravel can be a good option and gravel with smaller size is more favourable.

(5) Phase change materials can increase the production rate and the total daily water production significantly compared to the other materials. It achieved about 53% improvements in the total production.

It was also observed that water production starts when the temperature difference between the basin and the glass cover plate reaches about 7°C . The production delay occurs because it needs some time to build up the temperature difference between the basin and the cover, which also depends on the heat capacity of the energy storing material used. The round solid rods can absorb considerable amount of heat due to their mass; hence the temperature difference between the basin and the cover can take longer to reach 7°C . It was observed that the production delay was one hour longer for solar still with solid section rods. In comparison with solid section rods, the hollow section rods had no impacts on the production delay when solar still was used with hollow section rods only. It was concluded that the temperature difference between the basin and the cover is an important factor in terms of water production delay.

5. Chapter Five: Empirical and Theoretical Study of Solar Still Productivity

5.1 Introduction

Access to experimental equipment is not always available for the designers, and in many cases the experiments are sophisticated, and the cost is very high. Therefore, using empirical correlations and analytically derived formulas are strong tools for the design of any thermal system. This chapter presents an empirical and theoretical study for the total water production of the solar still. The effect of water depth and an example on the energy storing materials were investigated.

5.2 Empirical Study of Total Production (Y)

Using empirical techniques not only saves time and costs but it also helps to better understand the process and the relation between the main parameters. For example, as presented in chapter 2, Kandasamy et al. (2013) proposed two correlations for the prediction of the total water production (y) as a function of water depth (d) for a single slope (Eq. 2.3) and double slope (Eq. 2.4) solar stills.

In the present study, five different values of water depth were investigated; see Table 5.1 for the depths and the corresponding total daily production. These values are plotted in Figure 5.1 and the best fit equation obtained using MS Excel is shown on the figure with the R^2 value. The data of the present study are correlated in the form given by Eq. 5.1 below. This equation is nearly similar to Eq. 2.4 given by Kandasamy et al. (2003) except that the constant in the front of the correlation is slightly smaller. In other words, the correlation of Kandasamy et al. (2003) predicts values which are 13% higher than the values predicted using Eq. 5.1 given in the present study.

$$y = 5.308d^{-0.3} \tag{5.1}$$

Depth, d(cm)	5	10	15	20	25
Total daily production, y(L/m ²)	3.4	2.4	2.4	2.2	2

Table 5.1 Measured total production in terms of water depth

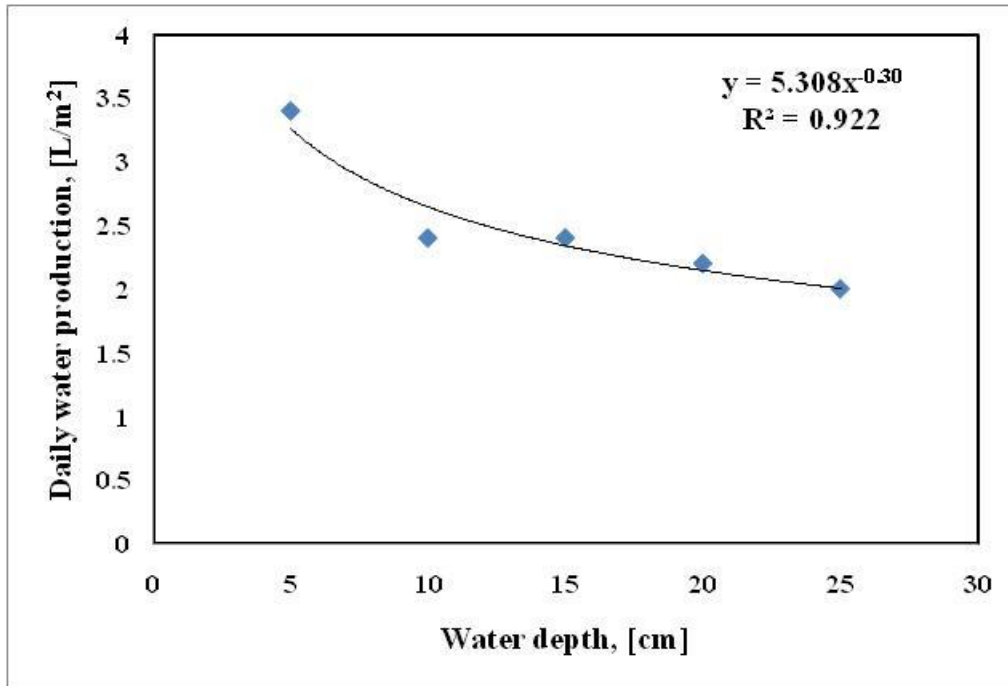


Figure 5.1 The daily water production as a function of water depth inside the basin

5.3 The Effect of Ambient Temperature

The effect of the ambient temperature (T_{av}) on the daily production and production rate is investigated in this section. Figure 5.2 shows the variation of temperatures of basin, basin water, vapour, ambient and cover in August in Kuwait on the test site. The test was carried out for a solar still with no modifications. It was observed that the maximum basin temperature, cover and basin water temperatures occurred at about 1 pm when the ambient temperature was at maximum value. The maximum ambient temperature also corresponds to maximum solar radiation time. The highest recorded temperature for vapour was 67°C which occurred at about 1 pm. The highest recorded cover temperature was 59-60 °C between 1pm and 3pm. The basin temperature and basin water temperature were found almost the same throughout the experimental period. The daily water production as a function of the ambient average temperature is presented in Table 5.2.

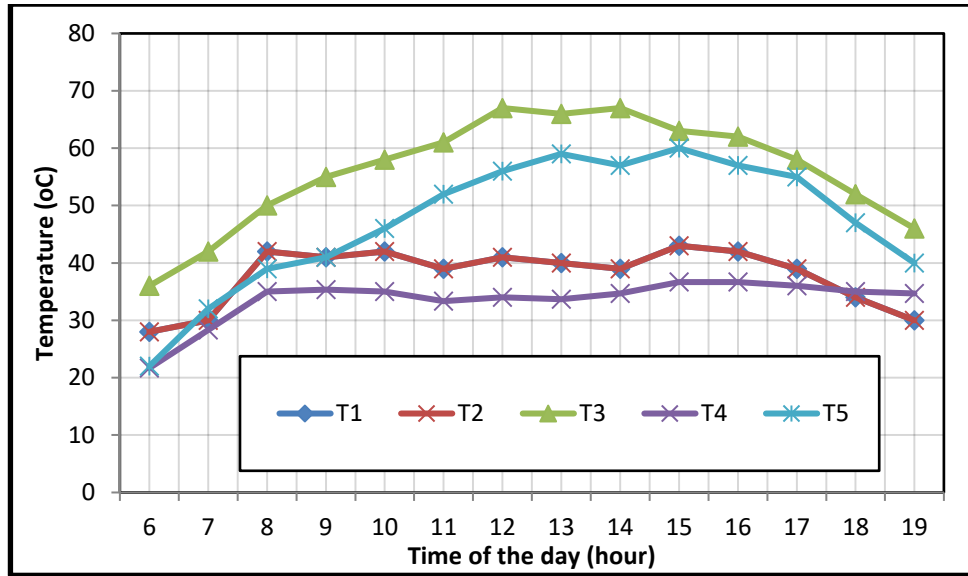


Figure 5.2 Variation of basin temperature (T1), basin water temperature (T2), vapour temperature (T3), ambient temperature (T4) and cover temperature (T5) in August in Kuwait

Daily ambient average temperature, [$^{\circ}\text{C}$]	33.71	34.51	34.8	36.11	38.15
Daily water production, [ml/m^2]	1900	1750	1800	2300	3200

Table 5.2 Daily ambient temperature against daily water production

Figure 5.3 shows the results summarized in Table 5.2 and the best fit equation was obtained using Excel software. According to this figure, the daily water production increases as the ambient temperature increases. Equation 5.2 indicates the linear correlation for the daily water production in terms of the ambient average temperature.

$$y = 329.32T_{av} - 9486.3 \quad (5.2)$$

where y is the daily water production and T_{av} is the ambient average temperature. This equation shows a strong relation between the daily water production and the ambient average temperature. When the maximum water production rate (Table 5.3) was plotted versus the ambient temperature, a similar trend was obtained, and the best fit equation is given by Eq. 5.3 below.

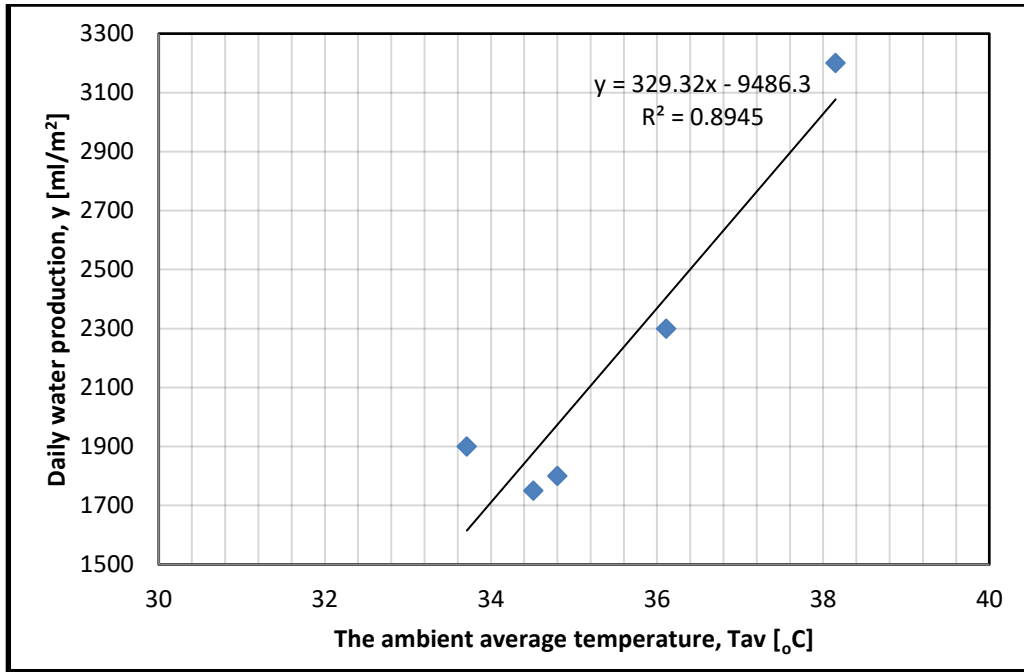


Figure 5.3 The variation of daily water production against the ambient average temperature

$$x = 93.74T_{av} - 2752.86 \quad (5.3)$$

Daily ambient average temperature $^{\circ}C$	Maximum water production rate l/hm^2
33.71	300
34.51	340
34.8	320
36.11	420
38.15	520

Table 5.3 Maximum water production rate versus the daily ambient average temperature

5.4 Energy Storing Materials

It is well known that the higher the water temperature, the higher the productivity of the solar still. Energy storing materials are one of the options to improve water production and speed up the heating process in the water basin. Using energy storing materials can reduce the equivalent specific capacity of solar still. Therefore, for a given solar energy, the basin water temperature will be raised rapidly and consequently the water production will be improved. Many materials were used as an energy storing materials in the published literature. The effect

of energy storing materials on efficiency has been discussed and compared in the literature review chapter in this study. In this section the effect of energy storing materials are quantified and discussed in order to explain the results presented previously in chapter 4.

5.5 Heat Capacity of Energy Storing Materials

Figure 5.4 shows a typical double slope solar still. The energy balance Equation, in a very simple form, for this solar still which contains only water in the water basin can be expressed by (5.4).

$$Q_I = m_w C_w \Delta T_1 + Q_{LI} \quad (5.4)$$

where Q_I is the total solar energy received from the sun (J) in a period of time t (s), Q_{LI} is the total heat losses (J) in period of time t , m_w is the mass of water in the basin (kg), C_w is the specific heat capacity of water in the basin ($J/kg.K$) and ΔT_1 is the magnitude of increase in basin water temperature (K). Figure 5.5 shows a double slope solar still with some energy storing materials in the basin.

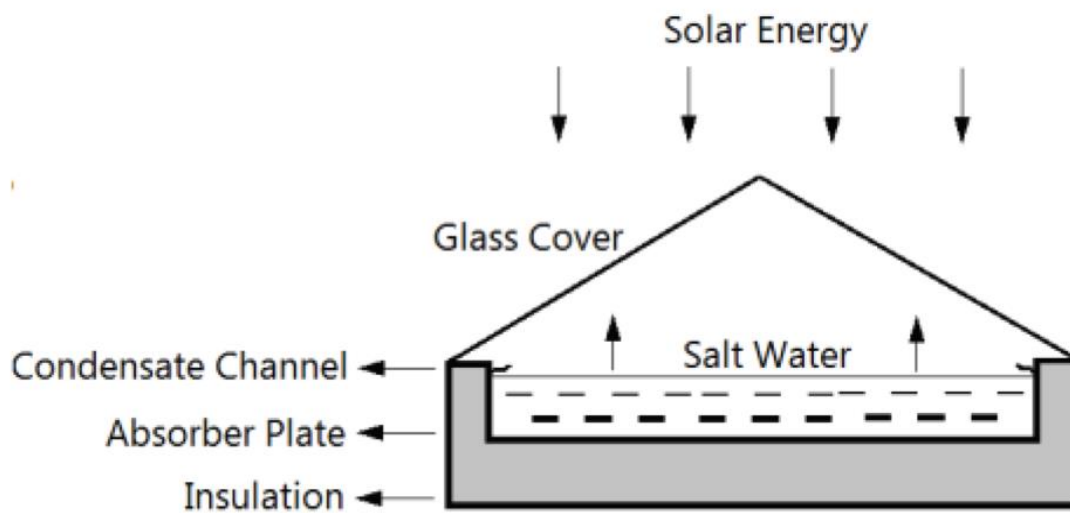


Figure 5.4 A typical double solar still with no energy storing materials used in the basin

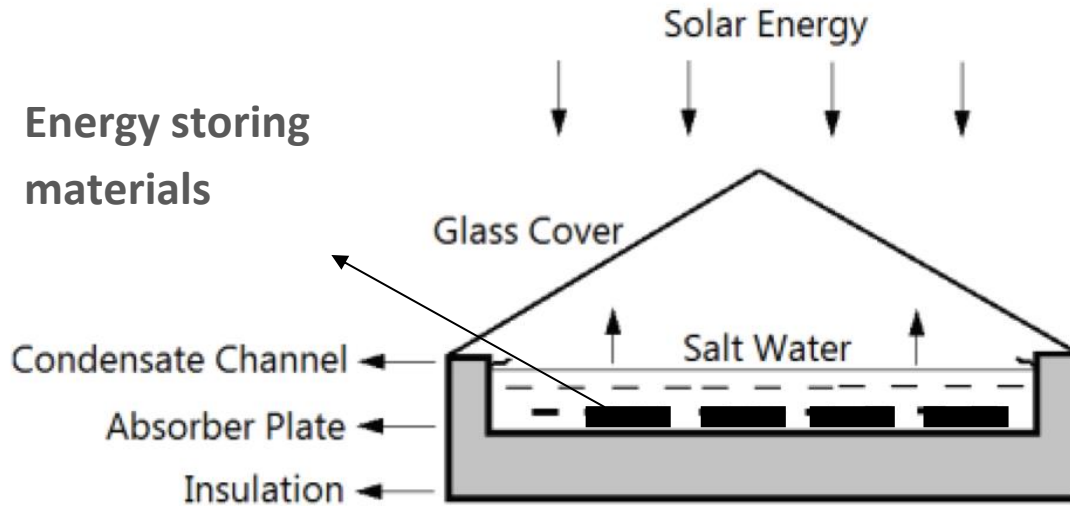


Figure 5.5 Double solar still with energy storing materials used in the basin

The energy balance equation for the double slope solar still with energy storing materials can be expressed in form of Eq. 5.5.

$$Q_2 = (m_w - m_s)C_w\Delta T_2 + m_s C_s \Delta T_2 + Q_{L2} \quad (5.5)$$

where Q_2 is the total solar energy received from sun in period of time t when the solar still was used by energy storing materials as in Figure 5.5. Similarly m_s is the mass of energy storing materials, ΔT_2 is the magnitude of increase of basin water temperature, C_s is the specific heat capacity of energy storing material and Q_{L2} is the total heat loss from the solar still to environment in the period of time t . the value of $m_w - m_s$ presents the mass of basin water when solar still is in use with energy storing material. Since the tests were carried out on consecutive days, it can be assumed that the amount of solar energy on two consecutive days is almost the same.

$$Q_1 = Q_2$$

(5.6)

The effect of temperature differences ΔT_1 and ΔT_2 on heat loss is not significant and therefore it is a good assumption to consider the heat losses in two consecutive days are equal.

$$Q_{L1} = Q_{L2} \quad (5.7)$$

By equating the Eq. (5.4) and (5.5) and removing Q_{L1} and Q_{L2} from both sides of the equations and with further simplifications Eq. 5.8 below can be obtained. The derivation calculation of Eq. 5.8 can be found in appendix 2.

$$\frac{\Delta T_1}{\Delta T_2} = 1 + \left(\frac{\rho_s C_s - \rho_w C_w}{m_w C_w} \right) V \quad (5.8)$$

where ρ_s is the density of energy storing materials (kg/m^3), ρ_w is the density of water (kg/m^3) and V is the volume of water replaced with energy storing material (m^3). The left-hand side of Eq. 5.8 expresses the temperature difference ratio which is a positive value but smaller than 1. The only condition to have the temperature difference ratio less than 1 satisfying Eq. 5.8 is:

$$\left(\frac{\rho_s C_s - \rho_w C_w}{m_w C_w} \right) V < 0 \quad (5.9)$$

Further simplification to Eq. 5.9 results in Eq. 5.10 below.

$$\rho_s C_s < \rho_w C_w \quad (5.10)$$

Equation 5.10 expresses the condition required for improving the performance of energy storing materials. It is concluded that the only parameters which can affect the performance of energy storing materials are density and specific heat capacity of energy storing materials.

5.5.1 Energy Storing Factor (β)

A new dimensionless parameter called *Energy storing factor* (β) can be defined using Eq. 5.11 below.

$$\beta = \frac{\rho_s C_s}{\rho_w C_w} \quad (5.11)$$

According to the above equation, for values of β smaller than 1, the energy storing material can cause an increase in temperature in comparison with the solar still without modification. For values of β greater than 1, the material will not be effective for energy storing. The value of β can be used to compare the performance of different energy storing materials in terms of their effect on the temperature difference (ΔT_2).

Equation 5.8 mentioned above expresses the relation between ΔT_1 and ΔT_2 in terms of ρ and C for energy storing material and basin water and also V and can be rearranged as:

$$\Delta T_1 = \left\{ 1 + \left(\frac{\rho_s C_s - \rho_w C_w}{m_w C_w} \right) V \right\} \Delta T_2 \quad (5.12)$$

The value of $1 + \left(\frac{\rho_s C_s - \rho_w C_w}{m_w C_w} \right) V$ in the above equation constant for a given solar still and therefore it can be expressed as:

$$\Delta T_1 = k \cdot \Delta T_2 \quad (5.13)$$

where k is a constant that depends on the properties of the energy storing material, basin water and the volume of basin water in the solar still. Figure 5.6 shows the variation of ΔT_1 against ΔT_2 for Steel, Copper, Aluminium, stone and glass.

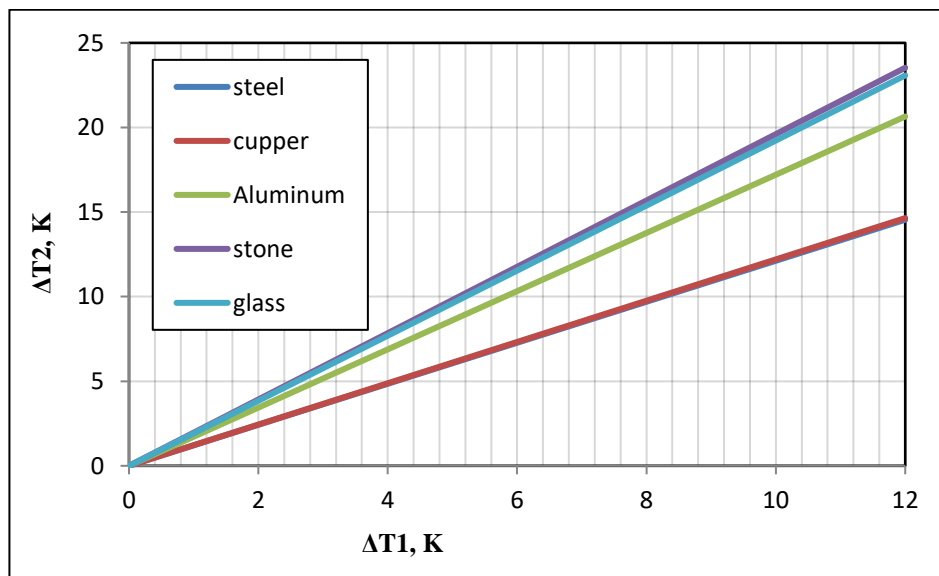


Figure 5.6 Water temperature rise for a modified solar still using energy storing materials versus water temperature rise for a solar still without modifications

According to Figure 5.6, steel, copper, aluminium, stone and glass can increase the basin water temperature in comparison with the basin water temperature in solar still without modifications. Consequently, the water production can be improved by using those materials as energy storing materials. Figure 5.7 shows the values of β for steel, copper, aluminium, stone and glass, which were used as an energy storing material in many studies. According to this figure, materials with the same value of energy storing factor have similar performance when they are used as an energy storing material. Table 5.4 expresses the values of ρ and C for steel, copper, aluminium, stone, glass and water. The results of Figure 5.7 are in a good agreement with the literature. As the value of β decreases, the performance of the energy storing material in the solar still improves.

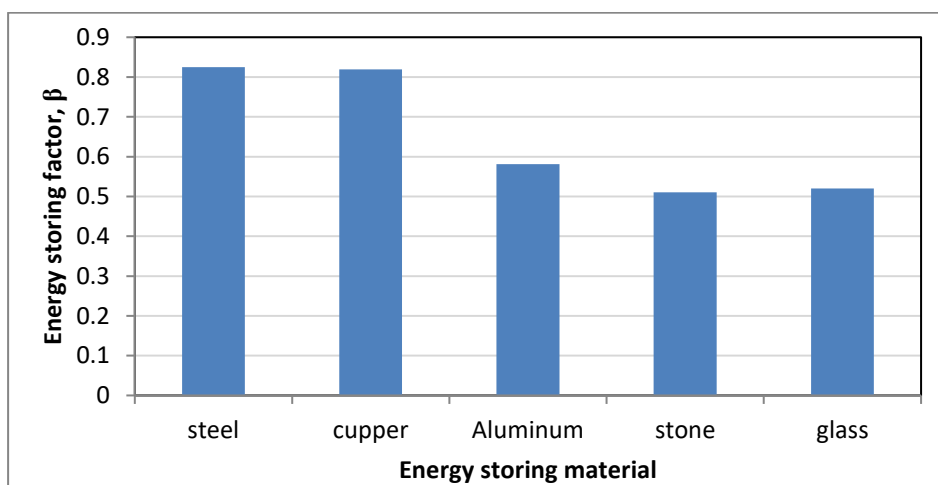


Figure 5.7 Variation of Energy storing factor, β for steel, copper, aluminium, stone and glass

Material	Density ρ (kg/m ³)	Specific heat capacity C (J/kg.K)
steel	7700	450
copper	8940	385
Aluminium	2712	900
stone	2550	840
glass	2600	840
water	1000	4200

Table 5.4 Density and specific heat capacity values

5.5.2 The Effect of The Shape of Energy Storing Materials

According to the experimental and analytical results in this study, the density and specific heat capacity of energy storing materials are the two main factors which affect the value of Energy storing factor β . It was also found that the value of β is proportional to the performance of energy storing materials. Two different shapes of steel with the same mass were included in the discussion given in this section. This could be due to the heat transfer performance for two different shapes. The performance of the two round shape samples in this study can be expressed by Eq. 5.14.

$$Q_1 = hA_1\Delta T_1 \quad (5.14)$$

where Q_1 is the rate of heat transfer which exposed to basin water from the solid shape (W), h is the convective heat transfer coefficient (W/m^2K) and ΔT_1 is the temperature difference for the solid shape in period of time t (s). Similarly, the performance of hollow shape can be expressed by Eq. 5.15.

$$Q_2 = hA_2\Delta T_2 \quad (5.15)$$

The samples were kept in a refrigerator to make sure the samples were started by the same temperature at the beginning of water production. The final temperature at period of t is assumed the same if the gradient of temperature in the basin is not considerable and therefore it can be concluded that $\Delta T_1 = \Delta T_2$. Equation (5.14) can be divided by Eq. (5.15) as follows.

$$\frac{Q_2}{Q_1} = \frac{h_2A_2\Delta T_2}{h_1A_1\Delta T_1} \quad (5.16)$$

Further simplification results in Eq. (5.17).

$$\frac{Q_2}{Q_1} = \frac{h_2A_2}{h_1A_1} \quad (5.17)$$

The convective heat transfer coefficient is a function of material, surface roughness, colour and size of materials. The two samples were the same materials and mass and surface roughness and colour and therefore it is a good assumption to consider $h_1=h_2$. Simplifying Eq. (5.17) results in Eq. (5.18).

$$\frac{Q_2}{Q_1} = \frac{A_2}{A_1} \quad (5.18)$$

The ratio of the two areas in Eq. (5.18) can be calculated for hollow and solid shapes.

$$\frac{A_2}{A_1} = \frac{R_2^2 - r_2^2 + R_2 l_2}{R_1^2 + R_1 l_1} \quad (5.19)$$

where R_2 , r_2 and l_2 are the external radius, internal radius and height in m , respectively for hollow sample. Similarly, R_1 and l_1 are the radius and height in m , respectively for solid sample. By considering the values for R_2 , r_2 , R_1 , l_2 and l_1 for solid and hollow samples it can be concluded that.

$$\frac{Q_2}{Q_1} > 1 \quad (5.20)$$

Or

$$Q_2 > Q_1 \quad (5.21)$$

Equation (5.21) expresses that the rate of heat exposed to basin water is greater for the hollow sample in comparison to solid sample. Therefore, the basin water temperature is raised rapidly for hollow sample in comparison to solid sample. Consequently, the water production started for the hollow sample earlier in comparison to solid sample. In other words, the time of water production for solar still is longer in comparison to solid sample. It is concluded that the shape of energy storing materials can affect their performances as well as density and specific heat capacity of energy storing materials. It was also concluded the wetted area is an important factor in relation to shape of energy storing materials. A larger wetted area can improve the energy storing material performance.

5.6 Theoretical Analysis

In the sections above, simple analysis was conducted in order to quantify the effect of shape and material of the energy storing media. In this section a full theoretical analysis is conducted in order to predict the temperature distribution and productivity of a double slope solar still. Figure 5.8 depicts a schematic drawing for the solar still that illustrates the flow of energy through the different zones in the still. The total incident solar radiation on the glass cover is not complexly absorbed by water. Instead, a fraction of this radiation is reflected to the ambient, another fraction is absorbed by the glass cover and the rest can penetrate the glass and reach the water inside the basin. These fractions depend on the material coefficients of reflection (R), absorption (α) and transmittance (τ). These three processes occur wherever the radiation hits any surface, i.e. water surface and the basin surface. Because the bottom surface of the still is usually painted black, the reflection from this surface can be ignored. In what follows, the analysis starts with an energy balance for each zone in the still. The current analysis is based on the following assumptions:

1. There is no vapour leakage in the still,
2. There is no temperature gradient along the glass cover thickness and the water depth,
3. The level of water in the basin is constant,
4. The condensation on the inner surface of the glass cover is film-wise condensation.

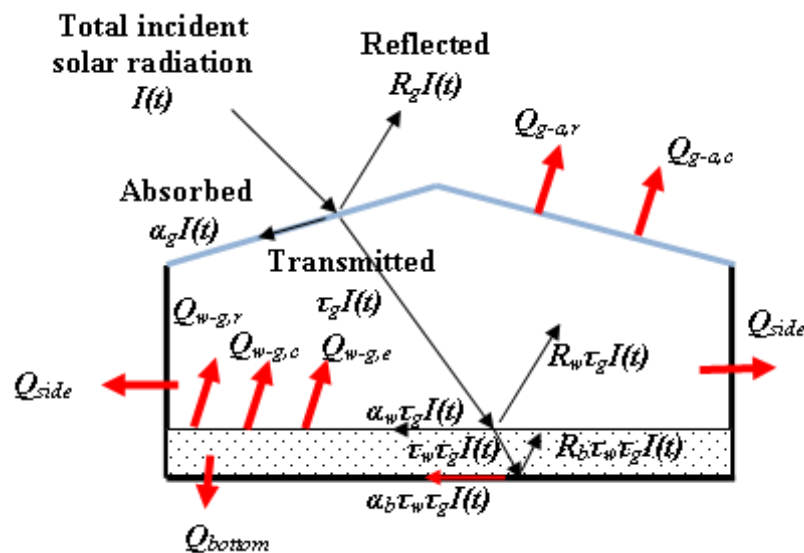


Figure 5.8 The energy flow inside a double slope solar still

For the glass cover, the summation of the absorbed solar energy and the heat transfer from the water inside the basin is balanced with the energy lost from the glass cover to the ambient. This balance equation can be written as follows in terms of W/m²:

$$\alpha_g I(t) + h_{rw}(T_w - T_g) + h_{cw}(T_w - T_g) + h_{ew}(T_w - T_g) = h_{tg}(T_g - T_a) \quad (5.22)$$

where $q_{rw}, q_{cw}, q_{ew}, q_{rg}, q_{cg}$ are the radiation heat flux from water to glass, the convection heat flux from water to glass, the evaporation heat flux, the radiation heat flux from the glass to the ambient and the convection heat flux from the glass surface to the ambient. The energy equation for the solar basin bottom plate is given by:

$$\alpha_b I(t) = q_b + q_{bg} + q_s \frac{A_{bw}}{A_{sw}} \quad (5.23)$$

where q_b, q_{bg}, q_s are the heat flux from the basin liner to water, from the basin liner to the ground and from the basin liner to the side walls of the still. The energy balance equation for the water mass is given by:

$$\alpha_w I(t) + q_b = m_w c_w \frac{dT_w}{dt} + q_{rw} + q_{cw} + q_{ew} \quad (5.24)$$

The heat transfer coefficients required for the above equations are obtained from Dutt et al. (1989) as follows.

$$h_{rw} = \frac{\varepsilon_{eff} \sigma (T_w^4 - T_g^4)}{T_w - T_g} \quad (5.25)$$

where ε_{eff} is the effective diffusivity, σ is the Stefan Boltzmann constant, T_w is the water temperature. The effective diffusivity is given by:

$$\varepsilon_{eff} = \frac{1}{\frac{1}{\varepsilon_w} + \frac{1}{\varepsilon_g} - 1} \quad (5.26)$$

where $\varepsilon_w = 0.96$ and $\varepsilon_g = 0.88$ are the emissivity of water and glass, respectively.

$$h_{cw} = 0.884 \left[T_w - T_g + \frac{(P_w - P_g)T_w}{268900 - P_w} \right]^{1/3} \quad (5.27)$$

where P_w and P_g are the vapour pressure estimated at the water and glass temperature, respectively.

$$P_w = \exp \left[25.317 - \frac{5144}{T_w} \right] \quad (5.28)$$

$$P_g = \exp \left[25.317 - \frac{5144}{T_g} \right] \quad (5.29)$$

$$h_{ew} = 0.016273 h_{cw} \frac{P_w - P_g}{T_w - T_g} \quad (5.30)$$

The combined radiation and convection heat transfer coefficient from the glass cover to the ambient depends on the wind speed (V) and is given by:

$$h_{ig} = 5.7 + 3.8V \quad (5.31)$$

Equations (5.22), (5.23) and (5.24) can be written in the following forms:

$$I(t)\alpha_g + h_{tw}(T_w - T_g) = h_{tg}(T_g - T_a) \quad (5.32)$$

$$I(t)\alpha_w + h_w(T_b - T_w) = m_w c_w \frac{dT_w}{dt} + h_{tw}(T_w - T_g) \quad (5.33)$$

$$I(t)\alpha_b = h_w(T_b - T_w) + h_b(T_b - T_a) \quad (5.34)$$

The glass and basin temperature can be obtained from Eq. (5.32) and (5.34), respectively.

$$T_g = \frac{\alpha_g I(t) + h_{tw}T_w + h_{tg}T_a}{h_{tw} + h_{tg}} \quad (5.35)$$

$$T_b = \frac{\alpha_b I(t) + h_w T_w + h_b T_a}{h_w + h_b} \quad (5.36)$$

Substituting T_g and T_b into Eq. (5.33) and with some re-arrangements, the following equation can be obtained:

$$\frac{dT_w}{dt} + aT_w = f(t) \quad (5.37)$$

Solving this differential equation with the boundary conditions $T_w = T_{w0}$ at time $t = 0$ and $T_g = T_{g0}$ at time $t = 0$, the water temperature can be obtained as follows:

$$T_w = \frac{f(t)}{a}(1 - \exp(-at)) + T_{w0} \exp(-at) \quad (5.38)$$

Using Eq. (5.35), the glass temperature can be obtained. The hourly distillate output can be obtained from the following equation:

$$m = \frac{h_{ew}(T_w - T_g)}{h_{fg}} \times 3600 \quad (5.39)$$

where:

$$a = \frac{U}{m_w c_w}, \quad f(t) = \frac{(\alpha\tau)_{eff} I(t) + UT_a}{m_w c_w}$$

$$(\alpha\tau)_{eff} = \alpha_b \frac{h_w}{h_w + h_b} + \alpha_w + \alpha_g \frac{h_{tw}}{h_{tw} + h_{tg}}$$

$$U = \frac{1}{\frac{1}{h_w} + \frac{L_{ins}}{k_{ins}} + \frac{h_{rb} + h_{cb}}{h_{rb} + h_{cb}}} + \frac{h_{tw} h_{tg}}{h_{tw} + h_{tg}}$$

$$h_b = \frac{1}{\frac{L_{ins}}{k_{ins}} + \frac{h_{rb} + h_{cb}}{h_{rb} + h_{cb}}}$$

The equations above were applied and solved for the conventional solar still with no modifications in order to verify the experimental measurements. Figure 5.9 and Figure 5.10 depict the measured water and glass temperature versus time, respectively, compared with the predictions using the equations above. It is obvious that the model predicts the trend very well with some deviations from the measured values. These deviations may be arising from the uncertainties in the empirical correlations that were used to predict the heat transfer coefficients required for the model. However, when the cumulative water production was predicted and compared with the measurements in Figure 5.11, the predicted values are in a good agreement with the measured values. This figure was created using Eq. (5.39). This means that although the model has some deviations in the predicted temperatures, the temperature difference between water and glass is predicted very well. This explains the success of the model in

predicting the cumulative water production. The results of this analysis conducted in the present study indicate that the measurement system is verified.

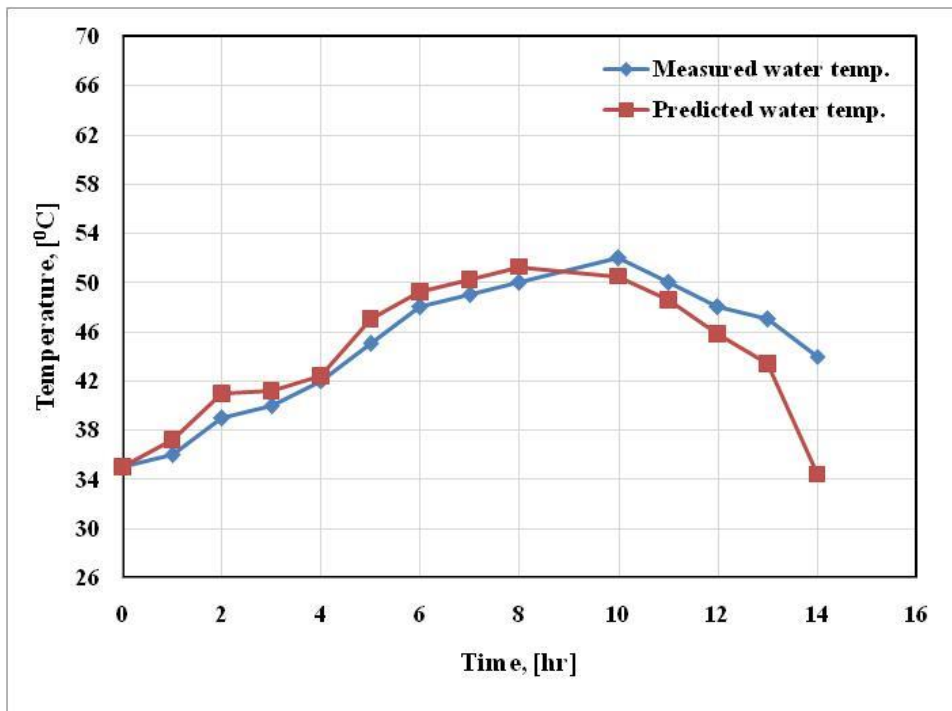


Figure 5.9 The measured basin water temperature versus time compared with the prediction using the theoretical model

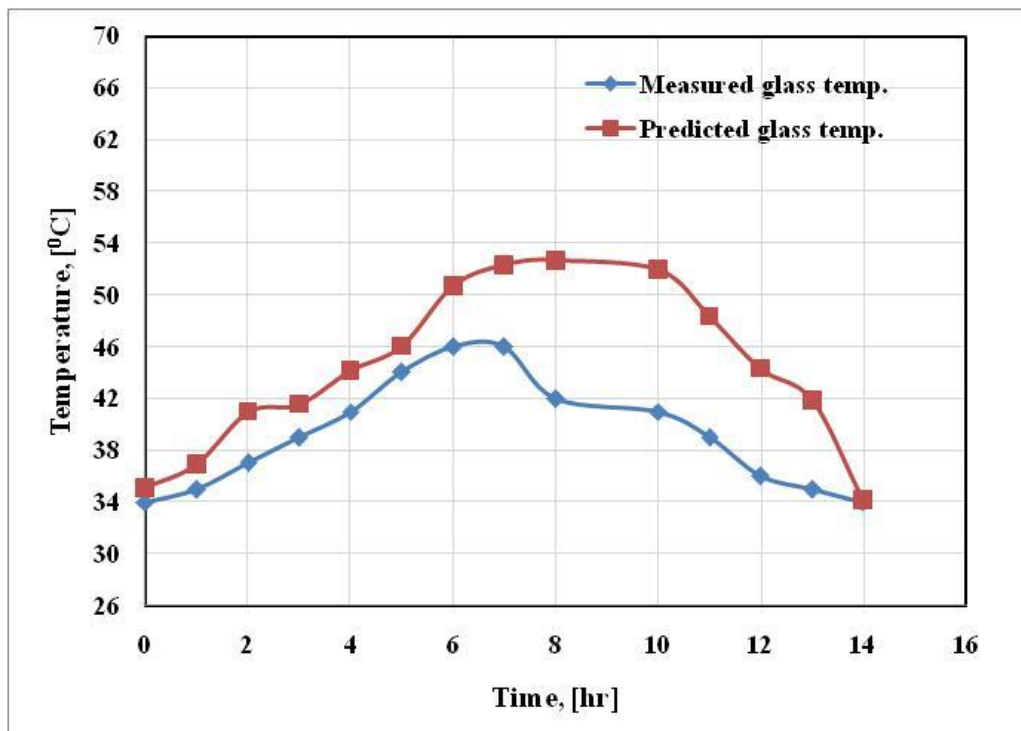


Figure 5.10 The measured glass temperature versus time compared with the prediction using the theoretical model

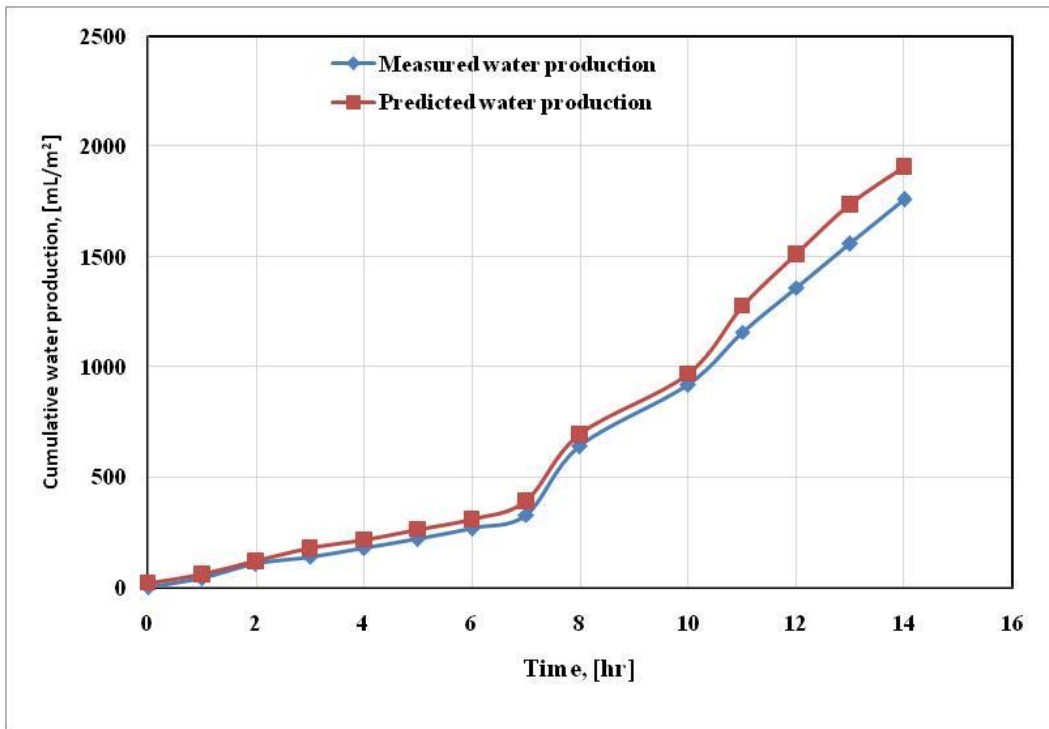


Figure 5.11 The measured cumulative water production versus time compared with the prediction using the theoretical

5.7 Summary

In this chapter, the effect of water depth and ambient temperature on the thermal performance and productivity of the solar still was correlated by fitting the experimental data using the best fit equation. Additionally, the effect of energy storing materials was quantified and it was found that the material density and heat capacity are the important factors. In the end, a theoretical analysis was conducted only for one case, which is the conventional solar still with no modifications. The results indicated that there is a reasonable agreement with the predictions and the measurements. This can verify the experimental measurements system.

6. Chapter Six: Conclusions and Future Work

6.1 Conclusions

Solar stills have been studied analytically and experimentally in this thesis. It has concluded that solar stills are one of the best solution for the problems of obtaining fresh water in the world. The main achievements of this study are listed as follows:

1. Solar stills are the most available and affordable technique to prepare fresh water particularly in remote or coastal areas in the Kuwaiti climate conditions.

The quality of water produced by solar still was tested in terms of main parameters (PH value, electrical conductivity (Ec), total dissolved solids (TDS) and salinity (Sa). the study has found that the main quality parameters are all within the WHO standard range.

2. The study has concluded that energy storing materials can increase the daily water production in solar stills. The performance of energy storing materials is related to their size, material and shape. A new dimensionless parameter called Energy storing factor (β) is the main factor which can affect the performance of energy storing materials in terms of increasing water production in solar stills.

$$\beta = \frac{\rho_s C_s}{\rho_w C_w}$$

Where ρ_s is the density of energy storing materials (kg/m^3), ρ_w is the density of basin water (kg/m^3), C_s is the specific heat capacity of energy storing material ($J/kg.K$) and C_w is the specific heat capacity of water in the basin ($J/kg.K$).

3. The study has found that for the values of $\beta < 1$ the energy storing materials can improve the water production and for values of $\beta > 1$ using energy storing materials can cause a reduction in water production.
4. The study has found that in addition to density and specific heat capacity of energy storing materials, the shape of energy storing materials is an important factor which can affect the water production in solar stills. It was found that greater wetted area for energy storing materials corresponds to higher water production performance.

5. The study has found that daily water production is linearly depended on maximum production rate. Higher maximum production rate is corresponding to higher daily water production. A linear correlation was developed to express the relation between maximum production rate and daily water production.

6. The study has found that the water depth (d) can influence water production (y) significantly. The correlation below was developed using experimental measurements.

$$y = 5.3085d^{-0.3031}$$

7. The water production is proportional to ambient average temperature (T_{av}) linearly. A linear correlation was developed using the experimental data.

8. Maximum production rate is proportional to average ambient temperature linearly. A linear correlation was developed to express the relation between maximum production rate and average ambient temperature. The calculated values for production using the correlation were in a good agreement with measurements.

9. The round hollow steel pieces are the best among the investigated shapes. The external cooling of the glass cover plate is not very effective.

10. The total water production increases significantly as the water depth decreases.

11. Using gravel as energy storing material can improve the productivity of a solar still, which is slightly lower than the productivity of solar stills with metallic energy storing materials. If the cost was considered, gravel could be a good option and gravel with smaller size is more favourable.

12. Phase change materials can increase the production rate and total daily water production significantly compared to the other materials. It achieved about 53% improvements in the total production.

6.2 Future Work

For further improvements in the performance of double slope solar stills, the following recommendations can be adopted for future work:

- 1.** The test of a different design configurations
- 2.** Testing a wide range of phase change materials to as energy storage materials.
- 3.** Incorporation of photovoltaic and electric heaters to increase the evaporation rate.
- 4.** The use of heat pump driven by renewable energy to work as a heat source and to supply cooling to the external transparent cover plate

REFERENCES

Abbaszadehmosayebi, G., Ganippa, L. (2014a). “Determination of specific heat ratio and error analysis for engine heat release calculations”. *Applied Energy* .Vol.122, pp, 143–150

Abbaszadehmosayebi, G. and Ganippa. L. (2014b). “Characterising Wiebe Equation for Heat Release Analysis based on Combustion Burn Factor (Ci)”. *Fuel*. Vol. 119, pp. 301-307.

Abdullah. A. S. (2013). “Improving the performance of stepped solar still”. *Desalination*. Vol. 319, pp. 60-65.

Abdul-Wahab, S. A. and Al-Hatmi, Y.Y. (2013). “Performance evaluation of an inverted absorber solar still integrated with a refrigeration cycle and an inverted absorber solar still”. *Energy for Sustainable Development*. Vol. 17, No. 6, pp. 642-648.

Abu-Zeid M. A. E., Yaqin Zhang, Hang Dong, Lin Zhang, Huan-Lin Chen, Lian Hou, (2015), A comprehensive review of vacuum membrane distillation technique, *Desalination* 356 (2015) 1–14

Ahsan, A., Islam, S. M. K., Fukuhara T., and Ghazali H.A. (2010). “Experimental study on evaporation, condensation and production of a new tubular solar stil”. *Desalination* . Vol. 260, No. 1-3, pp. 172-179.

Ahsan A., Rahman A., Shanableh, A., Daud, N. N. N., Mohammed, T. A., and Mabrouk, A.N.A. (2013). “Life cycle cost analysis of a sustainable solar water distillation technique”. *Desalination and Water Treatment*. Vol. 51, No. 40-42, pp. 7412-7419.

Ahsan, A., Imteaz, M., Thomas, U. A., Azmi, M., Rahman, A., and Daud, N. N. N. (2014). “Parameters affecting the performance of a low cost solar still”. *Applied Energy*. Vol. 114, pp. 924-930.

Al Otaibi, A. and Al Jandal, S. (2011). “Solar photovoltaic power in the state of Kuwait”, 37th IEEE Photovoltaic Specialists Conference (PVSC), IEEE.

Alaudeen, A., Johnson, K., Ganasundar, P., Abuthahir, A. S., and Srithar, K . (2014). “Study on stepped type basin in a solar still”. *Journal of King Saud University - Engineering Sciences* Vol. 26, No. 2, pp. 176-183.

Al-shorfa.com (2015) Al-Mashareq, Available at: http://al-shorfa.com/en_GB/articles/meii/features/2013/11/01/feature-03; Accessed: 30.01.2015

Akash B. A., M. S. Mohsen, O. Osta, Y. Elayan, Experimental evaluation of a single-basin solar still using different absorbing materials, *Renewable Energy*, vol. 14, pp. 307 – 310, 1998.

Arjunan, T.V., Aybar, H. S., and Nedunchezian, N. (2009). “Status of solar desalination in India”. *Renewable and Sustainable Energy Reviews*. Vol. 13, No. 9, pp. 2408-2418.

Arunkumar, T., Denkenberger, D., Ahsan, A., and Jayaprakash, R. (2013). “The Augmentation Of Distillate Yield By Using Concentrator Coupled Solar Still With Phase Change Material”. *Desalination*. Vol. 314, pp. 189-192.

authors.library.caltech.edu (2016) “Overview of Electron Microscopy”, Available at: http://authors.library.caltech.edu/5456/1/hrst.mit.edu/hrs/materials/public/ElectronMicroscope/EM_HistOverview.htm. Accessed on: 22.02.2016.

Aybar, H. S and Assefi, H. (2009). “Simulation of a Solar Still to Investigate Water Depth and Glass Angle”. *Desalination Water Treat.* Vol. 7, pp. 35-40

Ayoub, G. M., Malaeb. L. and Saikaly, P.E. (2013). “Critical variables in the performance of a productivity-enhanced solar still”. *Solar Energy*. Vol. 98, Part C, pp. 472-484.

Ayuthaya, R. P, N., Namprakai, P., and Ampun, W. (2013). “The thermal performance of an ethanol solar still with fin plate to increase productivity”. *Renewable Energy*, Vol. 54, pp. 227-234.

V. Belessiotis, S. Kalogirou, E. Delyannis, *Thermal Solar Distillation, Methods and Systems*, Academic Press, Elsevier 2016.

Boubekria, M., Cheknane, A., and Ali, M. (2013). "Modeling and simulation of the continuous production of an improved solar still coupled with a photovoltaic/thermal solar water heater system". *Desalination*. Vol. 331, pp. 6-15.

Deshmukh H. S. and S.B. Thombre, (2017), Solar distillation with single basin solar still using sensible heat storage materials, *Desalination* 410 (2017) 91–98

El-Bahi, A., and Inan, D. A.(1999). "Solar still with minimum inclination, coupled to an outside condenser". *Desalination*; Vol. 123, No. 1, pp.79-83.

El-Agouz, S. A. (2014). "Experimental investigation of stepped solar still with continuous water circulation". *Energy Conversion and Management*. Vol. 86, pp. 186-193.

El-Dessouky H. T. and Ettouney H. M., *Fundamentals of salt water desalination*, Elsevier Science B. V., 2002.

Elfasakhany A., Performance assessment and productivity of a simple-type solar still integrated with nanocomposite energy storage system, *Applied Energy* 183 (2016) 399–407.

El-Samadony, Y.A.F., and Kabeel, A. E. (2014). "Theoretical estimation of the optimum glass cover water film cooling parameters combinations of a stepped solar still". *Energy*, Vol. 68, pp. 744-750.

El-Sebaili, A. A., Aboul-Enein, S., and El-Bialy, E. (2000). "Single Basin Solar Still With Baffle Suspended Absorber". *Energy Conversion and Management*. Vol. 41, No. 7, pp. 661-675.

El-Sebaili, A. A., Al-Ghamdi, A. A., Al-Hazmi, F. S., and Faidah, A. S. (2009). "Thermal performance of a single basin solar still with PCM as a storage medium". *Applied Energy*, Vol. 86, No. 7-8, pp. 1187-1195.

El-Sebaili A. A., M. El-Naggar, Year round performance and cost analysis of a finned single basin solar still *Applied Thermal Engineering* 110 (2017) 787–794.

Eltawil, M. A., and Omara. Z. M. “Enhancing the solar still performance using solar photovoltaic, flat plate collector and hot air”. *Desalination*. Vol. 349, pp. 1-9.

en.wikipedia.org (2014) “Adelaide Desalination Plant”, Available at: http://en.wikipedia.org/wiki/Adelaide_Desalination_Plant. Accessed: 23.11.2014

en.wikipedia.org (2015) “Transmission electron microscopy”, Available at: http://en.wikipedia.org/wiki/Transmission_electron_microscopy, Accessed: 15.03.2015.

Esfahani, J. A., Rahbar, N., and Lavvaf, M. (2011). “Utilization of thermoelectric cooling in a portable active solar still-An experimental study on winter days”. *Desalination*. Vol. 269. No.1-3, pp. 198-205.

Farid, M. and Hamad, F. (1993). “Performance of a single-basin solar still”. *Renew Energy*, Vol. 3, No.1, pp. 75-83.

Fatani, A. A., Zaki, G. M., and Al-Turki, A. (1994). “Improving the yield of simple basin solar stills as assisted by passively cooled condensers”. *Renew Energy*, Vol. 4, No. 4, pp. 377-386.

forum.daffodilvarsity.edu.bd (2015) “Transmission Electron Microscope (TEM)”, Available at: <http://forum.daffodilvarsity.edu.bd/index.php?topic=9749.0>, Available at: 15.03.2015.

Gao, C. J. and Chen, G. H. (2004). *Handbook for desalination technology and engineering*. China: Chemical Industry Press.

Ghaffour, N., Missimer, T. M., and Amy, G. L. (2013). “Technical review and evaluation of the economics of water desalination: Current and future challenges for better water supply sustainability”. *Desalination*. Vol. 309, pp. 197-207.

Ghaffour, N., Bundschuh, J., Mahmoudi, H., and Goosen, M.F.A. (2015). “Renewable energy-driven desalination technologies: A comprehensive review on challenges and potential applications of integrated systems”. *Desalination*. Vol. 356, pp. 94-114.

Ghoneyem, A. and Lleri, A. (1997). "Software to analyze solar stills and an experimental study on the effects of the cover". *Desalination*. Vol. 114, No. 1, pp. 37-44.

González D., José Amigoa, Francisco Suáreza, Membrane distillation: Perspectives for sustainable and improved Desalination, *Renewable and Sustainable Energy Reviews* 80 (2017) 238–259

Gorjian, S., Ghobadian, B., Hashjin, T.T., and Banakar, A. (2014). "Experimental performance evaluation of a stand-alone point-focus parabolic solar still". *Desalination*. Vol. 352, pp. 1-17.

Greenlee, L. F., Lawler, F. D., Freeman, B. D., Marrot, B., and Moulin. P. (2009). "Reverse osmosis desalination: Water sources, technology, and today's challenges". *Water Research*. Vol. 43, No. 9, pp. 2317-2348.

Halima, H. B., Frikha, N. and Slama, R. B. (2014). "Numerical investigation of a simple solar still coupled to a compression heat pump". *Desalination*. Vol. 337, pp. 60-66.

Hoffman, A. R. (2008). *Water security: a growing crisis and the link to energy*. AIP Conference Proceedings; pp. 55-63.

Kabeel, A. E., Omara, Z. M. and Essa. F. A. (2014). "Improving the performance of solar still by using nanofluids and providing vacuum". *Energy Conversion and Management*. Vol. 86, pp. 268-274.

Kabeel, A. E., Hamed, A.M., and El-Agouz, S. A. (2010). "Cost analysis of different solar still configurations". *Energy*. Vol. 35, pp. 2901-2908.

Kabeel A.E., Mohamed Abdelgaied Improving the performance of solar still by using PCM as a thermal storage medium under Egyptian conditions *Desalination* 383 (2016) 22–28.

Kalogirou, S. A. (2005). "Seawater desalination using renewable energy sources". *Progress in Energy and Combustion Science*. Vol. 31, No. 3, pp. 242-281.

Kamal, W. A. (1988). "A theoretical and experimental study of the basin-type solar still under the arabian gulf climatic conditions". *Solar and Wind Technology*. Vol. 5, No. 2, pp. 147-157.

Kandasamy, S., Vellingiri, M., Sengottain, S., and Balasundaram, J. (2013). "Performance correlation for single-basin double-slope solar still". *International Journal of Energy and Environmental Engineering*. Vol. 4, No. 4, pp.1-6.

Kannan, R., Selvaganesan, C., Vignesh, M., Babu, B. R., Fuentes, M., Vivar, M., Skryabin, I., and Srithar, K. (2014). "Solar still with vapor adsorption basin: Performance analysis". *Renewable Energy*. Vol. 62, pp. 258-264.

Kaviti A.K., Akhilesh Yadav, Amit Shukla, Inclined solar still designs: A review *Renewable and Sustainable Energy Reviews* 54 (2016) 429–451.

Kaushal, A. And Varun. (2010). "Solar stills: A review". *Renewable and Sustainable Energy Reviews*. Vol. 14, No.1, pp. 446-453.

Khalifa, A. J. N., and Ibrahim, H. A. (2010). "Effect of inclination of the external reflector of simple solar still in winter: An experimental investigation for different cover angles". *Desalination*. Vol. 264, No. 1-2, pp. 129-133

Khalifa A. J. N., Ahmad M. Hamood, Performance correlations for basin type solar stills, *Desalination* 249 (2009) 24–28

J. Kucera, *Desalination: Water from Water*, Scrivener Publishing LLC and John Willey and Sons Inc. 2014.

Kumar, S., and Tiwari, G. N. (2009). "Life cycle cost analysis of single slope hybrid (PV/T) active solar still". *Applied Energy*. Vol. 86, No. 10, pp. 1995-2004.

Maalej, A.Y. (1991). "Solar still performance". *Desalination*, Vol. 82, pp. 197-205.

Madhlopa, A. (2014). "Modelling radiative heat transfer inside a basin type solar still". *Applied Thermal Engineering*. Vol. 73, No.1, pp. 707-711.

Madhlopa, A., and Clarke, J. A. (2013). “Computation of irradiance in a solar still by using a refined algorithm”. *Renewable Energy*. Vol. 51, pp. 13-21.

Malaeb, L., Ayoub, G. M., and Al-Hindi, M. (2014). “The Effect of Cover Geometry on the Productivity of a Modified Solar Still Desalination Unit”. *Energy Procedia*. Vol. 50, pp. 406-413.

Malik, M. A. S., Tiwari, G. N., Kumar, A. and Sodha, M. S. (1982). *Solar Distillation*, Oxford, U.K: Pergamon Press 1982.

Mamouri, S. J., Deramia, G. H., Ghiasib, M., Shafii, M.B and Shiee, Z. (2014). “Experimental investigation of the effect of using thermosyphon heat pipes and vacuum glass on the performance of solar still”. *Energy*. Vol. 75, pp. 501-507.

Manju S., Sagar N., (2017), Renewable energy integrated desalination: A sustainable solution to overcome future fresh-water scarcity in India, *Renewable and Sustainable Energy Reviews* 73 (2017) 594–609

Manokar, A. M., Murugavel, K. K., and Esakkimuthu, G. (2014). “Different parameters affecting the rate of evaporation and condensation on passive solar still – A review”. *Renewable and Sustainable Energy Reviews*. Vol. 38, pp. 309-322.

Martin, C. L, and Goswami, D. Y. (2005). “Solar Energy Pocket Reference”. *International Solar Energy Society*, pp. 1-96. Freiburg, Germany.

Mathioulakis, E., and Belessiotis, V. (2003). “Integration of solar still in a multi-source, multiuse environment”. *Solar Energy*; Vol. 75, No. 5, pp. 403-411.

Mehanna, M., Saito, T., Yan. J., Hickner, M., Cao, X., Huang, X., and Logan, B. E. (2010). “Using microbial desalination cells to reduce water salinity prior to reverse osmosis”. *Energy and Environmental Science*, Vol. 3, pp. 1114-1120.

Methnani M. Influence of fuel costs on seawater desalination options. *Desalination*. 2007; 205(1-3):332-9.

Muftah, A. F., Alghoul, M. A., Fudholi, A., Abdul-Majeed, M.M., and Sopian. K. (2014). "Factors affecting basin type solar still productivity: A detailed review". *Renewable and Sustainable Energy Reviews*. Vol. 32, pp. 430-447.

Murugavel, K. K., Chockalingam, Kn. K. S. K., and Srithar, K. (2008). "Progresses in improving the effectiveness of the single basin passive solar still". *Desalination*. Vol. 220. No. 1-3, pp. 677-686.

Murugavel, K. K., Anburaj, P., Hansen, S., and Elango, T. (2013). "Progresses in inclined type solar stills". *Renewable and Sustainable Energy Reviews*. Vol.20, pp. 364-377.

Nafey A. S., M. Abdelkader, A. Abdelmotalip, A.A. Mabrouk, Solar still productivity enhancement, *Energy Conversion and Management*, 42, 1401 – 1408, 2001.

Naim M. M., M. A. Abd El Kawi, Non conventional solar still, Part 1: Nonconventional solar stills with charcoal particles as absorbing medium, *Desalination* 153, 55 – 64, 2002a.

Naim M. M., M. A. Abd El Kawi, Non conventional solar still, Part 1: Nonconventional solar stills with energy storage element, *Desalination* 153, 71 – 80, 2002b.

Naim, M. M., Mervat, A., and El Kawi, A. (2003). "Non-conventional solar stills Part1. Non-conventional solar stills with charcoal particles as absorber medium. *Desalination*. Vol. 153, No. 1-3, pp. 55-64.

Namprakai, P. and Hirunlabh, J. (2007). "Theoretical and experimental studies of an ethanol basin solar stil". *Energy*; Vol. 32, No. 12, pp. 2376-2384.

Nithyanandam C., G. Baskar and Nalin Kant Mohanty, Design and fabrication of the passive solar still using blue metal stone, *International Journal of Ambient Energy*, 2017, Vol. 38, No. 2, 171–177.

Omara, Z. M., Eltawilb, M. A., and ElNashar, A. E. (2013). “A new hybrid desalination system using wicks/solar still and evacuated solar water heater”. *Desalination*. Vol. 325, pp. 56-64.

Omara, Z. M., Kabeel, A. E., and Younes, M. M. (2014). “Enhancing the stepped solar still performance using internal and external reflectors”. *Energy Conversion and Management*. Vol. 78, pp. 876-881.

Omaraa, Z. M., A.S. Abdullah, A.E. Kabeel, F.A. Essaa, The cooling techniques of the solar stills' glass covers – A review, *Renewable and Sustainable Energy Reviews* 78 (2017) 176–193

Panchal, H. N. (2015). “Enhancement of distillate output of double basin solar still with vacuum tubes”. *Journal of King Saud University - Engineering Sciences*. Vol. 27, No. 2, pp. 170-175.

Panchala H. N. Sanjay Patel, An extensive review on different design and climatic parameters to increase distillate output of solar still, *Renewable and Sustainable Energy Reviews* 69 (2017) 750–758.

Porta, M. A, Chargoy, N., and Fernandez, J. L. (1997). “Extreme operating conditions in shallow solar stills”. *Solar Energy*. Vol. 61, No. 4, pp. 279-286.

Qiblawey, H. M., and Banat, F. (2008). “Solar thermal desalination technologies”. *Desalination*. Vol. 220, pp.633-644.

Rahbar, N. and Esfahani, J. A. (2012). “Experimental study of a novel portable solar still by utilizing the heatpipe and thermoelectric module”. *Desalination*. Vol. 284, pp. 55-61.

Rajaseenivasan, T., Elango, T., and Murugavel. K. K. (2013a.). “Comparative study of double basin and single basin solar stills”. *Desalination*. Vol. 309, pp. 27-31.

Rajaseenivasan, T., Murugavel, K. K., Elango, T. And Hansen, S. R. (2013b.). “A review of different methods to enhance the productivity of the multi-effect solar stil”. *Renewable and Sustainable Energy Reviews*. Vol.17, pp. 248-259.

Rajaseenivasan, T. and Murugavel, K. K. (2013c). “Theoretical and experimental investigation on double basin double slope solar still”. *Desalination*. Vol. 319, pp. 25-32.

Rijsberman FR. Water scarcity: Fact or fiction?. *Agricultural Water Management*. 2006; 80(1-3):5-22.

Rao SM, Mamatha P. Water quality in sustainable water management. *Current science*. 2004; 87(7):942-7.

Sadineni S. B., Hurt, R., Halford, C. K, and Boehm, R. F. (2008). “Theory and experimental investigation of a weir-type inclined solar still”. *Energy*. Vol. 33, No. 1, pp. 71-80.

Sakthivel, M., Shanmugasundaram, S., and Alwarsamy, T. (2010). “An experimental study on a Regenerative solar still with energy storage medium – jute cloth”. *Desalination*. Vol. 264, No.1-2, pp. 24-31.

Samee, M. A., Mirza, U. K., Majeed, T., Ahmad, N. (2007). “Design and performance of a simple and single basin solar still”. *Renewable and Sustain-able Energy Reviews*. Vol. 11, No. 3, pp. 543-549.

Sampathkumar, K., and Senthilkumar, P. (2012). “Utilization of solar water heater in a single basin solar still-An experimental study”. *Desalination*. Vol. 297, No. 3, pp. 8-19.

Sampathkumar. K., Arjunan, T.V., Pitchandi, P., and Senthilkumar, P. (2010). “Active solar distillation – a detailed review”. *Renewable and Sustainable Energy Reviews*. Vol.14, No. 6, pp. 1503-1526.

Samuel D. G. H., P.K. Nagarajan, Ravishankar Sathyamurthy, S.A. El-Agouz, E. Kannan, Improving the yield of fresh water in conventional solar still using low cost energy storage material, *Energy Conversion and Management* 112 (2016) 125–134.

Sathyamurthy, R., Kennady, H. J., Nagarajan, P. K., and Ahsan, A. (2014). “Factors affecting the performance of triangular pyramid solar still”. *Desalination*. Vol. 344, pp. 383-390.

Sathyamurthy R. P.K. Nagarajan, S.A. El-Agouz, V. Jaiganesh, P. Sathish Khanna, Experimental investigation on a semi-circular trough-absorber solar still with baffles for fresh water production, *Energy Conversion and Management* 97 (2015) 235–242.

Shalaby S. M., E. El-Bialy, A.A. El-Sebaii, An experimental investigation of a v-corrugated absorber single-basin solar still using PCM, *Desalination* 398 (2016) 247–255.

Seametrics.com (2014) “5 Countries Most Threatened by Water Shortages”, Available at: <http://www.seametrics.com/blog/5-countries-most-threatened-by-water-shortages/>. Available: 22.11.2014.

Sharshir S. W., Guilong Peng, Lirong Wu, F.A. Essa, A.E. Kabeel, Nuo Yang, The effects of flake graphite nanoparticles, phase change material, and film cooling on the solar still performance, *Applied Energy* 191 (2017) 358–366.

Shukla, A. Karunesh Kant, Atul Sharma, Solar still with latent heat energy storage: A review, *Innovative Food Science and Emerging Technologies* 41 (2017) 34–46

Sivakumar, V. and Sundaram, E. G (2013). “Improvement techniques of solar still efficiency: A review”. *Renewable and Sustainable Energy Reviews*, Vol. 28, pp. 246-264.

Srivastava, P. K and Agrawal, S. K. (2013a). “Winter and summer performance of single sloped basin type solar still integrated with extended porous fins”. *Desalination*. Vol. 319, pp. 73-78.

Srivastava, P. K, and Agrawal, S.K. (2013b). “Experimental and theoretical analysis of single sloped basin type solar still consisting of multiple low thermal inertia floating porous absorbers”. *Desalination*. Vol. 311, pp. 198-205.

Suneesh, P.U., Jayaprakash, R., Arunkumar, T., and Denkenberger. D. (2014). “Effect of air flow on “V” type solar still with cotton gauze cooling”. *Desalination*. Vol. 337, pp. 1-5.

Taghvaei, H., Taghvaei, H., Jafarpur, K., Estahbanati, K. R.M., Feilizadeh, M., Feilizadeh, M., and Ardekani, S. A (2014). “A thorough investigation of the effects of water depth on the performance of active solar stills”. *Desalination*, Volume 347, 15 August 2014, Pages 77-85.

Tiwari, G. N., Singh, H. N and Tripathi, R. (2003a). “Present status of solar distillation”. *Solar Energy*. Vol. 75, No. 5, pp. 367-373.

Tiwari, G. N., Shukla, S. K., and Singh, I. P. (2003b). “Computer modeling of passive/active solar stills by using inner glass temperature”. *Desalination*. Vol. 154, No. 2, pp. 171-185.

Tiwari, G. N., Dimri, V., and Chel, A. (2009). “Parametric study of an active and passive solar distillation system: Energy and exergy analysis”. *Desalination*. Vol. 242, No. 1-3, pp. 1-18.

unwater.org (2014) <http://www.unwater.org/worldwaterday/about-world-water-day/world-water-day-2014-water-and-energy/en/>. Accessed: 19.11.2014

Velmurugan. V, and Srithar, K. (2007). “Solar stills integrated with a mini solar pond - analytical simulation and experimental validation”. *Desalination*. Vol. 216, No. 1-3, pp. 232-241.

Velmurugan. V, and Srithar, K. (2011). “Performance analysis of solar stills based on various factors affecting the productivity- a review”. *Renewable and Sustainable Energy Reviews*. Vol. 15, No. 2, pp. 1294-1304.

Voropoulos, K., Mathioulakis, E., and Belessiotis, V. (2001). “Experimental investigation of a solar still coupled with solar collectors”. *Desalination*. Vol. 138, No. 1-3, pp. 103-110.

Voropoulos, K., Mathioulakis, E., and Belessiotis, V. (2003). “Experimental investigation of the behaviour of a solar still coupled with hot water storage tank”. *Desalination*. Vol. 156, No.1-3 pp. 315-322.

WWAP (United Nations World Water Assessment Programme), Water for a sustainable world. The United Nations World Water Development Report. Paris, UNESCO: 2015.

The World Health Organization, *Water Facts & Water Stories from Across the Globe*, http://www.theworldwater.org/water_thefacts.php (2010).

Weather and climate.com (2015) “Weather and Climate Information”, Available at: <http://www.weather-and-climate.com>. Accessed: 27.12.2015.

www.technologystudent.com (2015) “Advantages and Disadvantages of Solar Power”, Available at: <http://www.technologystudent.com/energy1/solar7.htm>. Accessed: 11.01.2015

www.imeche.org (2015) “Promoting sustainable energy use and engineering sustainable supply is vital to our economy and modern lifestyles”, Energy Theme, Available at: <http://www.imeche.org/knowledge/themes/energy/energy-supply/fossil-energy/when-will-oil-run-out>. Accessed: 11.01.2015.

www.sciencedirect.com (2015) “ScienceDirect”, Available at: <http://www.sciencedirect.com/>; Accessed: 11.01.2015

Xiao, G., Wang, X., Ni, M., Wang, F., Zhu, W., Luo, Z., and Cen, K. (2013). “A review on solar stills for brine desalination”. *Applied Energy*. Vol. 103, pp. 642-652.

Zeroual, M., Bouguettaia, H., Bechki, D., Boughali, S., Bouchekima, B., and Mahcene, H. (2011). “Experimental investigation on a double-slope solar still with partially cooled condenser in the region of Ouargla (Algeria)”. *Energy Procedia*. pp. 6:736-42.

Zerrouki, M., Settou, N., Marif, Y., Belhadj, M. M. (2014). “Simulation study of a capillary film solar still coupled with a conventional solar still in south Algeria”. *Energy Conversion and Management*. Vol. 85, pp. 112-119.

Ziabari, F. B., Sharaka, A. Z., Moghadam, H. and Tabrizi, F.F (2013). “Theoretical and experimental study of cascade solar still”. *Solar Energy* . Vol. 90, pp. 205-211.

Appendix 1: On Balance Mtt-500 Mini Table Top Scale

On Balance MTT-500 Mini Table Top Scale

- Capacity: 500g / 17.64oz / 7716gn / 2500.0ct
- Readability: 0.1g / 0.01oz / 0.1gn / 0.5ct
- Sperarate Lid/ Bowl
- 4 Modes: g, oz, gn, ct
- Backlit Display
- Auto Shut Off
- Tare & calibration Facility
- 2 x AAA Batteries (Included)
- Weighing Platform Size: 69 x 69mm
- Dimensions: 75 x 105 x 23mm
- Weight: 150g

Appendix 2: Derivation of Equation (5.8)

$$Q_1 = m_w C_w \Delta T_1 + Q_{L1}$$

$$Q_2 = (m_w - m_s) C_w \Delta T_2 + m_s C_s \Delta T_2 + Q_{L2}$$

$$Q_1 = Q_2$$

$$Q_{L1} = Q_{L2}$$

$$\frac{\Delta T_1}{\Delta T_2} = 1 + \left(\frac{\rho_s C_s - \rho_w C_w}{m_w C_w} \right) v$$

$$\left(\frac{\rho_s C_s - \rho_w C_w}{m_w C_w} \right) v < 0$$

$$\rho_s C_s < \rho_w C_w$$

Appendix 3: Figures – Experimental Setup



Fig. App 3.1 Solar still basin. The edges were welded from both sides.



Fig. App 3.2 The connection of supply pipe to solar still inside the basin



Fig. App 3.3 The connection of level sensor.



Fig. App 3.4 The level sensor was connected to basin wall.



Fig. App 3.5 level sensor was connected to alarm circuit.



Fig. App 3.6 K-type thermocouple was connected to basin to record the temperature.



Fig. App 3.7 The connection of drain pipe to the side of basin.



Fig. App 3.8 Wood sheet attached on outer basin.



Fig. App 3.9 Wood sheet protects the insulation layer.

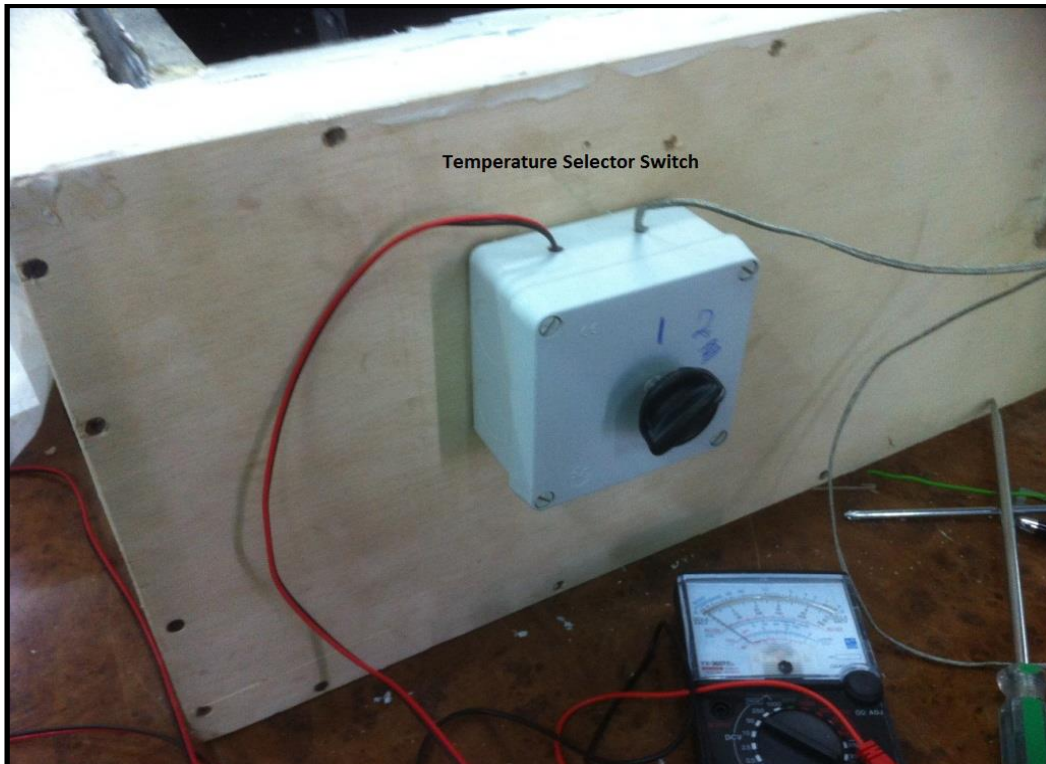


Fig. App 3.10 Temperature selector switch.

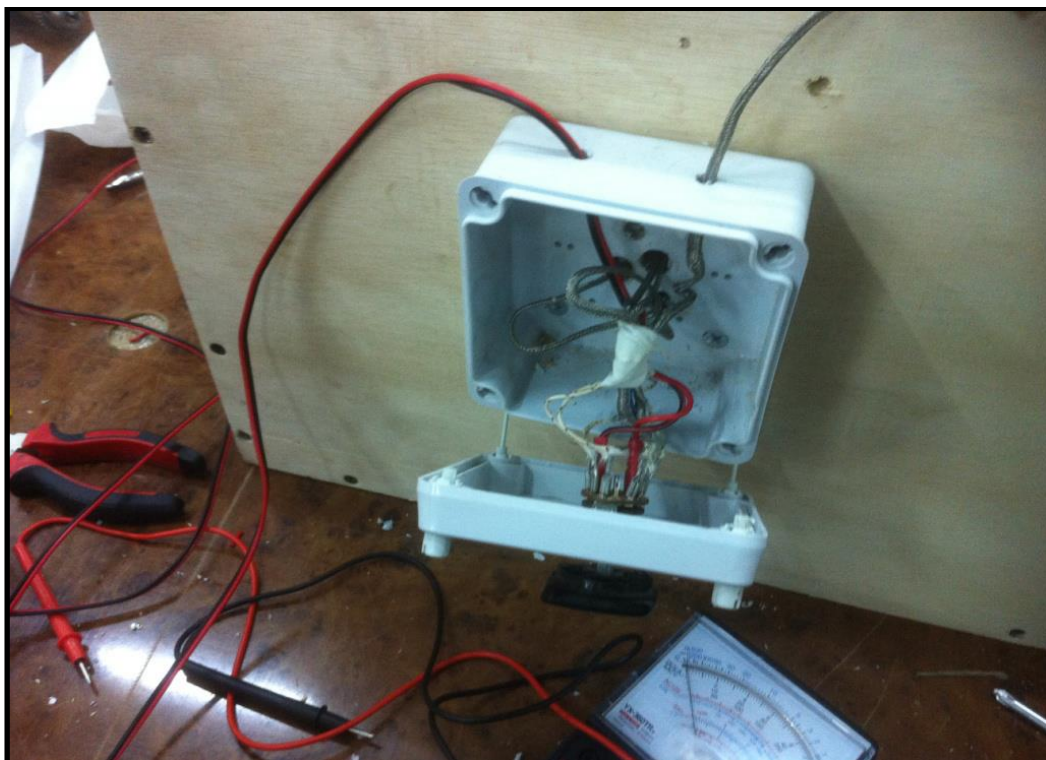


Fig. App 3.11 Electrical parts were tested on daily basis.



Fig. App 3.12 Glass sheets were used to construct double slope cover.



Fig. App 3.13 The solar still cover was built by using glass sheets at angle 35°.



Fig. App 3.14 Flexible anti mould, water proof silicone was used to connect the cover to still main body.



Fig. App 3.15 Thermocouples were connected to cover glass to measure the temperature of outer face of cover.



Fig. App 3.16 Control value was connected on the side basin.



Fig. App 3.17 The measurements were carried out where sun light could hit the solar still cover directly.

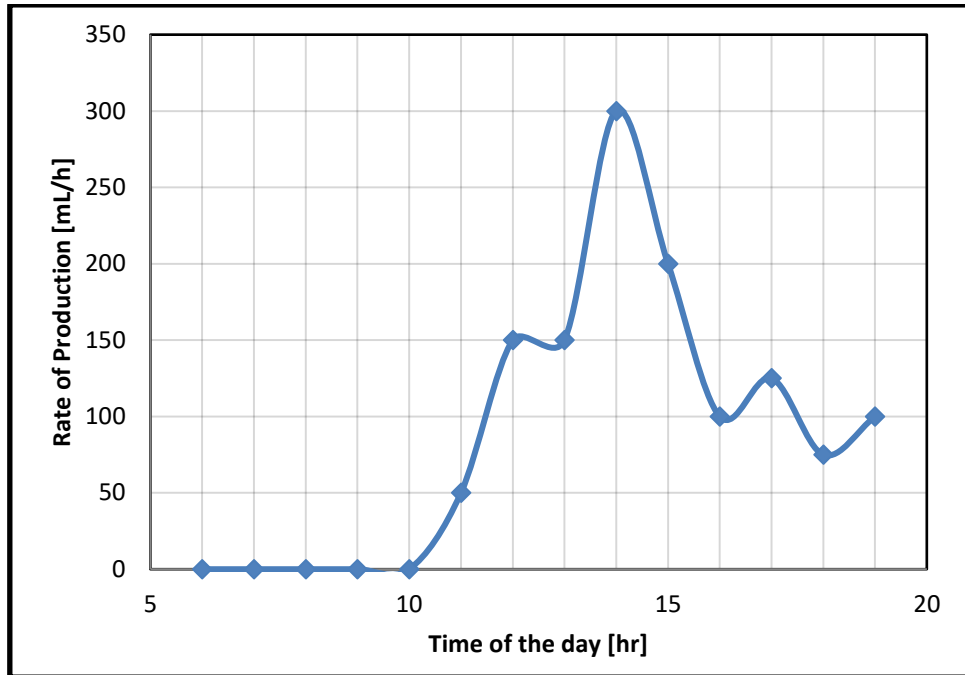


Fig. App 3.18 Variation of water production rate during a day with no modification.

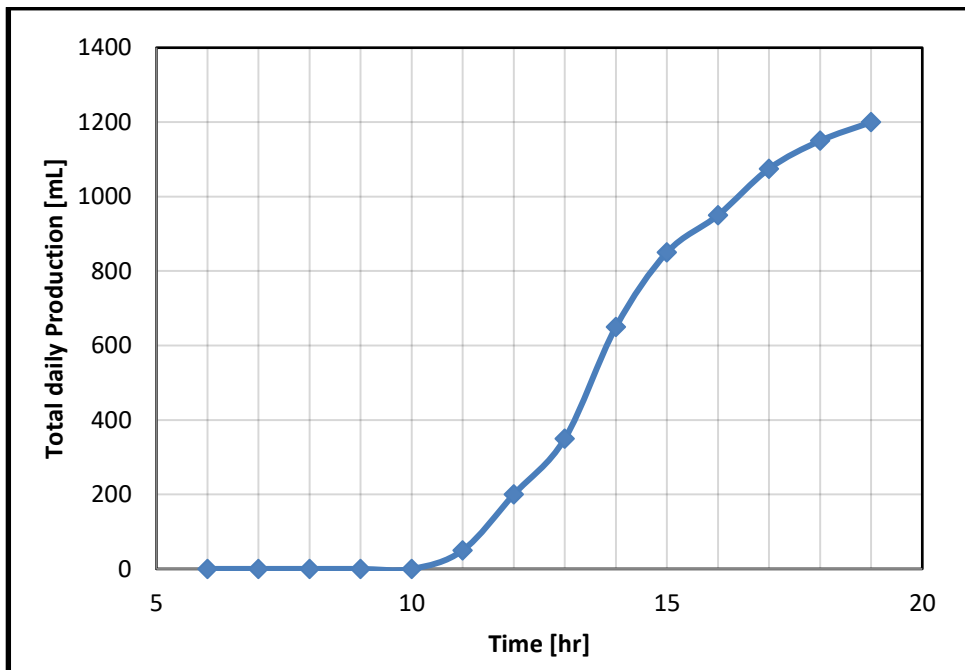


Fig. App 3.19 Variation of total daily water production during a day with no modification.

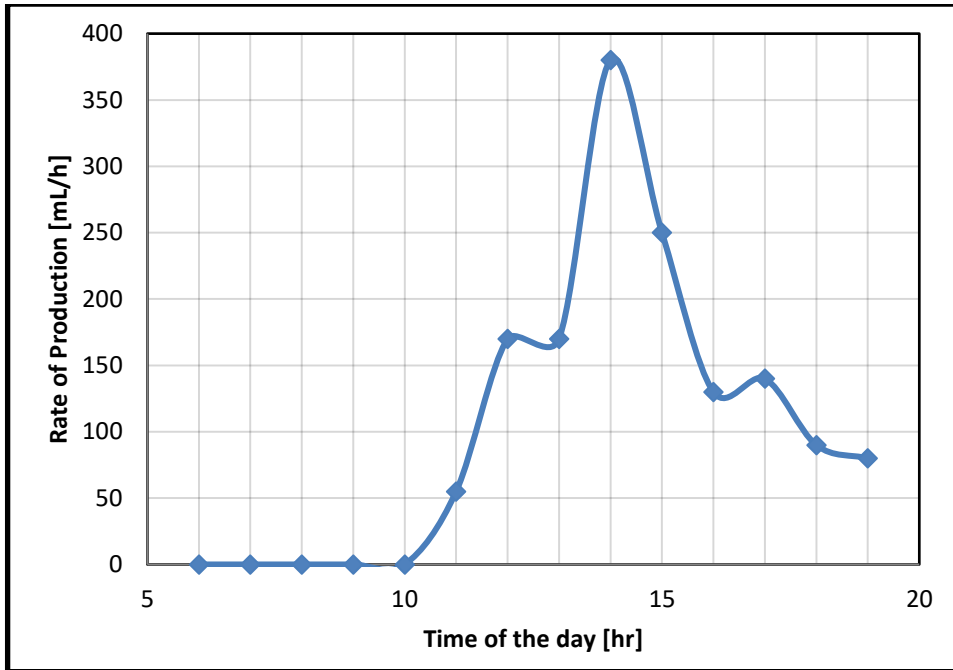


Fig. App 3.20 Variation of water production rate during a day by using hollow shape energy storing materials.

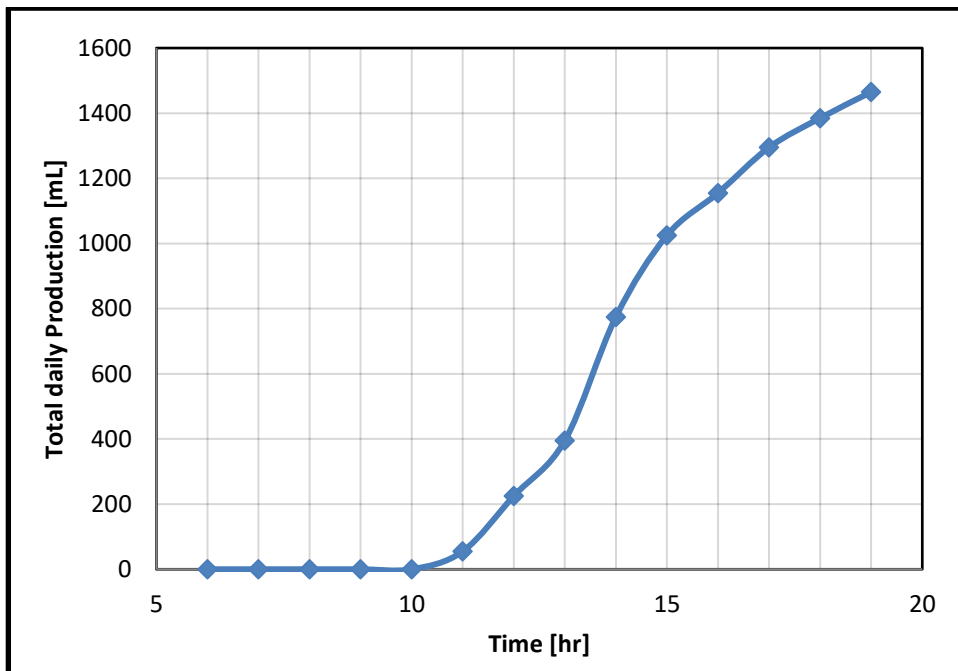


Fig. App 3.21 Variation of total daily water production during a day by using hollow shape energy storing materials.

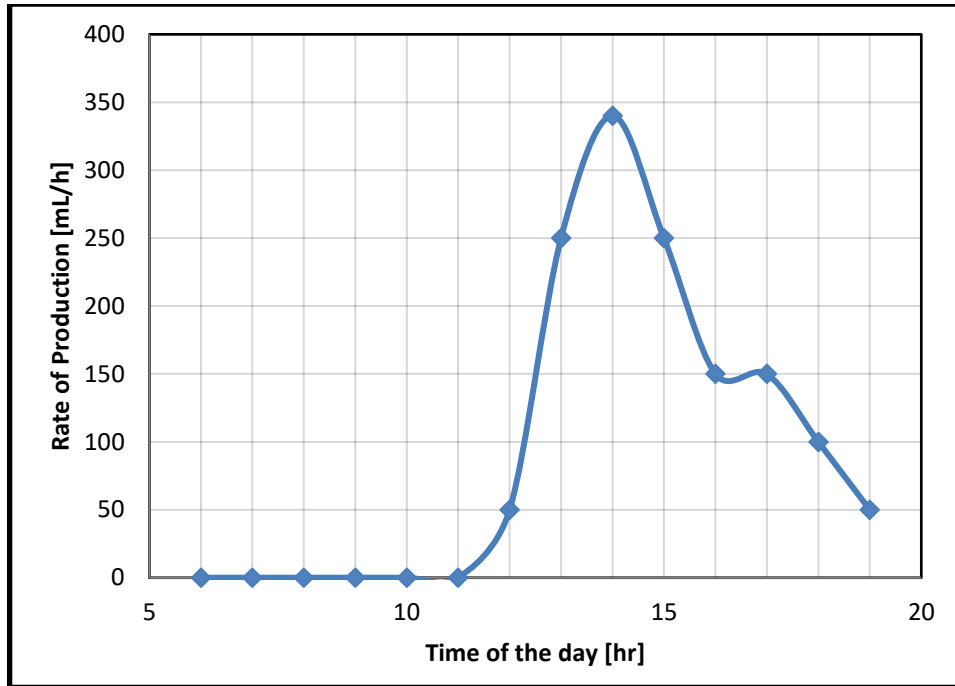


Fig. App 3.22 Variation of water production rate during a day by using solid shape energy storing materials.

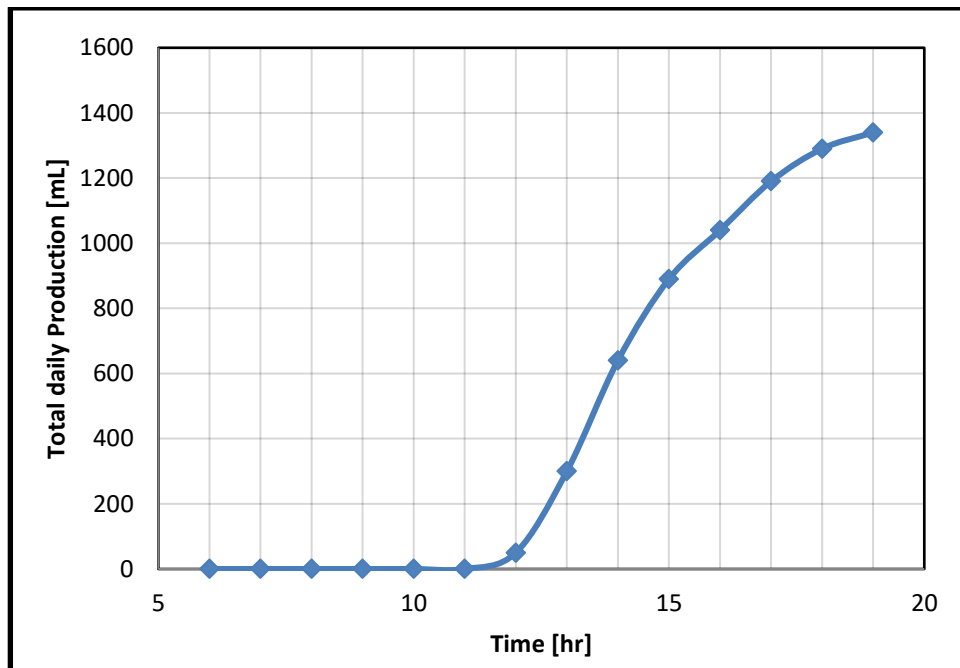


Fig. App 3.23 Variation of total daily water production during a day by using solid shape energy storing materials.